A NEW APPROACH TO MITIGATE THE IMPACT OF DISTRIBUTED GENERATION ON THE OVERCURRENT PROTECTION SCHEME OF RADIAL DISTRIBUTION FEEDERS

A Thesis

by

HAMED B. FUNMILAYO

Submitted to the Office of Graduate Studies of
Texas A&M University
in partial fulfillment of the requirements for the degree of

MASTER OF SCIENCE

December 2008

Major Subject: Electrical Engineering

A NEW APPROACH TO MITIGATE THE IMPACT OF DISTRIBUTED GENERATION ON THE OVERCURRENT PROTECTION SCHEME OF RADIAL DISTRIBUTION FEEDERS

A Thesis

by

HAMED B. FUNMILAYO

Submitted to the Office of Graduate Studies of
Texas A&M University
in partial fulfillment of the requirements for the degree of

MASTER OF SCIENCE

Approved by:

Chair of Committee,	Karen Butler-Purry
Committee Members,	B. Don Russell
	Natarajan Sivakumar
	Takis Zourntos
Head of Department,	Costas N. Georghiades

December 2008

Major Subject: Electrical Engineering

ABSTRACT

A New Approach to Mitigate the Impact of Distributed Generation on the Overcurrent Protection Scheme of Radial Distribution Feeders. (December 2008)

Hamed B. Funmilayo, B.Sc., Kansas State University

Chair of Advisory Committee: Dr. Karen Butler-Purry

Increased Distributed Generation (DG) presence on radial distribution feeders is becoming a common trend. The existing Overcurrent Protection (OCP) scheme on such feeders consists mainly of overcurrent protection devices (OCPDs) such as fuses and reclosers. When DG is placed on the remote end of a 3-phase lateral, the radial configuration of the feeder is lost. As a result, OCP issues may arise which lead to permanent outages even when the fault is temporary. This thesis presents a new approach that revises the existing OCP scheme of a radial feeder to address the presence of DG. The fuses on the laterals with DGs are removed and multi-function recloser/relays (MFRs) are added to address three specific OCP issues; fuse fatigue, nuisance fuse blowing, and fuse misoperation.

The new approach requires no communication medium, provides backup protection for the DG unit, and allows the remaining laterals to retain their existing protective devices. The results are reported using the IEEE 34 node radial test feeder to validate the new approach and the IEEE 123 node radial test feeder to generalize the approach. The new approach completely mitigated the fuse misoperation and nuisance fuse blowing issues and most of the fuse fatigue issues that were present on the radial test feeders. Specifically, the approach demonstrates that coordination between the existing protection devices on radial distribution feeders is maintained in the presence of DG.

ACKNOWLEDGEMENTS

Foremost, all thanks and praise be to God for providing me with the strength and knowledge to succeed. I am also very grateful to my advisor, Dr. Karen Butler-Purry, for her guidance, patience and support throughout my research work. Dr. Butler-Purry, thank you for providing me with the opportunity to work as a research assistant on this project, and thank you for all the time you dedicated to me throughout my master's study.

I thank Dr. B. Don Russell, Dr. N Sivakumar and Dr. T. Zourntos for investing their precious time to serve as my committee members. I also extend my gratitude to the Office of Graduate Studies and to the department faculty and staff for making my time at Texas A&M University a great experience.

Thanks to my colleagues at the Power System Automation Laboratory for their camaraderie. I wish you all success in your careers and in life. Last, countless thanks go to my siblings for their encouragement and to my wife for her patience and love. This thesis is in memory of my beloved parents for all their love, support and encouragement.

TABLE OF CONTENTS

CHAPTER Page

LIST OF TABLES

Page

Page

LIST OF FIGURES

Page

Page

CHAPTER I

INTRODUCTION

1.1. Background

The normal operation of an electrical power system involves the transfer of electricity from the generation points to various customers (commercial, industrial, and residential). The process integrates three major systems: generation, transmission, and distribution. The transmission system delivers the bulk electric power from the generation stations to substations where the distribution system begins.

In the distribution system, each substation is connected to the customers through one or more primary feeders. The majority of the distribution feeders are radial in which there is only one path for the electric power to flow from the substation to the customers. The feeder may operate at the primary voltage level (4 – 34.5kV) for industrial loads, or at secondary voltage levels (120/240V) for residential loads [1]. The feeder components include line segments, loads which may be in 3-phase, 2-phase or 1-phase configuration, in-line transformers, shunt capacitor banks, switches, voltage regulators, and overcurrent protection devices (OCPDs). The feeder lines may be in an overhead or underground configuration, although overhead lines are more common due to the economic benefits they provide. The feeder consist of the "main," typically a 3-phase 4 wire circuit, and laterals which tap into the main as 3-phase, 2-phase or 1-phase lines. Most loads on the feeder are located on the laterals. The feeder is inherently unbalanced because of the unequal spacing of the laterals and uneven distribution of the 1-phase loads [2] .

This thesis follows the style and format of *IEEE Transactions on Power Delivery.*

One of the primary objectives of operating a radial distribution feeder is to maintain a high level of service continuity with minimal loss of power during intolerable conditions. Because radial distribution feeders are mostly overhead lines, they are often exposed to the environment and easily affected by external disturbances such as lightning, thunderstorm, animals, and traffic accidents. These disturbances are known as faults, 80% of which are temporary and the remaining 20% are permanent [3]. The duration of the fault can range between ¼ cycle to a few cycles [4]. The resulting fault current is a function of the system impedances between the substation and the fault whose magnitude may be several orders higher than the normal operating current on the feeder. The fault can cause damage to the feeder components when not promptly cleared or isolated from the feeder. Owing to the radial nature of the feeder simple overcurrent protective devices, fuses and reclosers, are traditionally employed to reduce the impact of the fault on the feeder. The recloser is often located on the main, while most fuses are located on the laterals. The fuse is a single-shot device that isolates a fault by removing the faulted lateral, while the recloser is a multiple-shot device that clears and isolates a fault on the feeder with a preset sequence of openings and reclosures [5]. These OCPDs continuously monitor the phase current levels on the feeder and are coordinated such that faults on the feeder are isolated in order to affect fewer customers. Fuses are inexpensive and reliable devices that melt and blow within a few cycles due to a high magnitude fault current. Therefore, the fuse will have to be replaced often due to the damage created by the fault current. In order to minimize the number of fuse damages during a fault, a recloser is selected to temporarily de-energize the feeder to clear the fault prior to the fuse operation.This concept is known as a “fuse saving operation”. Hence, the main objective of an OCP scheme with fuse saving operation is to minimize the frequency of permanent outages [1], [6] .

Presently, the basic transfer of electric power is witnessing dramatic changes as active generation is now becoming a common trend at the distribution feeder level. The opposition to transmission expansion and the need to accommodate the growing electricity demand are major reasons that smaller sources known as distributed generators (DG) are added to the feeder. Some immediate benefits of operating DGs in parallel with feeders include reduction of feeder power losses to include transmission and distribution (T&D) costs [7]. However, the presence of one or more DGs on a feeder causes a redistribution of the normal and fault current through the OCPDs. In such situations, the magnitude of the phase current through the OCPDs may increase, decrease or remain the same. The variation in the current measurement may affect the coordination between the OCPDs and allow temporary faults to result in permanent outages. In addition, the feeder being no longer radial implies a need to revisit the selectivity of the existing OCPDs on the feeder.

1.2. Research Objective and Organization

The objective of this thesis work is to develop a new approach to mitigate the impact of DG on an existing OCP scheme of radial distribution feeders. The new approach requires minimal changes to the existing OCP scheme when the DG is added to the feeder and ensures that the OCPDs on the scheme still maintain their settings. To achieve the objective, an OCP scheme was implemented on two IEEE Radial Test Feeders and then DG was added to investigate the OCP issues that arose. Finally, the new approach was developed and applied to the existing OCP scheme to mitigate the issues. In the approach, protection changes occur only at the lateral on which the DG is located and the settings of the fuses and feeder reclosers are unchanged. The approach incorporates protection at the system, interconnection, and DG unit levels.

This thesis work consists of six chapters. In Chapter I, an introduction of this research work and an organization of the thesis are presented. The discussions in Chapter II are broad but mainly consist of the literature review and problem formulation. The chapter elaborates on the coordination of OCPDs on a typical radial feeder to include an analysis discussing the DG impact on the feeder's OCP scheme. In addition, the existing methods to mitigate the OCP problems caused by DG presence are introduced along with the merits and drawbacks of the methods. The problem formulation concludes the chapter. In Chapter III, the outline of the new approach to the existing OCP scheme as a solution to the formulated problem is presented. The system models used in the studies are presented in Chapter IV. The simulation studies and results are discussed in Chapter V. Finally, conclusions and future work are given in Chapter VI.

CHAPTER II

LITERATURE REVIEW AND PROBLEM FORMULATION

2.1. Introduction

Generally, the addition of DGs to a feeder implies that additional sources of fault current are present on the feeder. Therefore, faults which happen to be potentially temporary may likely result to permanent outages. It is a common theme that a single DG can cause temporary faults to result in permanent outages on the radial distribution feeder. However, as DG presence on the feeder becomes prominent, disconnecting the DG at every instance of a fault may be impractical and even uneconomical in some cases. Over the past decade, several researchers have dedicated considerable effort towards developing methods to mitigate the impact of DG on the OCP scheme of radial distribution feeders. Some of these methods address the protection issues by providing an entirely new scheme without the use of traditional OCPDs such as fuses. However, a typical distribution feeder has several dozens of laterals that are normally protected by fuses and it is unforeseeable that all the fuses would be replaced by more advanced devices due to DG. The first section of this literature review thus focuses on the radial distribution feeder and the conventional OCPDs found on the feeder.

2.2. Overcurrent Protection for Radial Feeders

The traditional OCPDs, fuses and reclosers are applicable for single or multiphase lines on radial feeders [8]. Fuses designed for voltages above 600V fall in the category of distribution/fuse cutouts or power fuses [1], though power fuses are specifically employed for voltages equal to 34.5kV and higher. Fuse cutouts can be expulsion or liquid-filled types based on their characteristics. The expulsion fuse consists of a fuse link that senses the fault current and blows after a prolonged time. The links are commonly available as K (fast) or T (slow). The

expulsion fuse extinguishes the fault arc when the fault current reaches the zero crossing. The circuit interruption is accompanied by a physical demonstration due to the arc energy generated in the fault. This fuse type is the most common in overhead lines [1]. On the other hand, the current limiting fuse forces the fault current magnitude to zero in order to extinguish the fault and no physical demonstration of the arc energy is exhibited in this process. Therefore, such fuses are found in locations such as vaults, where expulsion fuses would be hazardous. Fig. 1 illustrates the fuse's model, which is based on a Time Current Curve (TCC), and the expulsion fuse type device. The fuse model consists of two curves, minimum melt (MM) curve and maximum clear (MC) curve. From Fig. 1, the vertical axis represents the duration of the fault current through the fuse that would initiate the fuse operation on the MM or MC curve. The horizontal axis is the current through the fuse. Therefore, the fuse operates in a time-current band between the minimum melt times, when the fuse becomes partially damaged, and the maximum clearing times when the fuse is fully damaged. The difference between these times for any given fault current through the fuse corresponds to the arcing time of the fuse. The minimum melting time is important when the fuse overreaches other devices downstream of the fuse. The fuse model can be customized into software packages by using the fuse's TCC values from the manufacturer's database.

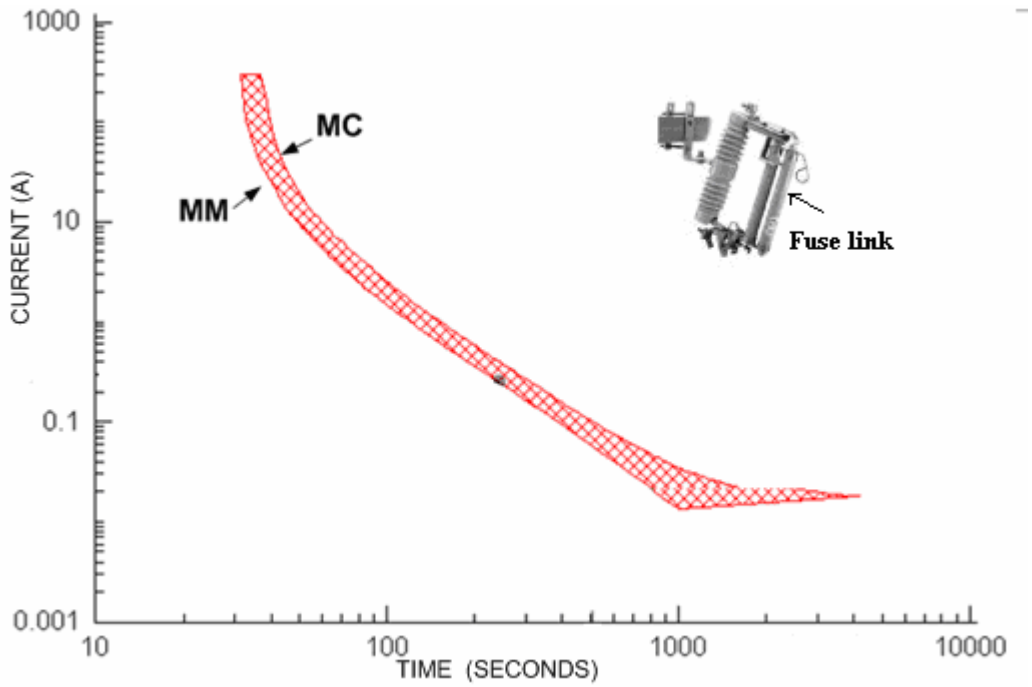

Fig. 1 Fuse Device and Time Current Characteristic Curve

The minimum operating limit for a fuse link is known as the continuous current rating, while the maximum limit is the symmetrical interrupting rating. In addition, the fuse is also rated based on the system voltage, maximum fault available at the point of application, X/R ratio at the point of application, and the load growth. Along with providing lateral protection, fuses protect the distribution feeder components such as in-line transformers and shunt capacitor banks.

Reclosers are circuit interrupters with self-contained controls and breaker. Reclosers are less costly than conventional breakers with relays therefore they are mostly used in distribution feeders. The recloser can be programmed to de-energize and re-energize the circuit at variable intervals in order to clear the fault. The recloser model consists of a fast and delayed curve. The first recloser was a hydraulic type introduced in 1939 to provide fault clearing and system restoration for 1-phase lines[9]. Since then, there have been hydraulic and electronic type reclosers with 1-phase and 3-phase capabilities. A 3-phase recloser includes phase and ground

units, while 1-phase reclosers do not have ground units. The 3-phase reclosers are generally recommended for protecting the main feeder in order to avoid damage to 3-phase motors and prevent potential ferroresonance [9]. Fig. 2 shows the recloser curves and an illustration of the 3-phase electronic recloser device. The recloser's fast curve is represented by the letter "A," while the delayed curve is given as "B".

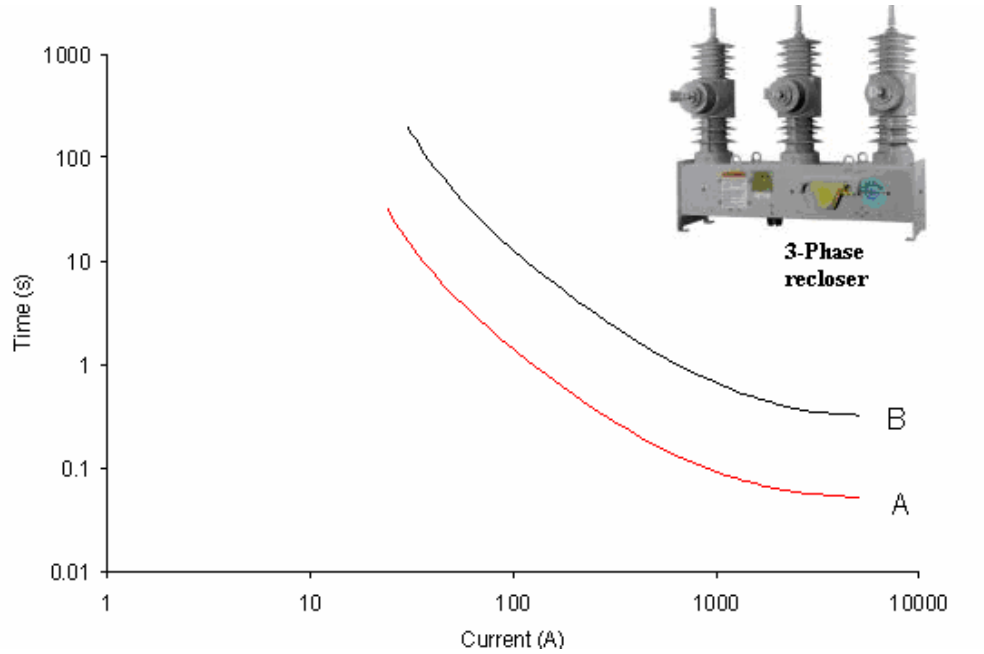

Fig. 2 Recloser Device and Time Current Characteristic Curve

The basic function of the recloser's fast curve is to clear the temporary fault and restore service with minimum delay. The reclosing action prevents the temporary fault from becoming permanent during which recloser switches from its fast curve to the delayed curve if the fault fails to clear initially. The delayed operation is characterized by longer time intervals and is followed by a lockout operation in case the fault still fails to clear. Afterwards, the recloser would have to be manually reset once it reaches the lockout position. The recloser's minimum operating limit is known as the minimum trip rating, while the maximum limit is the symmetrical

interrupting rating. Fig. 3 illustrates a typical operation of a recloser during a fault. The illustration presents a recloser programmed to operate in the A-B-B mode. This mode denotes one fast operation followed by two delayed operations and a lockout operation. The A-B-B sequence is one of the preferred modes of operation as it reduces the frequency of momentary outages and the duty on the substation transformer [9]. In the illustration, the recloser's contacts are initially closed when the load current flows through the recloser. When the fault occurs, the magnitude of the current through the recloser becomes several times larger than the normal current through the recloser. Therefore, the recloser undergoes the programmed multiple operations in which the contacts open for a defined period known as the reclosing time interval. The fast and delayed intervals are based on the settings of the recloser's TCC given in Fig. 2. The next section discusses the process of selecting, setting, and coordinating the OCPDs discussed.

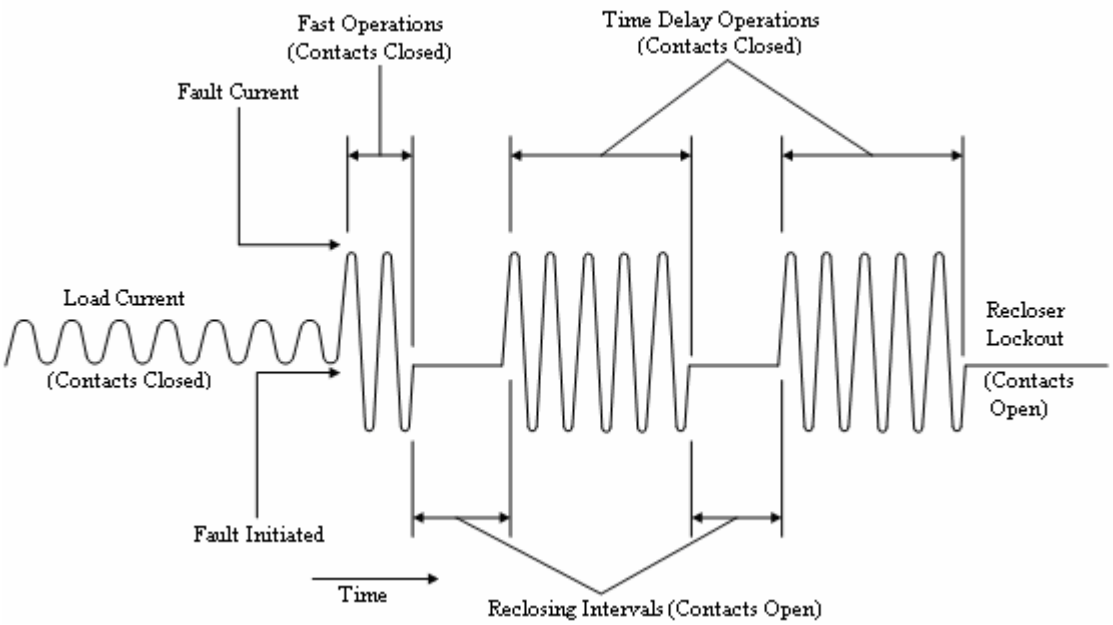

Fig. 3 Typical Recloser Operation during Faults (Adopted from [9])

2.3. Overcurrent Protection Coordination Rules

Adequate selection and coordination of OCPDs employs the peak load and fault current magnitudes at specific locations on a feeder where each OCPD would be applied. The peak load current results come from load flow studies that also involve the computation of real and reactive power values, and nominal voltage values on a feeder while the short circuit studies provide shunt fault current results on a feeder. The following subsections details the required parameters from a feeder and the OCPD ratings used to achieve adequate selection and coordination.

2.3.1. Load Flow Studies

In the load flow study, the parameter observed is the nominal phase current through the OCPD. The minimum trip rating for the selected recloser should be 200% of the nominal phase current in order to allow for inrush currents from the transformer and load growth [1],[9]. The equation in (2.1) assesses the load growth based on three parameters which are the load growth rate (g%), the initial and final values of the system load (P_0 and P_n), and the number of years considered (n^{th} year) [1], [10].

$$P_n = P_0 (1+g)^n \tag{2.1}$$

In this thesis work the load growth rate assumed was 1.25% for a five year period. For the fuse protecting a lateral, a continuous current rating value of 1.5 times the fuse's rating was used for the T and K tin link fuses [9]. The continuous current through the single fuses protecting a 3-phase lateral is based on the loading of that lateral. Therefore, each individual fuse on a 3-phase lateral may be of the same size [8]. In case of in-line transformers the maximum allowable rating for an in-line transformer's fuse should be 300% of the full load current through the transformer in question [11]. Regarding the capacitor fuses, the selected fuse link should have a

minimum rating of 135% of the rated load current to account for currents generated by harmonics [9].

2.3.2. Short Circuit Studies

In the short circuit study, the two parameters observed include the minimum and maximum branch fault current through the OCPD. For the purpose of the studies in this thesis work, the minimum fault branch current was a 1-phase grounded fault with a non-zero fault resistance placed at the farthest node downstream of the OCPD in question. The maximum branch fault current through the OCPD was a 3-phase to ground fault with no fault resistance (or 1-phase if the line was single phase) placed at the closest node downstream of that OCPD. The minimum fault current should exceed the recloser's minimum trip rating or the fuse's continuous current rating. Consequently, the maximum fault current should not exceed the OCPD's symmetrical interrupting rating.

Secondary-side (through) faults are considered to be the most difficult to interrupt by the transformer fuse. The method for calculating the through faults is provided in [12]. Equation (2.2) provides the primary fault current (I_{pri}) using the transformer's rated voltage (E), the impedance (Z_T), and KVA rating. The calculated primary fault current should be sensed by the selected transformer-primary fuse and interrupted in a timely fashion.

$$I_{pri} = \frac{E}{\sqrt{3} * Z_T} \tag{2.2}$$

where $Z_T(\Omega) = \frac{Z_{T\%} * 10 * E^2}{kVA}$

2.3.3. Coordination Studies

Coordination is defined as the process of selecting OCPDs with certain time-current settings and their appropriate arrangement in series to clear faults from the system's lines or components according to a preset sequence of operation [1]. The operating times of the primary device and the secondary or backup device are two parameters that determine coordination between the both OCPDs. The primary device is the closest OCPD that isolates the faulted section on the feeder, while the backup device is farther away and operates in case the primary device fails to trip. The backup OCPDs are located in an adjacent zone, which typically overlaps the primary zone. The backup OCPD device is intended to operate only if the primary device fails or is temporarily out of service. Recloser-fuse coordination through the TCC method employs the fault values obtained from the short circuit studies (minimum and maximum line/bus faults, capacitor faults and transformer faults).The criterion used to determine if the recloser and lateral fuses were properly coordinated was that the operating time of the primary device was less than that of the assigned backup device. The implication of the coordination statement is simplified through the illustration in Fig. 4 and Fig. 5.

Fig. 4 illustrates a portion of a typical distribution feeder with OCPDs and connected to the grid through a substation transformer. The feeder is characterized with six nodes (or buses) and includes the main and two laterals with loads. The main runs from node 2 – 4 and 4 – 5, while the laterals (assumed as 3-phase) branch out from the main, between node 2 – 4 and node 4 – 5. The feeder is divided into protection zones that are maintained by the OCPDs (the recloser and the fuses). The primary protection on the feeder laterals is provided with a backup protection. In Fig. 4, the recloser is denoted by REC and its primary protection zone is the main (between node 2 – 4 and node 4 – 5). The main is typically 3-phase, therefore REC is assumed as a 3-phase recloser. For the fuses (FUSE1 and FUSE2), the primary protection zones are their

respective laterals. The laterals can be 1-phase, 2-phase or 3-phase. The laterals are assumed as 3-phase. Three 1-phase fuses are placed on the individual phase of each lateral where FUSE1 and FUSE2 are assumed as one of the three 1-phase fuses on each lateral. In the illustration given in Fig. 4, the protection zone of the recloser overlaps those of the fuses. The overlap implies that the recloser's backup zone is the laterals [8]. The recloser is coordinated with the fuses for temporary and permanent faults on the feeder. If fuse saving is used, the preferred sequence for the recloser operation in this case is A-B-B. If a fault occurs at the location shown in Fig. 4, the current through the recloser (I_{REC}) and that through the fuse (I_{FUSE_2}) are sourced from the substation. FUSE2 is the primary OCPD that should isolate the faulted location if the fault is permanent while the recloser would be the backup device if FUSE2 failed to isolate the faulted location. FUSE2 operation would result in a permanent outage on the lateral after which the fuse would have to be replaced. Continuity of service would be maintained at the unfaulted sections of the feeder.

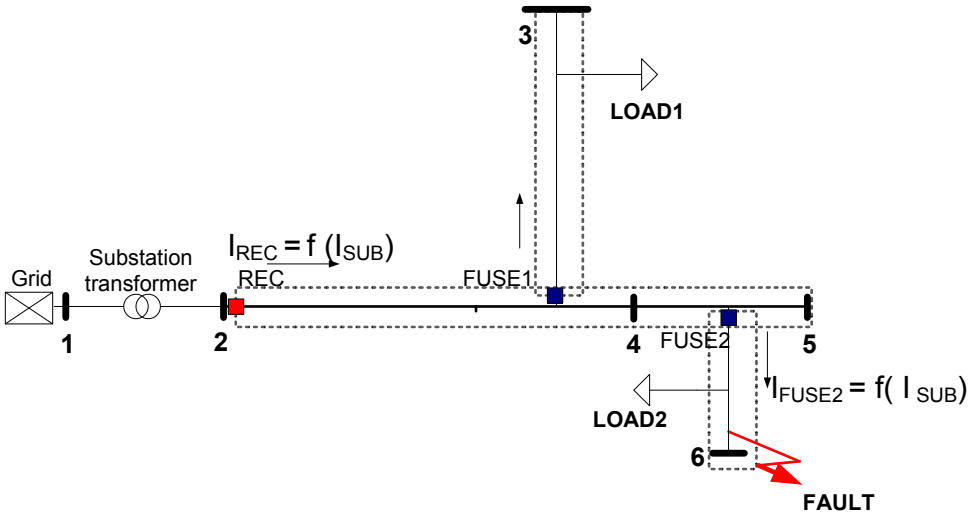

Fig. 4 A Portion of a Typical Radial Feeder with Recloser and Fuses

In Fig. 5, the points 1 and 2 indicate the fault current range (I_{fMIN} to I_{fMAX}) for which coordination between the recloser and FUSE2 holds. For the permanent fault (assuming a 3-phase fault on the lateral) shown in Fig. 4, point 3 represents the current seen by the recloser I_{REC_A} on the A curve and point 4 represents the current seen by FUSE2. Fig. 5 shows that $t(I_{REC_A})$ will be less than $t(I_{FUSE_2})$ for the fault which represents proper coordination of the devices to clear a potential temporary fault. Since the fault is permanent, the recloser will close its breaker after the breaker has been open for a prescribed amount of time. Point 5 represents the current seen by the recloser on the BB curve. Fig. 5 shows that $t(I_{FUSE_2})$ will be less than $t(_{REC_{BB}})$ for the fault which represents proper coordination of the devices to isolate the permanent fault.

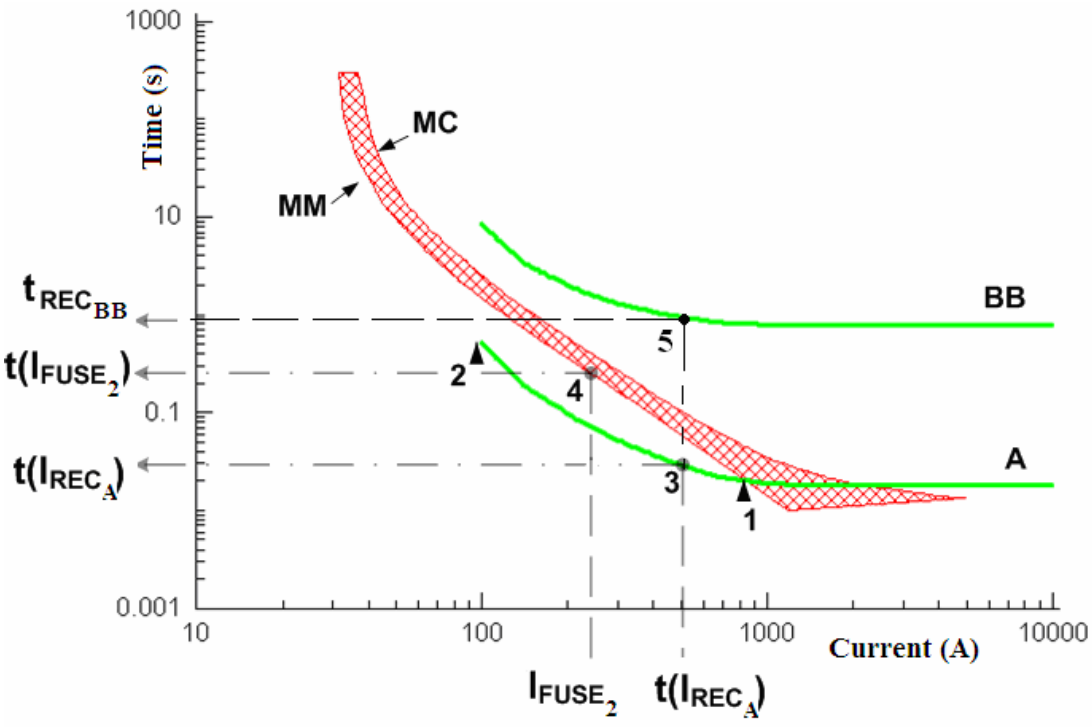

Fig. 5 Typical Coordination between a Recloser and a Fuse

From the illustration in Fig. 5, the following coordination rules apply to the OCPDs: For recloser-fuse coordination during minimum and maximum faults downstream of the lateral fuses, the recloser's scaled (A) curve operating time $t\left(I_{REC_A}\right)$ must be less than the fuse's minimum melt (MM) operating time $t\left(I_{FUSE_2}\right)$. Also, the fuse's maximum clear (MC) operating time must be less than the recloser's non-scaled delayed (BB) curve operating time.

For component protection devices such as capacitor banks and the in-line transformer fuses, the following rules apply: For recloser-fuse coordination during a capacitor fault at a capacitor fuse(not illustrated), the fuse's maximum clear operating time must be less than the recloser's scaled (A) curve operating time. For the coordination between a transformer fuse and the recloser during a transformer fault, the fuse's maximum clear (MC) operating time must be less than the recloser's scaled (BB) curve operating time. For fuse-fuse coordination, the ratio of operating time of the primary fuse's MC curve to that of the backup fuse's MM curve must be less than 0.75 [1], [9].

2.4. Distributed Generation (DG) in Radial Feeders

DG is defined as a subset of Distributed Resources (DR) that may be employed in smaller capacities as micro (~1W < 5kW), small (5kW < 5 MW), medium (5 MW < 50 MW), and large (50 MW < 300 MW). DG technologies include photovoltaics, wind turbines, fuel cells, small and micro-sized turbine modules, sterling-engine based generators, and internal combustion engine generators [13]. Many of these technologies use renewable energy resources. DG can serve as a viable option to provide additional substation and feeder capacity in anticipation of future load growth. Some immediate benefits of operating DG in parallel with the feeder include reduction of feeder power losses and Transmission & Distribution (T&D) costs.

The synchronous generator described in the next paragraph is the common generator used for DG employed on distribution feeder.

The DG unit consists of a synchronous generator directly connected to the associated power transformer [8]. The synchronous generator is an alternating-current machine in which the rotational speed of normal operation is constant when interconnected with the distribution feeder. The generator operates in synchronism with the system frequency and in step with the feeder's voltage. Synchronous generators have a direct current (dc) field winding to provide machine excitation and are generally capable of supplying sustained current for faults on the feeder [14]. The fault current infeed from the synchronous generator type depends on the prefault voltage, subtransient and transient reactances of the machine, and exciter characteristics. The resulting high magnitude of the short circuit from the generator redistributes the fault current level on the feeder, thus presents problems to existing overcurrent protection. The relevant modeling parameters for the DG include the real and reactive power ratings, per unit synchronous, transient, subtransient and zero sequence reactances [15],[16]. Since the synchronous generator exhibits non-linearity, the parameters are not linear with the increase in generator size and no interpolation or extrapolations are assumed. Therefore, this thesis work study is based on actual synchronous generator sizes from [17]. In addition, the default controller model from the software of choice as well as the automatic voltage regulator (AVR) for the generator was adopted.

There are five known transformer configurations through which the generator is connected to the feeder. These configurations are wye grounded-wye, wye grounded-delta, delta-wye grounded, delta- wye, and delta-delta. Most of the wye configuration is typically grounded, while delta-delta configuration type is ungrounded. The delta-delta is the most convenient configuration but causes overvoltage issues. However, the major advantages are the

reduction in the infeed fault current from the DG during grounded faults and the control of harmonics from non-linear loads [18]. The cause of overvoltages are the 1-phase or 2-phase grounded faults causing the voltage level on the un-faulted phase to increase up to 150% above the nominal level. The overvoltage issue was avoided by ensuring that there is no 1-phase protection device between the DG and the substation [9]. The KVA rating of the transformers matched the DG KVA rating[5].

2.5. Radial Feeder with DG and Overcurrent Protection Issues

The OCPDs on a radial distribution feeder normally operate on steady state fault current since the feeder is inherently passive. The generation and transmission systems are farther away from the feeder such that any transients from the generation system would have decayed over a period of time before the fault reaches the distribution feeder. However, when DG is added to the feeder lateral, generation is closer to the load and large transients may occur during a fault on the feeder. The addition of DG P_{DG} implies that less real power is required by the substation P_{SUB} to provide the total real power demand P_{demand} in (2.3). The combined power provided from the sources within the system P_{supply} is given in (2.4).

$$\sum (P_{load} + P_{losses}) = P_{demand} \tag{2.3}$$

$$\sum (P_{DG} + P_{SUB}) = P_{supply} \tag{2.4}$$

The DG penetration level is given by (2.5):

$$\text{Penetration level}\,(\%) = \frac{P_{DG}}{P_{supply}} \times 100 \tag{2.5}$$

Depending on the DG penetration level (size) on the laterals, the fuses may be subject to unnecessary damage especially during a fault. Three OCP problems that arise include fuse

fatigue, nuisance fuse blowing, and fuse misoperation [19], [20]. In earlier work conducted by the authors [21] , [22] to characterize the impact of DG on an OCP scheme for the IEEE 34 Node Radial Test Feeder [23], studies indicated that fuse fatigue and nuisance fuse blowing were more dependent on the total penetration level of the DGs, while fuse misoperation was dependent on the number of DGs at different locations on the feeder. For example, in one of the cases studied, three DGs with a total penetration level of 50% placed at different locations on the feeder showed the same number of recloser-fuse miscoordination issues as a single DG of the same total penetration level. Fig. 6 illustrates how these OCP problems develop after adding DG to a lateral of the feeder in Fig. 4.

For the given fault at the location shown in Fig. 6, two sources (the substation/Grid and the DG) now supply the fault current. Therefore, the current through the OCPDs now become functions of the substation (I_{SUB}) and the infeed current from the DG (I_{DG}). The recloser current (I_{REC}) is a function of the substation, the FUSE1 current (I_{FUSE1}) is a function of the DG, and the FUSE2 current (I_{FUSE2}) is a function of the substation and infeed current from the DG. The OCP problems may arise as a result of the redistributed fault current and other factors such as DG penetration level defined in (2.5). The next subsection discusses possible OCP problems that the addition of DG introduces on the existing OCP scheme.

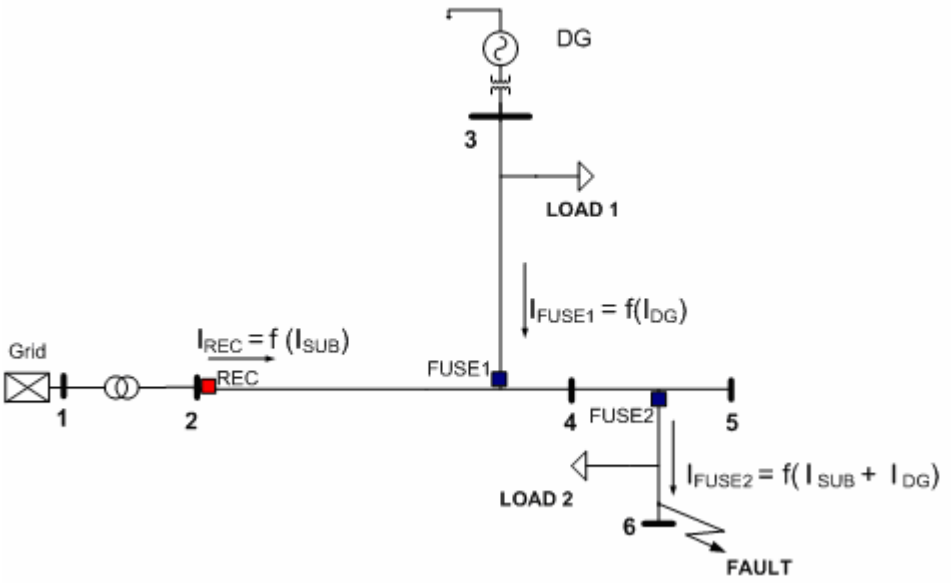

Fig. 6 A Portion of a Typical Radial Feeder with a DG, Recloser, and Fuses

2.5.1. Fuse Fatigue and Nuisance Fuse Blowing

Fuse fatigue or damage arises when the fuse link begins to melt before the recloser's fast operation [9]. In Fig. 6, the fault located downstream of FUSE2 may cause the fuse to become fatigued as shown in Fig. 7. Point 3 on the illustration corresponds to the current seen by the recloser I_{REC} on the A curve and point 4 represents the current seen by the FUSE2 on the MM curve. Fig. 7 shows that $t(I_{REC})$ will be more than $t(I_{FUSE2})$ for the fault downstream of the FUSE2 which represents fuse fatigue. The occurrence of fuse fatigue may reduce the lifetime of the fuse but will not cause the fuse to blow or result in a permanent outage.

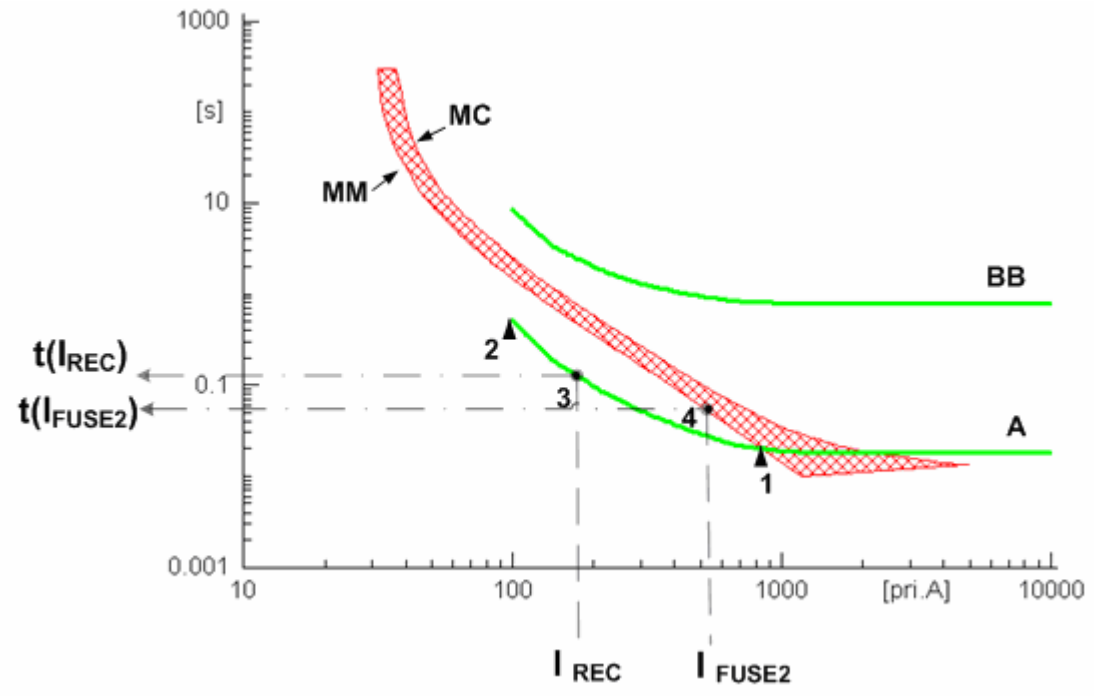

Fig. 7 Fuse Fatigue Problem

As the DG penetration level increases the fault current through FUSE2 may increase as well. The lateral may therefore suffer a permanent outage during a fault which may be potentially temporary. The illustration of the nuisance fuse blowing issue is given in Fig. 8 where the infeed current from the DG may cause the fuse to operate on the MC curve prior to the recloser's fast operation during a fault. Points 1 and 2 again represent the minimum to maximum current range for which coordination holds for the REC and FUSE2. For the permanent 3-phase fault on the lateral shown in Fig. 6, point 3 indicates the current seen by the recloser I_{REC_A} on the A curve and point 4 indicates the current seen by FUSE2. Fig. 8 shows that $t\left(I_{FUSE_2}\right)$ will be less than $t\left(I_{REC_A}\right)$ for the fault which represents nuisance fuse blowing. Even though this operation appears to be correct since FUSE2 isolates the permanent fault downstream of it, were the fault

temporary this would have been an incorrect operation and cause an unwarranted permanent outage.

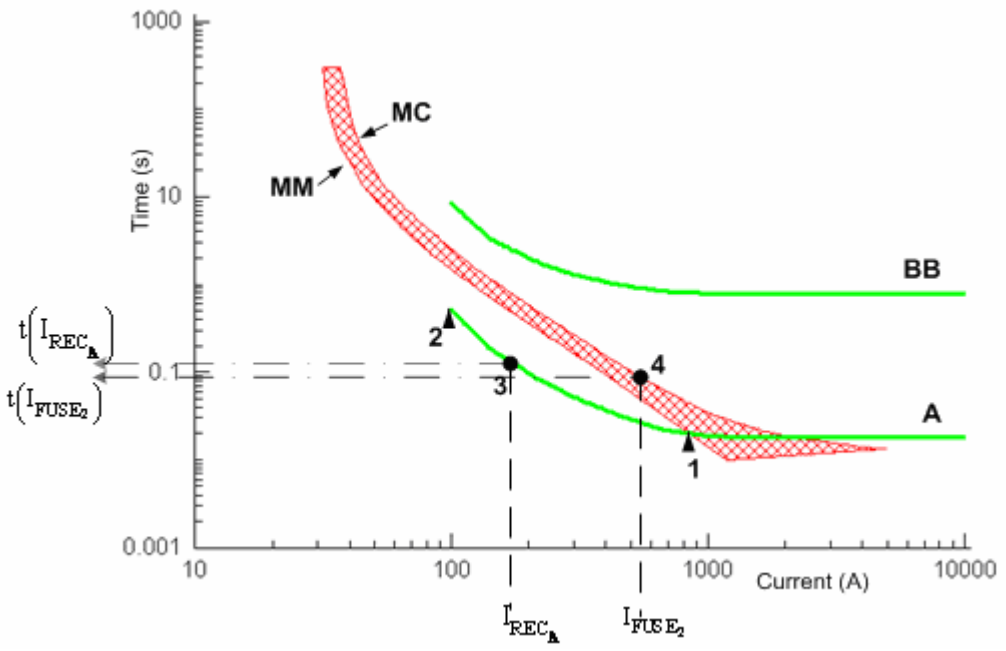

Fig. 8 Nuisance Fuse Blowing Problem

2.5.2. Fuse Misoperation

In the radial feeder, the protection zone for a fuse is the lateral and a fuse would operate to isolate all faults on the lateral protected by the fuse. However when the DG is added to the feeder lateral, the feeder is no longer radial and the fuse may operate for faults outside the lateral (on the main or on other laterals). This condition is known as fuse misoperation. In the illustration given in Fig. 6, the fault is on the protective zone for FUSE2. However, FUSE1 may misoperate during the fault due to the contribution of the infeed current from the DG to the fault. This condition will lead to the DG being isolated with lateral and result in an unwanted island. In the islanded section, there is a possibility that the total active power supplied by the DG may not

match the total load on the island. Therefore, damage to DG and the feeder components in the islanded section may occur in addition to other power quality issues [24].

The occurrence of the three described issues will affect the reliability of the feeder during temporary or permanent faults. The performance indices used in assessing the reliability of a feeder's OCP scheme are defined in [9], [25]. These indices include the Momentary Average Interruption Frequency Index (MAIFI) and the System Average Interruption Frequency Index (SAIFI). MAIFI pertains to momentary outages of 2 seconds or less, while SAIFI pertains to outages of more than 2 seconds [25]. Infeed current from DG during a temporary fault can potentially cause nuisance fuse blowing and result in permanent outages. Such circumstances will increase the SAIFI value and consequently decrease the feeder's reliability.

2.6. Methodologies Used to Address DG Impact on OCP

The need to re-coordinate OCPDs on the feeder may arise when OCP problems occur due to the presence of DG. Different methodologies have been presented implementing the coordination between the OCPDs to mitigate the impact of DG on the feeder's inherent overcurrent protection scheme. These methods are grouped into two, adaptive- and non-adaptive-based coordination techniques. The adaptive philosophy is very broad in its definition and applications. However, the theme of the technique involves the ability of an OCPD (typically a relay) to automatically alter its operating parameters in response to changing power system conditions in order to provide reliable relaying decisions [26]. The implementation of such technique requires OCPD settings that would accommodate for the changes in the state of the feeder. In most cases, such a process would require minimal or no human intervention.

An adaptive protection scheme with an emphasis on recloser-fuse coordination for a distribution feeder with a high penetration level of DG was the focus in [27], [28] . Brahma and Girgis in [27] discussed an adaptive method to implement a microprocessor based reclosing

scheme to achieve recloser-fuse coordination during a fault on a feeder with a high penetration level of DG. The scheme involved developing a user-defined recloser curve to achieve coordination between the recloser and fuse when DG is added to the feeder. The microprocessor based recloser's curve was adjusted through an online process in order to maintain coordination with the lateral fuses as changes in the feeder's branch current occurred. However, the scheme assumed that the DG would be disconnected before the first reclose operation when a fault occurred on the feeder. Brahma and Girgis in [28] provided another adaptive scheme for a radial feeder with multiple DG constituting a high penetration level. The scheme involved a relay at the main feeder that controlled the breakers at the laterals where the fuses were located. By using the synchronized vector phasor measurement unit (PMU), the relay measured and detected faults that occurred at a given location on the feeder and allowed the breaker to isolate the faulted section of the feeder. In the scheme, the fuses did not undergo any operation since isolation of the faulted zone was carried out by the breaker operation. The adaptive nature of the scheme was based on the ability of the relay to continuously monitor the feeder load flow and short circuit parameters following any change in the feeder topology. In the scheme, the relay was the only OCPD that provided the trip signal for isolating faults on the entire feeder. Therefore, coordination was not implemented. Furthermore, the accuracy of the scheme was dependent on the number of DG present in the feeder.

In the non-adaptive techniques the protective devices do not require online measurements to operate for a fault. References [9] and [29] suggested a selective replacement of the fuses following system studies for the newly connected DG. The approach was based on the fact that fuses were the prevalent OCPDs found on most laterals at the distribution level. The fuse sizes were selected based on the assumption that the DG remained connected to the feeder at a fixed location and a fixed penetration level.

Reference [30] suggested adding directional relays to the OCP scheme for radial distribution feeders with DG. In the approach, two directional relays were located at the interconnection point between the DG and the feeder. Both relays monitored the phase currents at the interconnection point to detect the fault and determine the fault's direction. Once the fault direction was determined, the relay operated the respective breaker to isolate the DG from the faulted area and minimize the possibility of recloser-fuse miscoordination.

2.7. Overall Assessment of Existing Methods

The IEEE 1547 standard [31] established the requirements for DG interconnection on distribution feeders. The standard maintains that DG should be disconnected from the feeder during any disturbance on the feeder. However, the standard does not emphasize specific OCP requirements for issues such as OCP coordination in the presence of DG [32]. Currently, the available methods, whether adaptive or non adaptive, can be viewed in terms of allowing island or non-island based operation. However, in practical terms, prolonged islanded operation of the DG with part of the feeder is currently not allowed for two major reasons—reduction in power quality of the feeder and complication of service restoration. First, the DG may not be able to maintain the voltage and frequency levels within the acceptable level required by the feeder resulting in power quality issues. Second, restoration of the feeder will also be complicated during delayed autoreclosing and manual switching following the recloser lockout because these two processes will require synchronizing the DG and the islanded load with the remaining feeder section. Therefore, the assessment of the existing methods will focus on schemes with non-islanded operation.

The adaptive protection methods that involve online selection of TCCs are only applicable to microprocessor based OCPDs. The adaptive methods involve altering the recloser curves automatically based on the DG status. However to be effective, most of these methods

require the use of communication links to continuously monitor the system's parameters and involve modifying the settings of the primary OCPD on the main feeder. Such requirements imply that the DG status needs to be constantly ascertained.

In the non-adaptive methods such as the selective replacement of the fuses, the selected fuse may operate incorrectly for faults if the DG penetration level is varied. In the case of the directional overcurrent relay scheme, the relay may require sensitive/low settings if the fault is several distances away from the DG. In addition, there must be sufficient quantities of current and voltage for a directional decision to be made, especially during close-in 3-phase faults.

The benefits of high-speed reclosing for distribution feeders employing DG was discussed in [33]. High speed reclosing is defined as the autoreclosing of a circuit breaker after a necessary time delay to permit fault arc deionization with due regard to coordination with all relay protective systems. The duration for the time delay is within 1 second, typically 0.2 seconds duration is reported in [34]. With high-speed reclosing, the DG is less prone to damage, and the risk of operating the DG in an islanded mode for an extended period of time is minimized. Two cycle breakers were proposed in [32] to eliminate the contribution of DG infeed to the fault and prevent the violation of the short circuit ratings of the OCPDs. Modern multi-functional reclosers and relays are equipped to combine both high-speed autoreclosing function and fast operating breakers. Upgrading the existing OCP scheme using a new approach improvises multi-functional reclosers/ relays at the lateral with DG to mitigate the OCP issues. This research work is a continuation of the studies carried out by the Power System Automation Laboratory at Texas A&M University in College Station.

2.8. Problem Formulation

Selective coordination for faults is one of the fundamental problems in radial distribution feeders. Addition of DG to the radial feeder implies that the nominal and fault current is

redistributed between the sources, the substation and the DG. The load and fault current through the OCPDs may decrease, increase, or remain the same thus coordination may be lost as a result. The problem is formulated as a time based coordination problem in which the selectivity rules apply. The selectivity rules can be expressed mathematically, as shown below in (2.6) and (2.7).

For all fault current values through a fuse in question (I_{FUSE_i}), the fuse operation time, $t\left(I_{FUSE_i}\right)$, should exceed the recloser's fast operation, $t(I_{REC})_A$:

$$t\left(I_{FUSE_i}\right) > t\left(I_{REC}\right)_A \qquad \forall I_{FUSE_i} \quad \begin{cases} I_{f\,min} \le I_{FUSE_i} \le I_{f\,max,} \\ I_{f\,min}, I_{f\,max} > 0 \end{cases} \tag{2.6}$$

For all fault current values through the fuse in question, the maximum clear time of the fuse, $t\left(I_{FUSE_i}\right)$, should not exceed the recloser's delayed time, $t\left(_{REC}\right)_{BB}$.

$$t\left(_{REC}\right)_{BB} > t\left(I_{FUSE_i}\right)_{MC} \qquad \forall I_{FUSE_i} \quad \begin{cases} I_{f\,min} \le I_{FUSE_i} \le I_{f\,max,} \\ I_{f\,min}, I_{f\,max} > 0 \end{cases} \tag{2.7}$$

DG added to the lateral of the feeder causes OCPDs to violate (2.6) and (2.7) when fuse fatigue and nuisance fuse blowing issues occur. Therefore, a new approach is added to the scheme to mitigate the three OCP issues. The new approach is realized through coordinating the added devices with the feeder recloser to ensure that infeed current from the DG can be limited during the worst fault conditions which may result in the issues.

The two radial feeders used for the purpose of this research work include the IEEE 34 Radial Node Test Feeder and the IEEE 123 Radial Node Test Feeder. The feeder description and preliminary assumptions include the following:

1. The feeder is radial with a single feeder consisting of mostly overhead distribution lines
2. The feeder loads are static and do not represent motor loads
3. The feeder has an existing overcurrent protection scheme comprising of a recloser (on the main feeder) and mostly fuses (on the feeder's laterals)
4. Fuse saving is implemented
5. All faults are initially assumed to be temporary
6. DG is added to reduce the substation's loading capacity and increase the feeder's capacity, making the feeder DG-dependent
7. DG is modeled as a synchronous generator, salient pole type
8. DG locations are the 3-phase laterals of the feeder in order to reduce overloading at the substation's transformer while maintaining close proximity to the loads
9. DG may be able to fully supply the load on the lateral in which the DG is located, and DG may be able to supply other loads outside the lateral
10. The DG unit has an inherent overcurrent protection

The constraints include the following:

a. The feeder's voltage level (V_{SYS}) remains within the rated value, V_{RATED} .

$$V_{RATED-MIN} \leq V_{SYS} \leq V_{RATED-MAX} \tag{2.8}$$

b. The generators operate within specified real and reactive power limits.

$$P_{DG-MIN} \leq P_{DG} \leq P_{DG-MAX} \tag{2.9}$$

$$Q_{DG-MIN} \leq Q_{DG} \leq Q_{DG-MAX} \tag{2.10}$$

c. The substation transformer is not overloaded.

Maximum loading (KVA) < 100% of the name plate rating (KVA) (2.11)

d. The limit on the total power provided by the *DG* is subject to a penetration level of 100% total load.

$$\sum P_{DG} \leq \sum P_{L} \tag{2.12}$$

$$\sum Q_{DG} \leq \sum Q_{L} \tag{2.13}$$

where P_L are the Q_L real and reactive loads of a radial feeder

2.9. Summary

Coordination in an OCP scheme refers to the overall protection design in which only the OCPDs closest to a fault will operate to isolate the faulted section or component. Selective coordination of the OCPDs ensures the continuity of service during temporary and permanent fault conditions. However, the presence of DG in parallel with the feeder may result in loss of coordination between the recloser and the fuses during a temporary or permanent fault, leading to issues such as fuse fatigue, nuisance fuse blowing, and fuse misoperation.

CHAPTER III

SOLUTION METHODOLOGY

3.1. A New Approach for a Fuse Saving OCP Scheme

The main purpose of the new approach is to mitigate the OCP problems with little modification to the existing OCP scheme of a feeder. Furthermore, the protection strategy of the feeder should ensure maximum protection at minimum cost. When DG is added to a radial feeder, temporary faults that are most common on the feeder laterals can result in unwarranted permanent outages. These outages are manifested as nuisance fuse blowing issues. Furthermore, permanent fault conditions on the main can result in an unwanted island due to fuse misoperation. Consequently, the DG and other equipment on the islanded section of the feeder may be damaged.

The new approach on the existing scheme accounts for all fault conditions on the laterals and the main. The protection changes involve replacing the fuse on the lateral with DG with a multi-function autorecloser (R_{LAT}). Although not a major contribution to this thesis work, an interconnection relay R_{DG}, and a differential relay are added as interconnection protection and backup protection for the DG unit respectively. The outline of the approach is discussed in the next section.

3.2. Outline of the New Approach

This section describes the new approach and coordination of the added OCPD with the recloser in the example feeder provided in Fig. 6. The focus is to determine the worst case conditions and coordinate the added OCPDs with the feeder recloser during the conditions. The process ensures that coordination will hold for the non-worst case conditions. The worst case condition is characterized by the maximum DG penetration level under the worst fault

conditions. The worst fault conditions may vary and depend on the line which is faulted. For example, in the 1-phase lines the worst fault condition was 1-ph grounded fault, while for the 3-phase laterals or main, the 3-ph grounded fault was the worst condition. To implement the new approach for the worst case conditions, a lateral recloser R_{LAT} and an interconnection relay (R_{DG}) are added to the list of OCPDs in the existing scheme. The added OCPD will allow each existing OCPD remaining on the feeder to maintain its settings and remain as the primary protection device of its zone. In short, the fuses would remain the primary protection device for the laterals, while the recloser would remain the primary device on the main feeder. The added OCPD are the primary protection devices for the lateral with DG. Fig. 9 illustrates the modification of the OCP scheme in the sample feeder discussed in Fig. 6. The protection zones are defined for the DG unit location, the feeder main, and the laterals. These OCPDs should operate for faults within the zones. Again, the fuses are the primary OCPDs for the laterals, while the recloser is the primary OCPD for the main feeder. R_{LAT} is the primary OCPD for the lateral with DG.

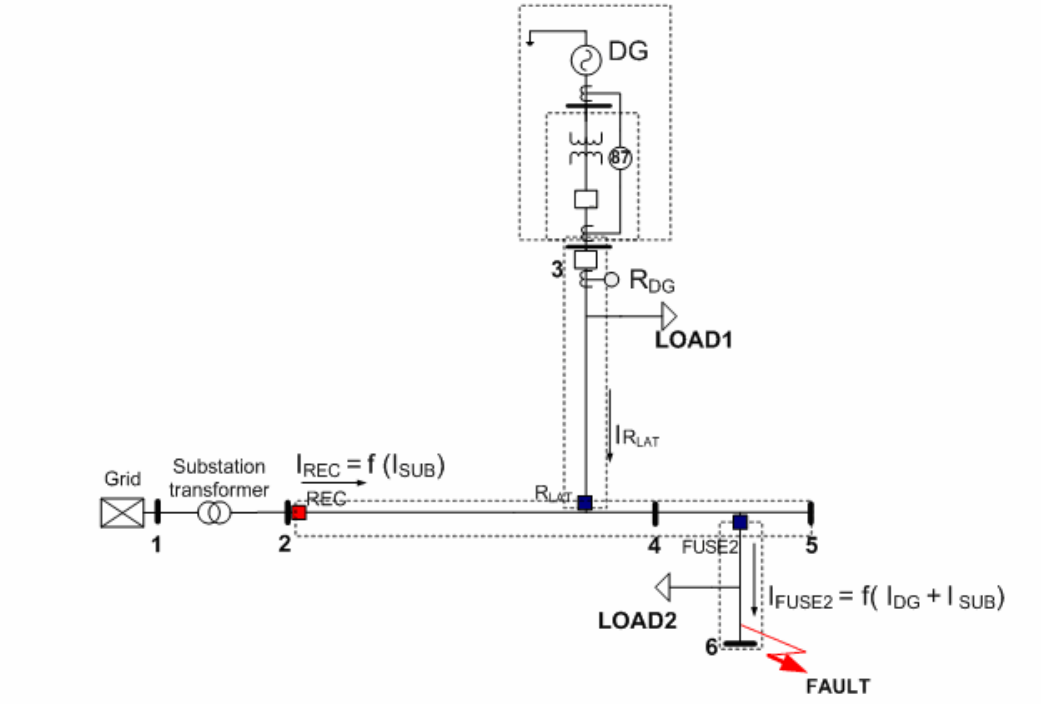

Fig. 9 A Portion of a Typical Radial Feeder with a DG and the OCPDs

The overlapped protection zones indicate a backup OCPD for the primary OCPD. The interconnection relay R_{DG} will trip the adjoining breakers at the interconnection point to prevent the DG from islanding with loads and equipment connected to the interconnection point. Overall, the feeder recloser provides the backup protection for all other devices to de-energize the entire feeder for permanent faults on the main or the laterals of the feeder. The protection changes made to the existing OCP scheme are described in next three sections.

3.3. System Protection

The system protection limits the infeed current from DG to prevent unnecessary permanent outages during a fault on the laterals. The three single fuses on a 3-phase lateral with DG is replaced with a recloser. The settings for the lateral recloser are based on knowledge of the OCPD settings in the existing OCP scheme—in particular, the operating time of the feeder

recloser in the existing OCP scheme. When DG is added to the feeder the fault current through the feeder recloser will decrease thus reducing the reach of the recloser. Therefore, the fastest operating time of the feeder recloser is achieved when the feeder is without DG.

The phase and ground settings of R_{LAT} and REC are coordinated using the composite method [35] to clear temporary faults on the feeder main and laterals during the worst case conditions. The settings for REC were the default settings used in the existing OCP scheme for multiple shot reclosing (1–fast, 2–delayed). The R_{LAT} recloser was configured for a single-shot reclosing (1–fast , 1–delayed) for its instantaneous trip and lockout operation. The choice of selecting reclosing interval for the lateral recloser is explained using the illustration in Fig. 10. The upper portion in Fig. 10 shows the status of the recloser ("1" for close status and "0" for open) during a time interval (in seconds) specified in the horizontal axis. The bottom illustration gives the corresponding frequency change during the time interval. When the fault occurs at t_f, the recloser opens at a time t_d and temporarily disconnects the lateral with the DG from the entire feeder until the recloser closes again at t_r seconds. The difference between t_d and t_r is the reclosing or dead time interval (t_i). Ref [33] defines the reclosing interval as a function of the frequency changes on feeder with DG. Therefore using (3.1), the reclosing interval of $R_{LAT's}$ fast operation was based on substituting an assumed frequency change of +/- 1.5 during contingencies such as a fault [36]. The instantaneous reclosing for R_{LAT} was high-speed with an 8–cycle reclosing interval. The reclosing interval for the feeder recloser was 10 cycles for the instantaneous and 60 cycles for the delayed operation.

$$\Delta f = \frac{\Delta P \, f_s}{2 S_n H} t_i \tag{3.1}$$

In (3.1), Δf is the frequency change between the islanded section frequency (f_i) and the synchronous frequency at the feeder (f_s). The remaining parameters (H, S_n and ΔP) are defined for the synchronous generator and the feeder where the paramter H is the inertia constant of the

generator whose rating is S_n. The difference between the active power from the DG and the islanded loads on the feeder is given by ΔP. In an attempt to provide service restoration following an instantaneous reclosing operation, a test was made to ensure that the reclosers were coordinated during the worst case situations. In the test, the recloser nearer to the weaker source of fault current (the DG) was the first to reclose. Then, the feeder recloser was reclosed afterwards. The stability studies of the DG unit during the high-speed reclosing operation were not performed in detail as it was assumed that the synchronizing power from the substation would stabilize the DG during the calculated reclosing interval [37]. Also, no voltage check or synchronism supervision was applied at the reclosers since the high-speed reclosing operation did not require an additional time delay [38] .

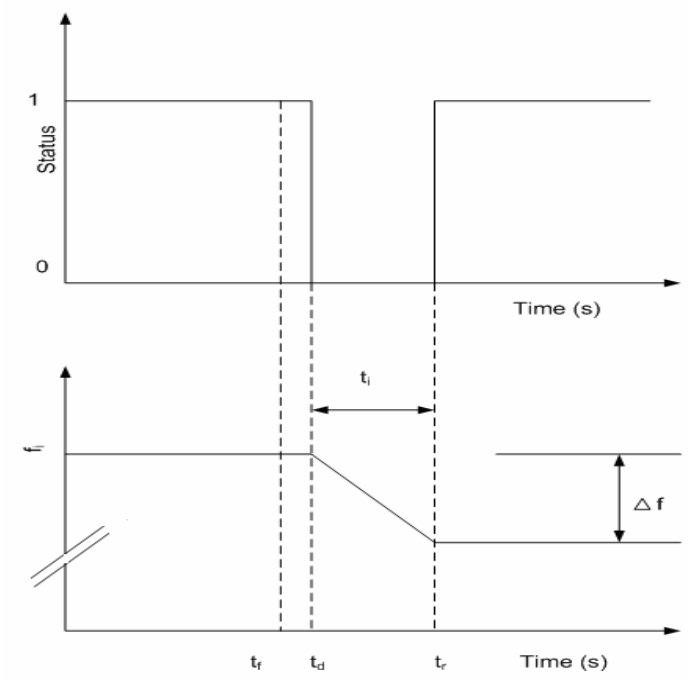

Fig. 10 Frequency Change during Autoreclosing

The settings for lateral fuses from the existing scheme were only based on either one or a combination of the phase current measurements I_a, I_b, and I_c, since fuses sense phase currents only. However, one criterion for selecting the added OCPDs was that the OCPD should be capable of operating using the phase and sequence current through the device. The reason for the condition is due to the bi-directional power flow introduced by the DG. In such situations, the fault current through R_{LAT} would be the vector sum of current from the two sources on the feeder. Such conditions may cause R_{LAT} to operate incorrectly for the fault or normal phase current. In addition, the unbalanced nature of radial distribution feeders allow the nominal values of the negative sequence and zero sequence measurements to be obtained to determine the settings of the MFRs. Results from [35] demonstrated that the sequence measurement improved the protection feeder performance. The pickup settings for the added OCPDs involved the use of both phase and sequence current measurements for the phase and ground settings. Ref. [2] defines the phase line currents as a function of the sequence currents as given by (3.2).

$$[I_{abc}] = [A_s] \bullet [I_{012}] \tag{3.2}$$

where $[A_s] = \begin{bmatrix} 1 & 1 & 1 \\ 1 & a_s^2 & a_s \\ 1 & a_s & a_s^2 \end{bmatrix}$

where $a_s = 1\angle 120^0$

Regarding the choice of time current curves for the added OCPDs, the lateral recloser, being a microprocessor based SEL351R offers the advantage of providing up to 38 various standard IEEE/IEC time current curves. The specific functional requirements of the recloser control employed in this research work include autoreclosing control, and phase fault and ground fault overcurrent protection. The phase fault OCP incorporates phase and negative-sequence overcurrent elements (51P and 51Q respectively) to detect phase faults, while the ground fault overcurrent protection recloser control incorporates the neutral ground overcurrent elements

(51N) for detection of ground faults [35],[39],[40]. Other features provided for additional security include directional elements, load encroachment logic, and torque-control capability. The added features were not the focus of this research work, and thus were disabled in the lateral recloser's model. The neutral overcurrent elements respond to the calculated neutral (residual or unbalanced) current $3I_0$ as the sum of the phase currents shown in (3.3):

$$3I_0 = I_a + I_b + I_c \tag{3.3}$$

3.4. Interconnection Protection

The primary purpose of interconnection protection is to prevent long term islanding operation of the DG unit with a feeder section. To achieve this objective, the relay (R_{DG}) is placed at the interconnection point to isolate the DG when it is not operating in parallel with the entire feeder [41]. This condition may arise during the feeder recloser's the time-delayed operation which may result in long-term islands lasting more than 1 second [38],[42]. The interconnection relay employs the 51P and 51Q elements to promptly isolate the DG unit. The 51Q element was used instead of the 51N element since no neutral line exists on the delta-delta connected transformer and most of the zero sequence current would be trapped in the delta-delta loop. Coordination of the 51Q element with the autorecloser's delayed curve elements was through the source-to-load coordination approach [35]. Although the frequency relay is primarily used for anti- islanding protection, the function was not implemented since the focus of this research work is on overcurrent protection.

3.5. DG Unit Protection

The DG unit is defined by the generator that is directly connected to the associated power transformer without a circuit breaker between both components [8]. This type of connection is the most common for large generators operating in parallel with the utility. The

differential (87TG) protection element shown in Fig. 11 is the most recommended form for DG units of this type and serves as backup if the DG has a primary protection device. The differential relaying concept eliminates the need to calculate fault currents and does not require precise relay settings [5]. Another benefit of applying the differential protection includes provision of high sensitivity for both phase and ground faults on the DG unit with the exception of high-impedance faults. The protection both isolates both the DG and transformer during transformer faults which may be external or internal [43]. External faults are those faults that occur outside the transformer. These faults present stress on the transformer and may shorten the transformer's life span. Internal faults occur within the transformer enclosure but such faults are not addressed in this research work.

The illustration in Fig. 11 shows how the differential relay operates to protect the DG unit. The current transformer (CT) locations in the differential protection set the protection zone for the DG unit. Two current measurement CTs located at the DG unit transformer's primary and secondary terminal provide backup for the DG. The CTs measure each phase current (A, B, C) of the line through the DG unit. CT1 is connected to the primary end of the DG unit, (Generator side), while the CT2 is connected to the secondary of the transformer.

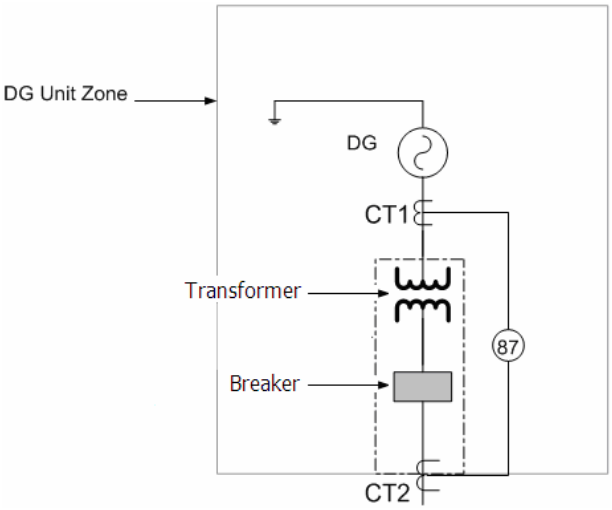

Fig. 11 DG Unit Backup Protection

The CTs are of the standard ratio type in which sensitivities on the order of 5A primary current can be obtained. The CT locations form the differential protection zone for the generator and transformer. The pickup settings for the CTs were based on the maximum DG size.

3.6. Protection Coordination in the New Approach

This section discusses the coordination of the existing and added OCPDs in the new approach for the worst case fault conditions (temporary or permanent maximum faults). During the worst case fault conditions, if coordination of the OCPDs holds to mitigate the OCP issues then it is assumed that the OCP issues are mitigated for the non-worst case situations. The lateral recloser and the interconnection relay operate in a 3-phase mode where the three phases are simultaneously disconnected during a fault.

When a fault is on the main feeder, the feeder recloser, the lateral recloser, and the interconnection relay operate to clear and isolate the fault. In Fig. 12, the vertical axis gives the OCPD status (“0” for open and “1” for close) and the horizontal axis provides the simulation period in seconds. For the illustration in Fig. 12, the feeder recloser (R) and lateral recloser (R_{lat})

operate on their fast curves to clear the fault if it was a temporary fault. Points 1 and 2 indicate the lateral recloser's fast operation (open and close), while points 1' and 3 give the feeder relcoser's operation. The status of both reclosers changes from 1 to 0 and back to 1 during this period. The DG unit remains in parallel with the lateral (on which the DG is located) during the operation of both reclosers. For a permanent fault, R_{DG} will operate (indicated by point 4) to isolate the DG unit from the feeder before the feeder recloser begin its first delayed operation indicated by point 5. The operation of the interconnection relay prevents long-term islanding of the DG unit with a section of the feeder. The feeder recloser then goes through two delayed operations indicated by points 5 – 6(open and close), and 7(open and lockout) after which the recloser will remain in the lockout status to isolate the entire feeder.

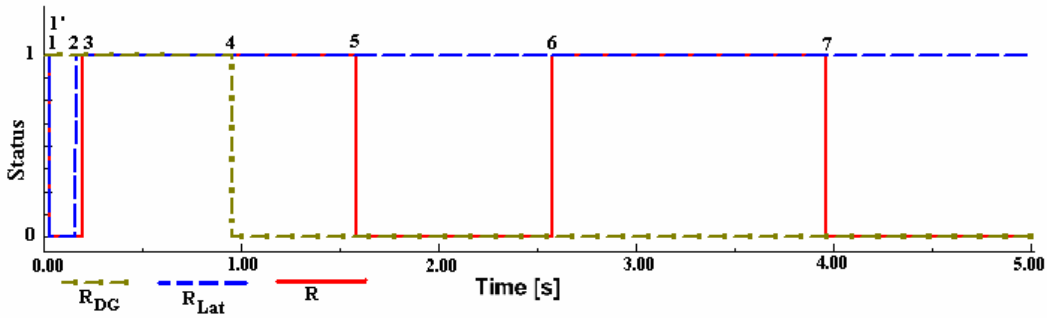

Fig. 12 Coordination for Faults on the Main Feeder Using the New Approach

Fig. 13 shows the coordination of protective devices for a fault on any of the feeder's laterals excluding the lateral with DG. Again, the vertical axis gives the OCPD status ("0" for open and "1" for close) and the horizontal axis provides the simulation period in seconds. For a potential temporary fault with duration of 4 cycles (staged from 0.01seconds to 0.08 seconds), the feeder recloser and the lateral recloser operate on their fast curves to clear the fault. For the illustration in Fig. 13, points 1 and 3 indicate the open and reclose operation of the lateral recloser while points 2 and 4 give the feeder recloser's operation. If the fault remains on the

lateral, the fuse protecting the lateral will blow to isolate the fault. Point 5 gives the fuse operation to isolate a permanent fault. The feeder recloser is the backup device for the fuse in case the fuse failed to isolate the fault. In the illustration the recloser does not operate on its delayed curve once the fault was isolated by the fuse. The lateral recloser will only operate on its delayed curve if the fault were on the lateral with DG.

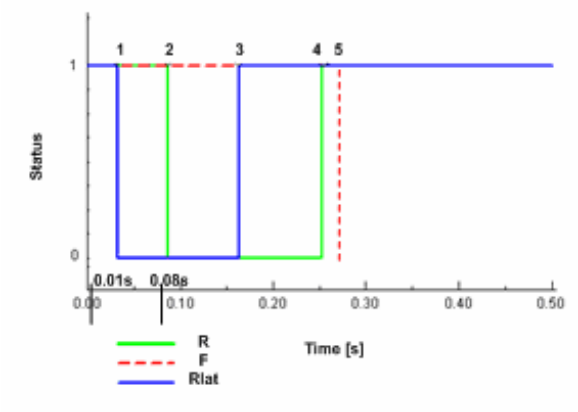

Fig. 13 Coordination for Faults on Laterals Using the New Approach

The afore-described coordination procedure in the new approach in which the primary and backup OCPDs' operation successfully clear and isolate a fault is listed as follows:

If the fault is on the laterals with fuses:

1. Lateral recloser (R_{LAT}) trips instantaneously,
2. Feeder recloser trips instantaneously,
3. R_{LAT} closes,
4. Feeder recloser closes,
5. Fault is cleared.
6. If the fault does not clear, the fuse in question blows,
7. Fault is isolated.

8. If the fault is not isolated due to primary OCPD failure,
9. R_{DG} trips open to isolate the DG,
10. Feeder recloser trips on the delayed curve and locks out,
11. Whole system is de-energized and fault is isolated.

For faults on the lateral with DG:

1. (R_{LAT}) trips instantaneously,
2. Faulted section is isolated (immediate fault clearing is not required at this location because no fuse saving is required for the lateral recloser),
3. R_{LAT} closes,
4. Feeder recloser trips instantaneously,
5. Feeder recloser closes,
6. R_{DG} opens to isolate DG and R_{LAT} trips on the delayed curve to lock out,
7. If the fault is not isolated due to primary OCPD failure,
8. Feeder recloser trips on the delayed curve and locks out,
9. Whole system is de-energized and fault is isolated.

If the fault is on the main feeder:

1. Lateral recloser (R_{LAT}) trips instantaneously,
2. Feeder recloser trips instantaneously,
3. R_{LAT} closes,
4. Feeder recloser closes,
5. Fault is isolated.
6. If the fault is not isolated due to primary OCPD failure,

7. R_{DG} trips open to isolate the DG; no current flows through R_{LAT} since fault is on the main,
8. Feeder recloser trips on the delayed curve and locks out,
9. Whole system is de-energized and fault is isolated.

Again, if coordination is established between the added MFRs and the feeder recloser, then coordination will be achieved for the downstream fuses since the fuses were already coordinated with the feeder recloser. The source-load procedure used to coordinate the negative-sequence overcurrent elements with the feeder recloser (since the negative sequence element was placed near the DG) is described as follows:

1. Establish coordination between the phase and ground overcurrent elements using standard methods and coordination philosophies. (This process was already established in the existing OCPDs, the recloser, and the fuses.)
2. Start at the most upline negative sequence overcurrent element (51Q of the interconnection relay [R_{DG}]) and identify the phase overcurrent element of the next downline device, R_{LAT}.
3. Derive the minimum pickup and curve settings for the 51Q element in terms of $3I_2$ to coordinate with R_{LAT} while maintaining appropriate coordination margins. The cold inrush current considerations can be ignored when deriving the settings.
4. In case the nominal branch current data on the feeder is not available, the minimum pickup setting of the 51Q element should not be lower than the minimum pickup value of the ground overcurrent 51N element. The negative sequence overcurrent is too low if the setting in terms of $3I_2$ is less than the minimum pickup of the 51N element in the device.

3.7. Summary

The new approach to upgrade the existing OCP scheme of radial distribution feeder involved protection changes at the lateral with the DG. The protection changes provided incorporate protection at the system, interconnection, and DG unit levels. Using the composite and source-load coordination approach, the added devices were coordinated with the feeder recloser such that the existing devices on the feeder retained their settings. The settings for the added protective devices were determined for DG sizes up to the maximum penetration level and provided in the Appendix.

CHAPTER IV

RADIAL TEST FEEDERS USED IN STUDIES

4.1. Introduction

In order to validate and generalize the performance of the new approach, physical radial distribution feeders with an existing overcurrent protection scheme are required. Since such requirements were not physically available, a feasible choice was to model two Radial Test Feeders, add OCPDs to the feeder, along with the DG model then simulate various case studies. The Radial Test Feeders were modeled using DIgSILENT Powerfactory software version 13.2 [44]. The model for the appropriate TCC based OCPDs and the salient-pole synchronous generators were customized into the software. The OCPDs TCC values were obtained from the manufacturer's database in DIgSILENT and PSS/ADEPT, while the DG model was obtained from [17], [45]. The case studies involved the steady state and transient studies. Table 1 provides the parameters of the four synchronous generator ratings used to model the various DG sizes. The first column gives the name and unit of the generator parameters. The remaining columns show the generator parameter for each of the four generators. The subtransient quadrature reactance (x_q'') and the stator resistance (R_s) were not available in [45] for the 3.85MVA DG. Therefore, the two parameters were duplicated from the 2.5MVA DG. Results of the OCPD operation during faults were obtained through Electromagnetic transient simulation (EMTP) in DIgSILENT. The simulation consisted of an instantaneous time interval with a 1ms time step.

Table 1 Synchronous Generator Parameters

Transient Parameters	Generator Size (MVA)			
	0.406	1.075	2.5	3.85
V_n (V_{rms})	460	460	460	4160
Freq (hz)	60	60	60	60
T_d' (s)	0.080	0.185	0.330	3.300
T_d'' (s)	0.019	0.025	0.030	0.015
T_q'' (s)	0.019	0.025	0.030	0.050
x_d (pu)	2.900	2.890	2.400	2.320
x_d' (pu)	0.170	0.250	0.200	0.260
x_d''(pu)	0.120	0.170	0.150	0.160
x_q (pu)	2.440	1.720	1.770	1.180
x_q'' (pu)	0.340	0.290	0.260	0.260*
x_l (pu)	0.070	0.080	0.050	0.150
H (s)	0.194	0.322	0.347	1.010
R_s (pu)	0.003	0.003	0.003	0.003

4.2. Radial Test Feeder Models

4.2.1. IEEE 34 Node Radial Test Feeder

The IEEE 34 Node Radial Test Feeder is shown in Fig. 14. The components found on the Radial Test Feeder include capacitor banks, a step-down transformer, and the defined main feeder and laterals. There are a total of six 1-phase laterals, labeled 1, 2, 3, 4, 6, and 8; and four 3-phase laterals labeled 5, 7, 8, and 11. Laterals 5 and 7 are completely 3-phase lines, while lateral 8 combines a 3-phase line with a 1-phase line. Also, laterals 5 and 7 are of special interest due to their unique characteristics with respect to the main feeder. Lateral 5, for example, operates on a different voltage level, 4.16kV, and produces an undervoltage at its farthest node (node 890). The reason for the undervoltage is mostly due to the high magnitude of the constant-current spot load and the line losses along the length of the lateral. Lateral 7, on the other hand, is the only location with reactive compensation as given in [23]. The two capacitor banks identified on the feeder are the extensions of nodes 844 and 848, respectively. Finally, Lateral

11, defined as the line section from node 836–840, shares similar characteristics to the main feeder. However, using some engineering judgment mentioned in [1, 6, 46], the line section is considered a lateral because of its location and proximity to the other 3-phase laterals with components. This situation implies that in the event of a fault at that location (836-840), only that section will be isolated. Consequently, the feeder's reliability will be enhanced.

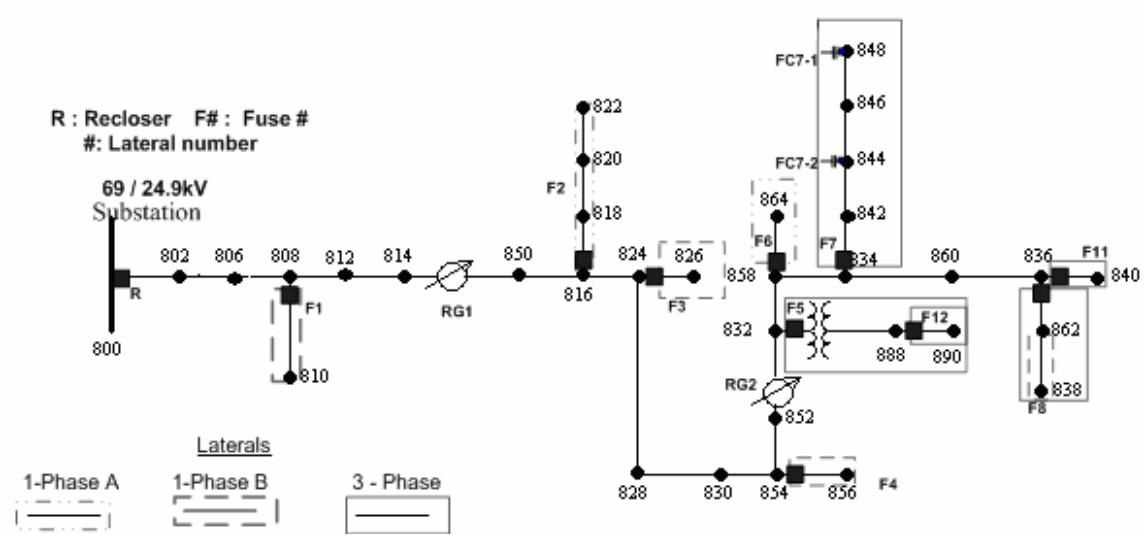

Fig. 14 IEEE 34 Node Radial Test Feeder (Adopted from [23])

4.2.2. IEEE 123 Node Radial Test Feeder

The IEEE 123 Node Radial Test Feeder shown in Fig. 15 operates at a 4.16 kV level. The feeder consists of two transformers, the substation transformer and a step-down transformer (XFM-1). A total of eleven switches, six of which are normally closed (NC) labeled as sw # and the remaining five are normally open, provide the feeder with different configuration options. The switches in the NO configuration include those near locations 451, 350, 251, and 195, 151 and 94. These switches are not required for the feeder's default operation, thus are disabled during the studies in this work. The normally closed switches include those switches connecting nodes 150-149, 18-135, 13-152, 60-160, 97-197, and 61-610. This feeder is mostly characterized

by overhead lines of 1-phase, 2-phase and 3-phase types. The feeder has an underground line segment that operates at the 4.16kV voltage level and consists of 3-phase lines.

In a similar fashion to the IEEE 34 Node, the IEEE 123 Node Radial Test Feeder consists of unbalanced loading with all combinations of load types (PQ, constant I, constant Z). However, all the loads are spot loads (totaling eighty-five in number) are located at the various nodes on the feeder. The total load is 4.023 MVA at a power factor of 0.8761. The feeder consists of four step-type voltage regulators, RG1-RG4 shown in Fig. 15. There are a total of four shunt capacitor banks consisting of one 3-phase shunt capacitor bank and three 1-phase shunt capacitor banks. These capacitor banks are connected in a wye-wye configuration. The 3-phase shunt capacitor bank is rated at 200kVar per phase and located at node 83 on the feeder. The 1-phase shunt capacitor banks are each rated at 50kVar located at nodes 88, 90, and 92 respectively.

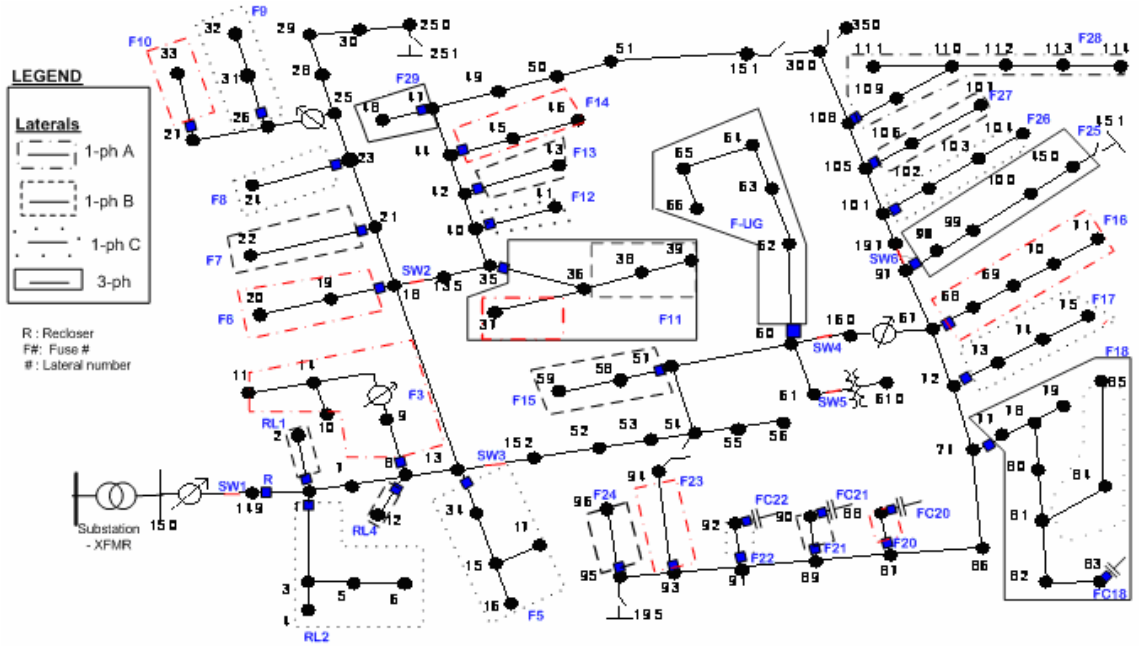

Fig. 15 IEEE 123 Node Radial Test Feeder (Adopted from [23])

A total number of 139 nodes is initially required to model the feeder in DIgSILENT. However, the number of nodes exceeded the software's requirement (120 nodes per active project). Therefore some nodes connected in series on the feeder were removed to satisfy the software's requirement. The assumptions made to construct the approximate model included modifying the old values of the test feeder's lines and loads, Z_{old} (mi) and P_{old} (KVA), to the new values (Z_{new} and P_{new}) . The voltage square rule described in [1] was used in the approximation of the feeder model. Equation (4.1) provides the mathematical relationship between the power and load ratio to the voltage V_{LN} ratio for the line in question.

$$\frac{P_{old}}{P_{new}} \times \frac{Z_{old}}{Z_{new}} = \left(\frac{V_{LNold}}{V_{LNnew}} \right)^2 \tag{4.1}$$

All the combined loads, totaling 49 in number, are indicated in Table 32 of Appendix B. The combined loads are assumed as constant PQ type connected in a wye configuration.

4.3. Preparation of Radial Test Feeders for Simulation Studies

In order to prepare the radial test feeders for further studies, the steady state results of the modeled feeders were compared with the IEEE's published results [23]. The load flow results include the node voltage, branch current and total power loss results. The short circuit studies involve the shunt fault current at the system nodes. Table 2, Table 3, and Table 4 show the comparison of the node voltage results of the IEEE 34 Node Radial Test Feeder modeled in DIgSILENT with the IEEE reference results. The first column of Table 2 provides the node on the feeder while the remaining columns compare the results of the voltage magnitude and angle values between the customized feeder and the IEEE reference. The asterisked section of the last column for node 800 implies that division by the base value (0.00) for that node was not possible. Table 3 and Table 4 provide similar results for phases B and C respectively. Using the

IEEE reference results as the base result, the error (pu) for each node voltage magnitude was less than 0.05 pu or 5%. The error margin for the voltage angle between the modeled feeder and the IEEE reference was higher especially the angles for phase A.

Similarly Table 5, Table 6, and Table 7 provide the comparison of the node voltage results of the IEEE 123 Node Radial Test Feeder modeled in DIgSILENT with the IEEE reference results. The first column of Table 5 provide the node on the feeder while the remaining columns compares the phase A voltage magnitude and angle results of the customized feeder and the IEEE reference. Table 6 and Table 7 provide similar results for phases B and C respectively.

Table 2 IEEE 34 Node Voltage - Phase A

PHASE A:						
	Magnitude(pu)			Angle(deg)		
Node	DIgSILENT	IEEE Ref	Error (p.u)	DIgSILENT	IEEE Ref	Error (p.u)
800	1.052	1.050	0.002	-4.089	0.000	**
802	1.050	1.048	0.002	-4.139	-0.050	81.774
806	1.048	1.046	0.002	-4.173	-0.080	51.162
808	1.032	1.014	0.018	-4.504	-0.750	5.006
812	0.996	0.976	0.021	-5.324	-1.570	2.391
814	0.968	0.947	0.022	-6.003	-2.260	1.656
RG10	1.032	1.018	0.014	-6.003	-2.260	1.656
816	1.032	1.017	0.014	-6.009	-2.260	1.659
818	1.031	1.016	0.015	-6.016	-2.270	1.650
820	1.009	0.993	0.017	-6.182	-2.320	1.664
822	1.007	0.990	0.017	-6.200	-2.330	1.661
824	1.024	1.008	0.016	-6.132	-2.370	1.587
828	1.023	1.007	0.016	-6.144	-2.380	1.581
830	1.008	0.989	0.018	-6.422	-2.630	1.442
832	1.046	1.036	0.009	-6.936	-3.110	1.230
834	1.041	1.031	0.010	-7.067	-3.240	1.181
836	1.041	1.030	0.010	-7.059	-3.230	1.185
840	1.041	1.030	0.010	-7.059	-3.230	1.185
842	1.041	1.031	0.010	-7.069	-3.250	1.175
844	1.041	1.031	0.010	-7.091	-3.270	1.168
846	1.041	1.031	0.010	-7.129	-3.320	1.147
848	1.041	1.031	0.010	-7.135	-3.320	1.149
850	1.032	1.018	0.014	-6.003	-2.260	1.656

Table 2 continued

PHASE A:						
	Magnitude(pu)			Angle(deg)		
Node	DIgSILENT	IEEE Ref	Error (p.u)	DIgSILENT	IEEE Ref	Error (p.u)
852	0.980	0.958	0.023	-6.936	-3.110	1.230
RG11	1.046	1.036	0.009	-6.936	-3.110	1.230
854	1.007	0.989	0.018	-6.429	-2.640	1.435
858	1.044	1.034	0.010	-6.996	-3.170	1.207
860	1.041	1.031	0.010	-7.062	-3.240	1.180
862	1.041	1.030	0.010	-7.059	-3.230	1.185
864	1.044	1.034	0.010	-6.996	-3.170	1.207
888	1.006	1.000	0.007	-8.560	-4.640	0.845
890	0.925	0.917	0.009	-9.435	-5.190	0.818

Table 3 IEEE 34 Node Voltage - Phase B

PHASE B:						
	Magnitude(pu)			Angle(deg)		
Node	DIgSILENT	IEEE Ref	Error (p.u)	DIgSILENT	IEEE Ref	Error (p.u)
800	1.054	1.050	0.004	-123.617	-120.000	0.030
802	1.053	1.048	0.004	-123.685	-120.070	0.030
806	1.052	1.047	0.004	-123.730	-120.110	0.030
808	1.043	1.030	0.013	-124.145	-120.950	0.026
810	1.043	1.029	0.013	-124.146	-120.950	0.026
812	1.024	1.010	0.014	-125.091	-121.920	0.026
814	1.009	0.995	0.015	-125.852	-122.700	0.026
RG10	1.028	1.026	0.003	-125.852	-122.700	0.026
816	1.028	1.025	0.003	-125.859	-122.710	0.026
824	1.020	1.016	0.004	-126.095	-122.940	0.026
826	1.020	1.016	0.004	-126.097	-122.940	0.026
828	1.019	1.015	0.004	-126.113	-122.950	0.026
830	1.004	0.998	0.006	-126.557	-123.390	0.026
832	1.043	1.035	0.008	-127.358	-124.180	0.026
834	1.039	1.030	0.009	-127.565	-124.390	0.026
836	1.038	1.029	0.009	-127.570	-124.390	0.026

Table 3 continued

PHASE B:						
	Magnitude(pu)			Angle(deg)		
Node	DIgSILENT	IEEE Ref	Error (p.u)	DIgSILENT	IEEE Ref	Error (p.u)
838	1.038	1.029	0.009	-127.573	-124.390	0.026
840	1.038	1.029	0.009	-127.570	-124.390	0.026
842	1.039	1.029	0.009	-127.567	-124.390	0.026
844	1.039	1.029	0.009	-127.591	-124.420	0.025
846	1.039	1.029	0.009	-127.634	-124.460	0.026
848	1.039	1.029	0.009	-127.640	-124.470	0.025
850	1.028	1.026	0.003	-125.852	-122.700	0.026
852	0.978	0.968	0.010	-127.358	-124.180	0.026
RG11	1.043	1.035	0.008	-127.358	-124.180	0.026
854	1.004	0.998	0.006	-126.568	-123.400	0.026
856	1.004	0.998	0.006	-126.575	-123.410	0.026
858	1.041	1.032	0.009	-127.453	-124.280	0.026
860	1.038	1.029	0.009	-127.567	-124.390	0.026
862	1.038	1.029	0.009	-127.570	-124.390	0.026
888	1.004	0.998	0.006	-129.000	-125.730	0.026
890	0.932	0.924	0.009	-130.299	-126.780	0.028

Table 4 IEEE 34 Node Voltage - Phase C

PHASE C:						
	Magnitude (pu)			Angle (deg)		
Node	DIgSILENT	IEEE Ref	Error (p.u)	DIgSILENT	IEEE Ref	Error (p.u)
800	1.054	1.050	0.004	116.641	120.000	-0.028
802	1.053	1.048	0.004	116.591	119.950	-0.028
806	1.052	1.047	0.004	116.558	119.920	-0.028
808	1.043	1.029	0.014	116.258	119.300	-0.025
812	1.021	1.007	0.014	115.554	118.590	-0.026
814	1.004	0.989	0.015	114.988	118.010	-0.026
RG10	1.024	1.020	0.003	114.988	118.010	-0.026
816	1.023	1.020	0.003	114.983	118.010	-0.026
824	1.016	1.012	0.004	114.736	117.760	-0.026
828	1.015	1.011	0.005	114.716	117.750	-0.026
830	1.001	0.994	0.007	114.218	117.250	-0.026
832	1.046	1.036	0.010	113.302	116.330	-0.026
834	1.042	1.031	0.011	113.076	116.090	-0.026
836	1.042	1.031	0.011	113.073	116.090	-0.026
840	1.042	1.031	0.011	113.074	116.090	-0.026
842	1.042	1.031	0.011	113.073	116.090	-0.026
844	1.042	1.031	0.011	113.048	116.060	-0.026

Table 4 continued

PHASE C:						
Magnitude (pu)				Angle (deg)		
Node	DIgSILENT	IEEE Ref	Error (p.u)	DIgSILENT	IEEE Ref	Error (p.u)
846	1.043	1.031	0.011	113.003	116.010	-0.026
848	1.043	1.031	0.011	112.997	116.000	-0.026
850	1.024	1.020	0.003	114.988	118.010	-0.026
852	0.974	0.964	0.011	113.302	116.330	-0.026
RG11	1.046	1.036	0.010	113.303	116.330	-0.026
854	1.000	0.993	0.007	114.205	117.240	-0.026
858	1.044	1.034	0.010	113.199	116.220	-0.026
860	1.042	1.031	0.011	113.073	116.090	-0.026
862	1.042	1.031	0.011	113.073	116.090	-0.026
888	1.007	1.000	0.007	111.689	114.820	-0.027
890	0.924	0.918	0.007	110.594	113.980	-0.030

Table 5 IEEE 123 Node Voltage - Phase A

PHASE A:						
Magnitude (pu)				Angle (deg)		
Node	DIgSILENT	IEEE Ref	Error (pu)	DIgSILENT	IEEE 123	Error (pu)
1	1.026	1.031	0.005	-0.628	-0.660	-0.048
10	1.010	1.006	0.004	-1.405	-1.500	-0.063
101	1.031	1.034	-0.003	-3.310	-3.860	-0.143
105	1.029	1.032	-0.003	-3.364	-3.900	-0.137
108	1.028	1.031	-0.003	-3.438	-3.970	-0.134
109	1.026	1.027	0.000	-3.509	-4.050	-0.134
11	1.010	1.006	0.004	-1.410	-1.510	-0.066
110	1.026	1.025	0.001	-3.546	-4.090	-0.133
111	1.025	1.024	0.001	-3.557	-4.100	-0.133
114	1.025	1.022	0.003	-3.570	-4.150	-0.140
13	1.002	1.008	-0.005	-1.764	-1.870	-0.057
135	0.994	0.999	-0.004	-2.106	-2.290	-0.080
14	1.010	1.006	0.004	-1.401	-1.500	-0.066
149	1.037	1.044	-0.006	0.028	-0.020	-2.415
150	1.000	1.000	0.000			
151	0.987	0.990	-0.003	-2.298	-2.530	-0.092
152	1.002	1.008	-0.005	-1.764	-1.880	-0.062
160	0.986	0.988	-0.002	-2.973	-3.520	-0.155
18	0.994	0.999	-0.004	-2.106	-2.290	-0.080
197	1.032	1.035	-0.003	-3.262	-3.820	-0.146
20	0.994	0.997	-0.003	-2.130	-2.330	-0.086
21	0.994	0.998	-0.005	-2.137	-2.340	-0.087
23	0.993	0.998	-0.005	-2.165	-2.390	-0.094

Table 5 continued

PHASE A:							
	Magnitude (pu)				Angle (deg)		
Node	DIgSILENT	IEEE 123	Error (pu)		DIgSILENT	IEEE 123	Error (pu)
25	0.992	0.997	**-0.005**		-2.197	-2.450	**-0.103**
26	0.992	0.997	**-0.005**		-2.202	-2.480	**-0.112**
27	0.991	0.997	**-0.005**		-2.206	-2.490	**-0.114**
28	0.992	0.997	**-0.005**		-2.218	-2.480	**-0.106**
29	0.992	0.997	**-0.005**		-2.233	-2.500	**-0.107**
30	0.992	0.997	**-0.005**		-2.233	-2.500	**-0.107**
33	0.991	0.995	**-0.005**		-2.211	-2.520	**-0.123**
35	0.992	0.996	**-0.004**		-2.176	-2.380	**-0.086**
36	0.992	0.995	**-0.003**		-2.177	-2.400	**-0.093**
37	0.992	0.994	**-0.002**		-2.177	-2.410	**-0.097**
40	0.991	0.995	**-0.004**		-2.212	-2.420	**-0.086**
42	0.989	0.993	**-0.004**		-2.248	-2.450	**-0.082**
44	0.988	0.992	**-0.004**		-2.276	-2.480	**-0.082**
450	1.031	1.035	**-0.003**		-3.283	-3.820	**-0.141**
46	0.988	0.991	**-0.003**		-2.285	-2.500	**-0.086**
47	0.987	0.991	**-0.004**		-2.297	-2.500	**-0.081**
48	0.987	0.991	**-0.004**		-2.306	-2.510	**-0.081**
51	0.987	0.990	**-0.003**		-2.298	-2.530	**-0.092**
54	0.997	0.998	**0.000**		-1.986	-2.530	**-0.215**
56	0.997	0.997	**0.000**		-1.989	-2.530	**-0.214**
57	0.994	0.995	**-0.001**		-2.294	-2.830	**-0.189**
60	0.986	0.988	**-0.002**		-2.973	-3.510	**-0.153**
61-A	0.986	0.988	**-0.002**		-2.973	-3.510	**-0.153**
61-B	0.986	0.988	**-0.002**		-2.973	-3.510	**-0.153**
610	0.986	0.988	**-0.002**		-2.973	-3.510	**-0.153**
66	0.986	0.986	**0.000**		-2.984	-3.510	**-0.150**
67	1.033	1.036	**-0.003**		-3.206	-3.770	**-0.150**
7	1.017	1.022	**-0.005**		-1.066	-1.130	**-0.057**
71	1.032	1.030	**0.002**		-3.243	-3.860	**-0.160**
72	1.033	1.036	**-0.003**		-3.287	-3.860	**-0.149**
76	1.032	1.036	**-0.004**		-3.347	-3.920	**-0.146**
77	1.032	1.037	**-0.005**		-3.400	-3.990	**-0.148**
78	1.032	1.037	**-0.005**		-3.414	-4.010	**-0.149**
79	1.031	1.037	**-0.005**		-3.423	-4.020	**-0.148**
8	1.011	1.016	**-0.005**		-1.357	-1.440	**-0.058**
80	1.032	1.039	**-0.007**		-3.465	-4.070	**-0.149**
81	1.033	1.042	**-0.008**		-3.522	-4.140	**-0.149**
83	1.033	1.044	**-0.010**		-3.538	-4.200	**-0.158**
86	1.032	1.035	**-0.003**		-3.407	-3.950	**-0.137**
87	1.032	1.034	**-0.002**		-3.449	-3.970	**-0.131**
88	1.033	1.034	**-0.001**		-3.462	-4.000	**-0.135**
89	1.032	1.034	**-0.002**		-3.454	-3.960	**-0.128**
9	1.010	1.014	**-0.004**		-1.377	-1.470	**-0.063**
91	1.032	1.034	**-0.002**		-3.462	-3.960	**-0.126**
93	1.032	1.033	**-0.001**		-3.470	-3.970	**-0.126**
94	1.032	1.033	**-0.001**		-3.480	-3.980	**-0.126**
97	1.032	1.035	**-0.003**		-3.262	-3.820	**-0.146**
RG1	1.037	1.044	**-0.006**		0.028	0.000	
RG2-L14	1.010	1.008	**0.002**		-1.377	-1.470	**-0.063**
RG3-L26	0.992	0.997	**-0.005**		-2.197	-2.450	**-0.103**

Table 6 IEEE 123 Node Voltage - Phase B

PHASE B:						
	Magnitude (pu)			Angle (deg)		
Node	DIgSILENT	IEEE Ref	Error (pu)	DIgSILENT	IEEE Ref	Error (pu)
1	1.045	1.041	0.004	-118.836	-120.330	-0.012
101	1.032	1.030	0.002	-119.852	-122.220	-0.019
105	1.032	1.030	0.002	-119.879	-122.270	-0.020
107	1.032	1.028	0.004	-119.907	-122.320	-0.020
108	1.033	1.031	0.002	-119.879	-122.280	-0.020
12	1.041	1.038	0.003	-119.113	-120.740	-0.013
13	1.039	1.036	0.002	-119.267	-120.970	-0.014
135	1.033	1.032	0.001	-119.387	-121.230	-0.015
149	1.052	1.044	0.008	-118.681	-120.020	-0.011
150	1.014	1.000	0.014	-118.664	-120.000	-0.011
151	1.027	1.025	0.002	-119.587	-121.470	-0.015
152	1.039	1.036	0.002	-119.267	-120.980	-0.014
160	1.028	1.026	0.003	-119.697	-122.010	-0.019
18	1.033	1.032	0.001	-119.387	-121.220	-0.015
197	1.032	1.031	0.002	-119.834	-122.210	-0.019
2	1.045	1.041	0.004	-118.839	-120.330	-0.012
21	1.033	1.032	0.001	-119.387	-121.220	-0.015
22	1.032	1.031	0.002	-119.405	-121.250	-0.015
23	1.033	1.032	0.000	-119.376	-121.200	-0.015
25	1.033	1.033	0.000	-119.369	-121.200	-0.015
28	1.033	1.033	0.000	-119.365	-121.190	-0.015
29	1.033	1.033	-0.001	-119.359	-121.190	-0.015
30	1.033	1.033	-0.001	-119.350	-121.180	-0.015
35	1.031	1.029	0.001	-119.442	-121.310	-0.015
36	1.031	1.029	0.002	-119.442	-121.360	-0.016
39	1.031	1.028	0.003	-119.441	-121.380	-0.016
40	1.030	1.028	0.001	-119.484	-121.360	-0.015
42	1.029	1.027	0.001	-119.528	-121.410	-0.016
43	1.028	1.026	0.002	-119.545	-121.430	-0.016
44	1.028	1.026	0.001	-119.554	-121.440	-0.016
450	1.032	1.029	0.002	-119.860	-122.210	-0.019
47	1.027	1.025	0.001	-119.586	-121.470	-0.016
48	1.026	1.025	0.001	-119.593	-121.470	-0.015
51	1.027	1.025	0.002	-119.587	-121.470	-0.015
54	1.036	1.033	0.002	-119.281	-121.410	-0.018
56	1.036	1.033	0.002	-119.284	-121.430	-0.018
57	1.033	1.031	0.003	-119.425	-121.610	-0.018

Table 6 continued

PHASE B:						
	Magnitude (pu)			Angle (deg)		
Node	DIgSILENT	IEEE 123	% Error	DIgSILENT	IEEE 123	% Error
59	1.033	1.030	0.003	-119.433	-121.630	-0.018
60	1.028	1.026	0.003	-119.697	-122.000	-0.019
61-A	1.028	1.026	0.003	-119.697	-122.000	-0.019
61-B	1.028	1.026	0.003	-119.697	-122.000	-0.019
610	1.028	1.026	0.003	-119.697	-122.000	-0.019
66	1.027	1.022	0.006	-119.654	-121.870	-0.018
67	1.033	1.031	0.002	-119.807	-122.190	-0.020
7	1.043	1.040	0.003	-118.999	-120.570	-0.013
72	1.031	1.030	0.001	-119.863	-122.290	-0.020
76	1.030	1.030	0.001	-119.911	-122.380	-0.020
77	1.031	1.031	0.000	-119.950	-122.460	-0.020
78	1.031	1.031	0.000	-119.955	-122.480	-0.021
79	1.031	1.031	0.000	-119.956	-122.480	-0.021
8	1.041	1.038	0.003	-119.109	-120.740	-0.014
80	1.032	1.033	-0.001	-119.974	-122.540	-0.021
81	1.033	1.035	-0.002	-119.969	-122.570	-0.021
83	1.033	1.038	-0.004	-119.982	-122.630	-0.022
86	1.028	1.028	0.000	-119.976	-122.550	-0.021
87	1.027	1.027	0.000	-120.007	-122.630	-0.021
89	1.026	1.027	-0.001	-120.031	-122.680	-0.022
90	1.026	1.027	-0.001	-120.039	-122.720	-0.022
91	1.026	1.027	0.000	-120.040	-122.690	-0.022
93	1.026	1.027	0.000	-120.051	-122.710	-0.022
95	1.026	1.026	0.000	-120.066	-122.730	-0.022
96	1.026	1.026	0.000	-120.069	-122.730	-0.022
97	1.032	1.031	0.002	-119.834	-122.210	-0.019
RG1	1.052	1.044	0.008	-118.681	-120.000	-0.011
RG4-67	1.035	1.032	0.003	-119.697	-122.010	-0.019

Table 7 IEEE 123 Node Voltage - Phase C

PHASE C:						
	Magnitude (pu)			Angle (deg)		
Node	DIgSILENT	IEEE Ref	Error (pu)	DIgSILENT	IEEE Ref	Error (pu)
1	1.035	1.035	0.000	120.090	119.600	0.004
101	1.013	1.033	-0.020	118.606	117.590	0.009

Table 7 continued

PHASE C:							
	Magnitude (pu)				Angle (deg)		
Node	DIgSILENT	IEEE Ref	Error (pu)		DIgSILENT	IEEE Ref	Error (pu)
104	1.012	1.028	-0.016		118.561	117.490	0.009
105	1.013	1.034	-0.020		118.633	117.610	0.009
108	1.012	1.033	-0.020		118.663	117.650	0.009
13	1.014	1.020	-0.006		119.370	118.900	0.004
135	1.008	1.012	-0.004		119.140	118.830	0.003
149	1.046	1.044	0.002		120.424	119.980	0.004
15	1.013	1.018	-0.005		119.351	118.870	0.004
150	1.008	1.000	0.008		120.435	120.000	0.004
151	1.003	1.007	-0.004		118.888	118.580	0.003
152	1.014	1.020	-0.006		119.370	118.890	0.004
160	0.988	1.005	-0.017		118.750	117.750	0.008
17	1.013	1.018	-0.005		119.331	118.860	0.004
18	1.008	1.012	-0.004		119.140	118.830	0.003
197	1.014	1.034	-0.020		118.615	117.590	0.009
21	1.007	1.011	-0.004		119.099	118.810	0.002
23	1.007	1.010	-0.003		119.065	118.790	0.002
24	1.006	1.009	-0.002		119.045	118.770	0.002
25	1.006	1.009	-0.003		119.043	118.800	0.002
26	1.007	1.002	0.004		119.011	118.790	0.002
27	1.007	1.002	0.005		119.011	118.790	0.002
28	1.006	1.009	-0.003		119.038	118.800	0.002
29	1.006	1.008	-0.003		119.027	118.790	0.002
3	1.034	1.033	0.001		120.068	119.570	0.004
30	1.005	1.008	-0.003		118.998	118.770	0.002
32	1.007	1.001	0.005		118.995	118.770	0.002
34	1.014	1.019	-0.005		119.357	118.880	0.004
35	1.007	1.011	-0.004		119.063	118.770	0.002
4	1.034	1.033	0.002		120.061	119.560	0.004
40	1.006	1.010	-0.004		119.015	118.720	0.002
41	1.005	1.010	-0.004		119.009	118.710	0.003
42	1.005	1.009	-0.005		118.974	118.680	0.002

Table 7 continued

PHASE C:						
	Magnitude (pu)			Angle (deg)		
Node	DIgSILENT	IEEE 123	% Error	DIgSILENT	IEEE 123	% Error
450	1.013	1.033	-0.019	118.596	117.530	0.009
47	1.003	1.007	-0.005	118.893	118.610	0.002
48	1.003	1.007	-0.005	118.885	118.600	0.002
51	1.003	1.007	-0.004	118.888	118.580	0.003
54	1.008	1.014	-0.006	119.264	118.430	0.007
56	1.008	1.014	-0.006	119.261	118.430	0.007
57	1.002	1.011	-0.010	119.103	118.210	0.008
6	1.034	1.031	0.003	120.048	119.530	0.004
60	0.988	1.005	-0.017	118.750	117.760	0.008
61-A	0.988	1.005	-0.017	118.750	117.760	0.008
61-B	0.988	1.005	-0.017	118.750	117.760	0.008
610	0.988	1.005	-0.017	118.750	117.760	0.008
66	0.985	0.996	-0.010	118.758	117.700	0.009
67	1.015	1.035	-0.019	118.631	117.610	0.009
7	1.027	1.029	-0.002	119.828	119.350	0.004
72	1.013	1.034	-0.021	118.537	117.500	0.009
75	1.012	1.029	-0.017	118.500	117.400	0.009
76	1.012	1.035	-0.023	118.499	117.450	0.009
77	1.011	1.036	-0.024	118.468	117.370	0.009
78	1.011	1.036	-0.024	118.460	117.350	0.009
79	1.011	1.036	-0.024	118.466	117.360	0.009
8	1.022	1.025	-0.004	119.650	119.180	0.004
80	1.010	1.037	-0.025	118.408	117.240	0.010
81	1.010	1.037	-0.027	118.355	117.140	0.010
83	1.010	1.039	-0.028	118.340	117.070	0.011
85	1.009	1.034	-0.024	118.313	117.070	0.011
86	1.011	1.036	-0.025	118.449	117.420	0.009
87	1.010	1.037	-0.026	118.416	117.390	0.009
89	1.010	1.037	-0.027	118.408	117.380	0.009
91	1.010	1.038	-0.027	118.402	117.360	0.009
92	1.009	1.038	-0.027	118.391	117.310	0.009
93	1.010	1.038	-0.027	118.406	117.370	0.009
95	1.010	1.038	-0.027	118.407	117.370	0.009
97	1.014	1.034	-0.020	118.615	117.600	0.009
RG1	1.046	1.044	0.002	120.424	120.000	0.004
RG3-L26	1.007	1.003	0.004	119.043	118.800	0.002
RG4-67	1.019	1.037	-0.017	118.750	117.750	0.008

After comparing the results with the IEEE published reference, an overcurrent protection scheme with a fuse-saving philosophy was provided for the Radial Test Feeder as shown in Fig. 16. The OCP scheme included OCPDs, recloser and fuses. The recloser was added to the main while fuses were added to the laterals and the in-line components, capacitor banks and step-down transformer. Each fuse's protection zone is identified in Fig. 16 as the lateral on which the fuse is placed. The recloser's protection zone is the main. A similar approach was provided for the IEEE 123 Node Radial Test Feeder as shown in Fig. 17. In addition to the feeder recloser in Fig. 17, another recloser was used on lateral 1 and lateral 4 of the feeder because no fuse was available in the protection database that satisfied the selectivity criteria for the maximum fault on both laterals. The possible locations for DG placement are also provided in Fig. 16 and Fig. 17 in addition to the location of the overcurrent protective devices. These locations are numerically labeled and shown in the legend placed on both illustrations.

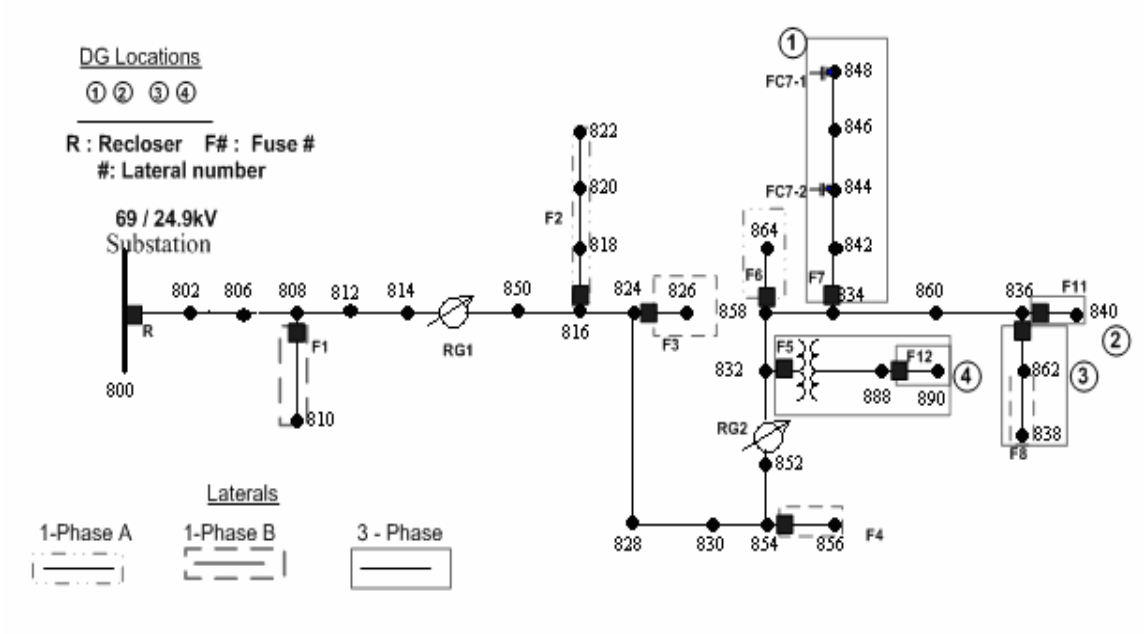

Fig. 16 IEEE 34 Node Radial Test Feeder with OCPDs and Possible DG Locations

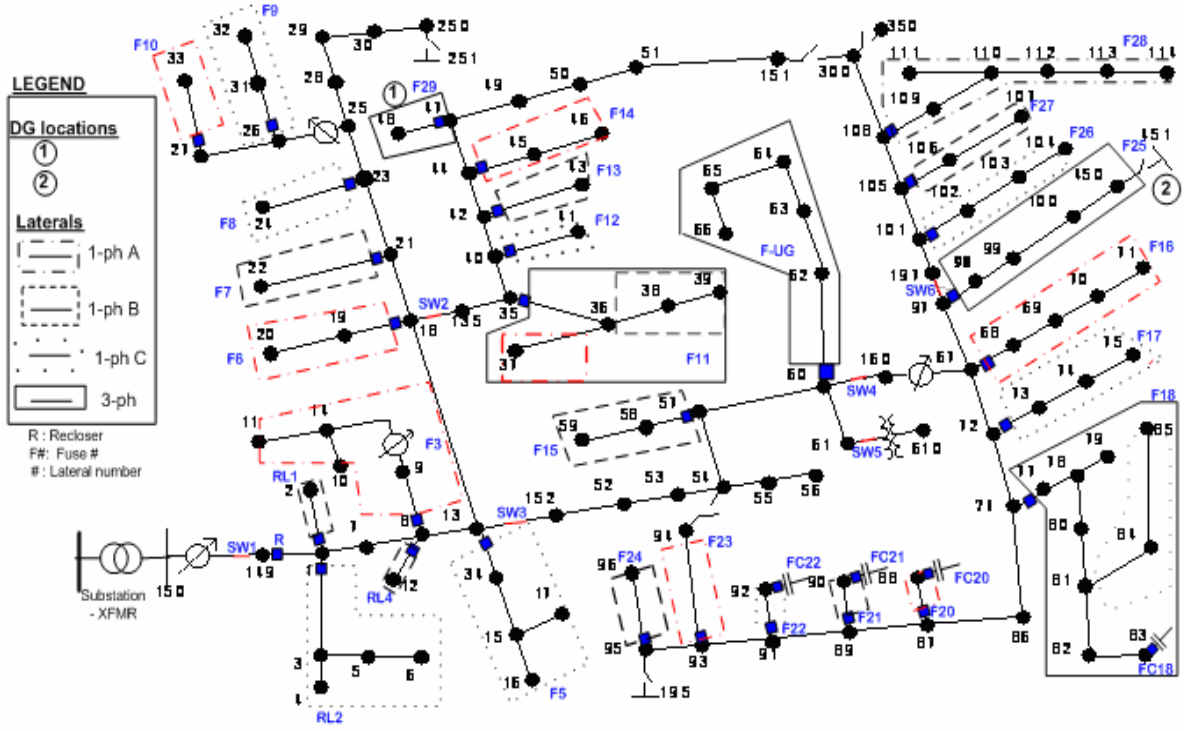

Fig. 17 IEEE 123 Node Radial Test Feeder with OCPDs (Adopted from [23])

4.4. Summary

In addition to the synchronous generator model for the DG, two radial test feeders, the IEEE 34 Node Radial Test Feeder and the IEEE 123 Radial Test Feeder were modeled in DIgSILENT as test beds for the thesis work. The steady state and transient simulation studies were conducted on both feeders. The steady state studies included load flow, short circuit studies to validate the base case results of the two feeders with the existing reference. The next chapter discusses the simulation studies conducted on both radial test feeders when DG is placed at strategic locations on the feeders.

CHAPTER V

SIMULATION STUDIES

5.1. Introduction

The transient simulation studies involved staging a temporary and permanent fault on the feeder to determine the impact of DG on the existing fuse saving based OCP scheme during the fault. The fault was placed at several locations on the feeder to include downstream of the laterals and on the main. In the transient simulation procedure, all the system conditions were initialized starting at –0.05s. The temporary fault duration was 5 cycles (assuming a short duration for the fault) or 10 cycles (assuming a longer duration for the fault) [4], [47]. The new approach was applied to the existing OCP scheme of both feeders to mitigate the three OCP issues which were identified.

Prior to adding DG to the feeder, the recloser and the fuse in the existing OCP scheme were coordinated and fuse saving was maintained. After DG was added to the feeder, coordination no longer held for some fuses. The next sections discuss the six main cases that were studied where each case corresponded to a potential DG location. Cases 1 through 4 involved the four DG locations on the IEEE 34 Node Radial Test Feeder while Cases 5 and 6 involved the IEEE 123 Node Radial Test Feeder. The cases provided results of the recloser and fuse operation prior to the applying the approach and after the approach was applied to the existing scheme.

5.2. Simulation Cases on the IEEE 34 Node Radial Test Feeder

Exhaustive studies were conducted on the IEEE 34 Node Radial Test Feeder to validate the performance of the new approach to mitigate the fuse misoperation, fuse fatigue and nuisance fuse blowing issues that were determined. The case studies involved the four DG

locations on the feeder illustrated in Fig. 16. For each case study, the minimum and maximum fault types (temporary and permanent) were staged on the feeder. Again, in each of the case study, a single DG (up to 2.5 MVA) was interconnected at the remote end of the 3-phase laterals located on the feeder after which the OCP issues were identified. The next subsections discuss the studies performed on the IEEE 34 Node Radial Test Feeder.

5.2.1. Case 1

This case described how the DG impacted the existing OCP scheme when the DG was placed at location 1 of the IEEE 34 Node Radial Test Feeder in Fig. 16. The DG location corresponded to the remote end of lateral 11, node 840.

In one example which typifies one of the worst case scenarios, a maximum (temporary and permanent L-L-L-G) fault was placed downstream of the three individual fuses (F7) on lateral 7 with a DG (sized at 2.5 MVA) connected to node 840. All the three individual fuses on the lateral underwent nuisance fuse blowing during the L-L-L-G fault. Fig. 18 illustrates a nuisance fuse blowing issue that developed as a result of the scenario described. In this situation, the fuse protecting phase B of the 3-phase lateral was the first to blow at 0.052s. As observed, the feeder recloser (denoted by R in the case studies) failed to operate to give the fault a chance to clear before the fuse blew. Therefore, the fuse saving philosophy adopted for the recloser-fuse coordination was lost during the 10 cycle fault duration. Consequently, an unwarranted permanent outage evolved during the temporary fault. One reason for the feeder recloser's failure to operate was due to the redistributed fault current between the DG and the substation which caused the fault current magnitude through the feeder recloser (which is near the substation) to decrease. The vertical axis in Fig. 18 gives the OCPD status ("0" for open and "1" for close) and the horizontal axis provides the corresponding operating time in seconds. As shown, the recloser status remained at 1 during the simulation period which indicated that the

recloser remained closed during the fault. On the other hand, the fuse's status changed from 1 to 0 at 0.052s, indicating a fuse blowing operation during the fault period.

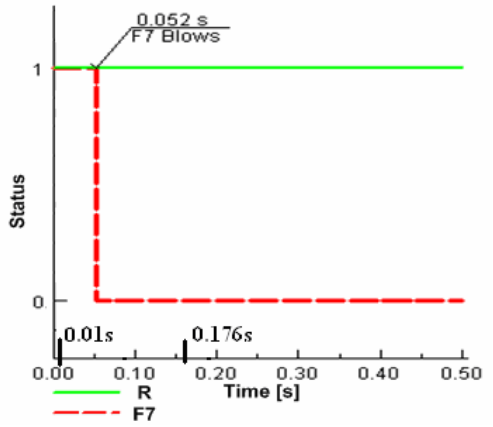

Fig. 18 Case 1: Nuisance Fuse Blowing before Applying the New Approach

Fig. 19 illustrates the current through the fuse during the fault and the horizontal axis corresponds to the simulation duration in seconds. As shown, the current became zero during the 10 cycle fault duration.

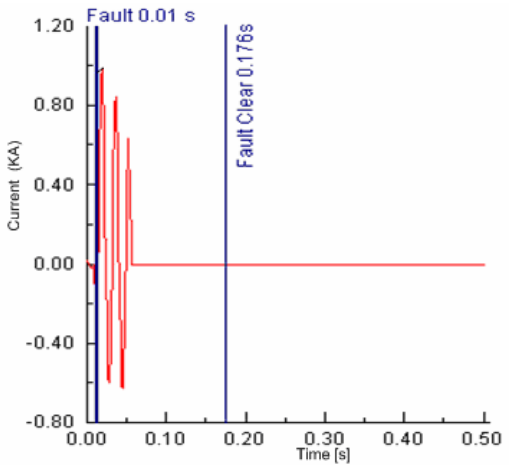

Fig. 19 Case 1: Fault Current through Fuse before Applying the New Approach

Fig. 20 displays the operation of the feeder recloser, the lateral recloser (R_{Lat}), and fuse (F7) after applying the new approach to the existing OCP scheme to mitigate the nuisance fuse blowing issue illustrated in Fig. 18. The vertical axis in Fig. 20 gives the OCPD status ("0" for open and "1" for close) and the horizontal axis corresponds to the duration of the simulation time in seconds. Again, the duration for the simulation was 0.5s. As the fault was initiated at 0.01seconds, the lateral recloser and the feeder recloser both operated to de-ionize the fault arc. R_{Lat} opened at 0.031s and reclosed at 0.163s. R opened at 0.081s and reclosed ten cycles later at 0.247s. As shown, the status of F7 did not change from 1 to 0 which meant that fuse did not blow during the temporary fault duration. Therefore the nuisance fuse blowing issue was mitigated. Consequently, an unwarranted permanent outage was prevented and the continuity of service was maintained at the lateral protected by the fuse as illustrated in Fig. 21.

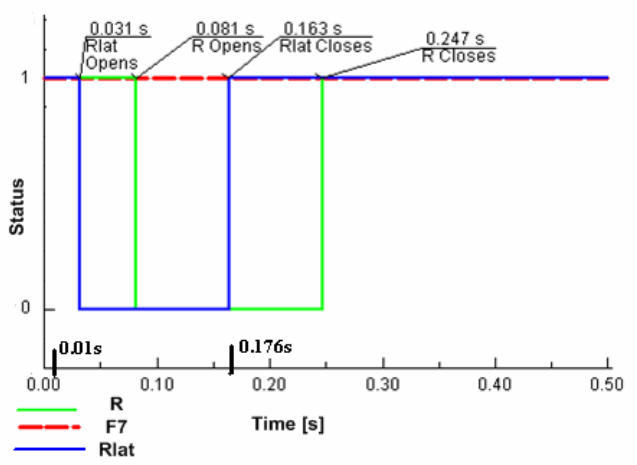

Fig. 20 Case 1: Nuisance Fuse Blowing Mitigated after Applying the New Approach

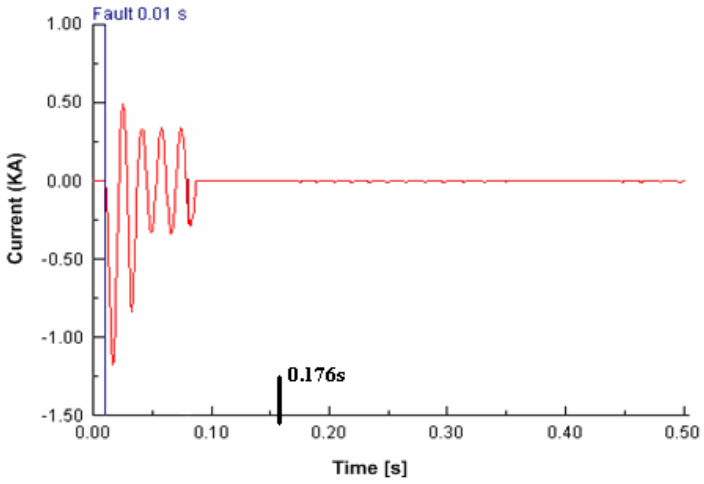

Fig. 21 Case 1: Fault Current through Fuse after the New Approach

During this period the lateral recloser's phase settings (51P1) comprised of a time dial settings (TDS) of 0.1 and the pickup of 80A. For the ground (51N1) settings, the TDS was 0.1 and the pickup was 3.2A. The TCC type was 102. The settings of the feeder recloser remained the same. The details of the devices' settings are listed in Appendix A of this thesis. The remaining two issues fuse misoperation and fuse fatigue also occurred for this case.

Table 8 provides the recloser fuse coordination results during the staged temporary fault which resulted in nuisance fuse blowing. The results include the worst case scenario where the maximum fault and maximum DG penetration level were applied. The first column of the table indicates a fuse number which protects a lateral and this number also corresponds to the lateral number (For example, fuse 1 protects lateral 1). The second column provides the fault type added downstream of the fuse. The third and fourth column give the recloser operation (open and reclose) for the fault while the final column indicates the fuse's operation.

Table 8 Case 1: Temporary Fault Coordination before the New Approach

Fuse #	Fault Type	R Opens (s)	R Closes (s)	Fuse blows (s)
1	1-ph-g	0.037	0.203	-
	1-ph-gZ_f	0.051	0.218	-
2	1-ph-g	0.065	0.232	-
	1-ph-gZ_f	0.354	0.520	-
3	1-ph-g	0.070	0.237	-
	1-ph-gZ_f	0.109	0.276	-
4	1-ph-g	0.141	0.307	-
	1-ph-gZ_f	0.215	0.381	-
6	1-ph-g	0.156	0.323	-
	1-ph-gZ_f	0.251	0.418	-
7	3-ph-g			0.052
	1-ph-gZ_f			0.286
8	3-ph-g			0.060
	1-ph-gZ_f			0.192

During the worst case situation, the individual fuses on lateral 7 and lateral 8 blew prior to the feeder recloser's operation on its fast curve. The nuisance blowing of the individual fuses resulted in permanent outages at the two laterals. The fuses on the 1-phase laterals, lateral fuses F1-F4, and F6 did not undergo nuisance fuse blowing during the worst case scenario. Table 9 provides the coordination results between the feeder recloser, the lateral recloser, and the fuses after the new approach was implemented on the existing OCP scheme to mitigate the nuisance fuse blowing issues that occurred during the temporary fault. The first column of the table indicates a fuse protecting a lateral while the second column gives the fault type on that lateral. The third and fourth column provide the operating time of the lateral recloser during the fault while the fifth and sixth column corresponds to the feeder recloser's operating time. The fuse blowing time is given in the last column (the "-" symbol signifies that the fuse did not blow). In addition, Table 10 provides the coordination results between the feeder recloser, lateral recloser and fuses for a permanent fault situation after the new approach was implemented on the existing

OCP scheme. The asterisked sections on the last column in Table 10 correspond to the slowest operation of the three single fuses on each of the 3-phase lateral. After this time, all the three phases of the 3-phase lateral would have operated.

Table 9 Case 1: Temporary Fault Coordination after the New Approach

Fuse #	Fault Type	R_{lat} opens (s)	R_{lat} Closes (s)	R Opens (s)	R Closes (s)	Fuse blows (s)
1	1-ph-g	0.034	0.167	0.037	0.203	-
	1-ph-gZ_f	0.041	0.175	0.051	0.218	-
2	1-ph-g	0.036	0.170	0.063	0.230	-
	1-ph-gZ_f	0.529	0.663	0.340	0.507	-
3	1-ph-g	0.033	0.167	0.065	0.232	-
	1-ph-gZ_f	0.039	0.173	0.098	0.265	-
4	1-ph-g	0.035	0.168	0.114	0.280	-
	1-ph-gZ_f	0.040	0.174	0.153	0.319	-
6	1-ph-g	0.037	0.170	0.130	0.296	-
	1-ph-gZ_f	0.037	0.171	0.165	0.331	-
7	3-ph-g	0.031	0.164	0.079	0.246	-
	1-ph-gZ_f	0.036	0.169	0.179	0.346	-
8	3-ph-g	0.031	0.164	0.085	0.252	-
	1-ph-gZ_f	0.034	0.184	0.168	0.351	-

Table 10 Case 1: Permanent Fault Coordination after the New Approach

Fuse #	Fault Type	R_{lat} opens (s)	R_{lat} Closes (s)	R Opens (s)	R Closes (s)	Fuse blows (s)
1	1-ph-g	0.034	0.167	0.037	0.203	0.225
	1-ph-gZ_f	0.041	0.175	0.051	0.218	0.290
2	1-ph-g	0.036	0.170	0.063	0.230	0.329
	1-ph-gZ_f	0.529	0.663	0.340	0.507	1.178
3	1-ph-g	0.033	0.167	0.065	0.232	0.292
	1-ph-gZ_f	0.039	0.173	0.098	0.265	0.377

Table 10 continued

Fuse #	Fault Type	R_{lat} opens (s)	R_{lat} Closes (s)	R Opens (s)	R Closes (s)	Fuse blows (s)
4	1-ph-g	0.035	0.168	0.114	0.280	0.459
	1-ph-gZ_f	0.040	0.174	0.153	0.319	0.666
6	1-ph-g	0.037	0.170	0.130	0.296	0.472
	1-ph-gZ_f	0.037	0.171	0.165	0.331	0.692
7	3-ph-g	0.031	0.164	0.079	0.246	0.254*
	1-ph-gZ_f	0.036	0.169	0.179	0.346	0.549*
8	3-ph-g	0.031	0.164	0.085	0.252	0.226*
	1-ph-gZ_f	0.034	0.184	0.168	0.351	0.581*

5.2.2. Case 2

This case describes how the DG impacted the existing OCP scheme of the feeder when the DG was placed at location 2 of the feeder in Fig. 16. Studies were performed with DG sizes up to 2.5 MVA at this location. Typically the OCP design of the radial feeder is such that the three single phase fuses protecting the lateral should only operate to isolate a fault on the 3-phase lateral. However, the fuses misoperated during an upstream fault (outside the lateral). In one example which typifies a worst case scenario, a L-L-L-G fault was placed upstream of (on node 834) the three single phase fuses with the DG penetration level at 100% (2.5MVA). Table 11 provides the operating time of the fuses on the 3-phase lateral during the fuse misoperation issue. The first column of the table indicates the fuse that is located on each phase of the lateral. The second and third columns provide the feeder recloser's operating time for the fault while the last column shows the fuse operating time during the fault. Of the three individual fuses protecting the lateral, the fuse on phase B was the first to misoperate followed by fuses on phase A, and C respectively.

Table 11 Case 2: Fuse Misoperation Issues before the New Approach

Fuse #	R Opens (s)	R Closes (s)	Fuse blows (s)
7 (Ph.A)	0.082	0.248	0.1767
7 (Ph.B)	0.082	0.248	0.153
7 (Ph.C)	0.082	0.248	1.179

Fig. 22 illustrates the operation of the fuse (labeled as F7) and the feeder recloser during the fault. As shown in the illustration, F7 on phase B blew at 0.153 seconds to isolate the unfaulted phase of the lateral causing permanent outage on that phase. As a result, the DG is islanded with the remaining two phases causing an unbalance on the unfaulted lateral. As illustrated in Fig. 22, the feeder recloser operated (opened at 0.081seconds and closed at 0.248 seconds) since the fault was on the main (node 834).

Fig. 23 shows the same case scenario after implementing the new approach on the existing OCP scheme. In the illustration, after the fault was initiated at 0.01seconds, the lateral recloser and the feeder recloser both operated to clear the fault. The lateral recloser opened all the three phases at 0.028 seconds and reclosed at 0.162 seconds (from status 1 to 0 and back to 1) in which the lateral was temporarily isolated. However, the lateral recloser did not operate on its delayed curve to permanently isolate the unfaulted 3-phase lateral. This situation implied that the device misoperation was mitigated. During the simulation duration the feeder recloser opened at 0.082 seconds and reclosed at 0.248 seconds.

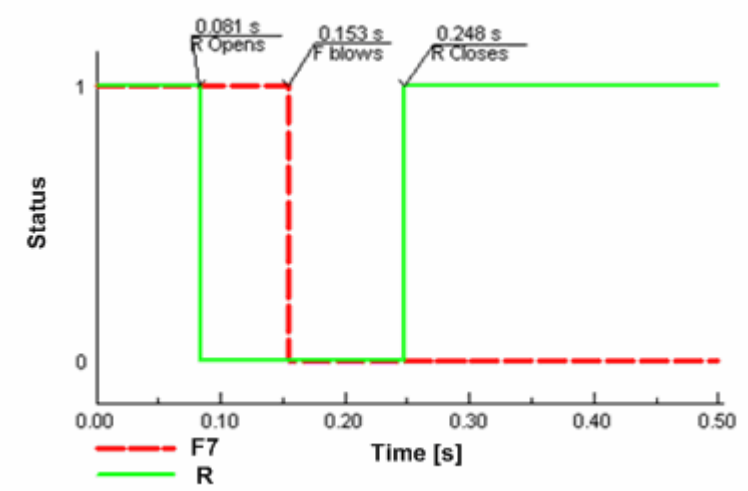

Fig. 22 Case 2: Fuse Misoperation of F7 before Applying the New Approach

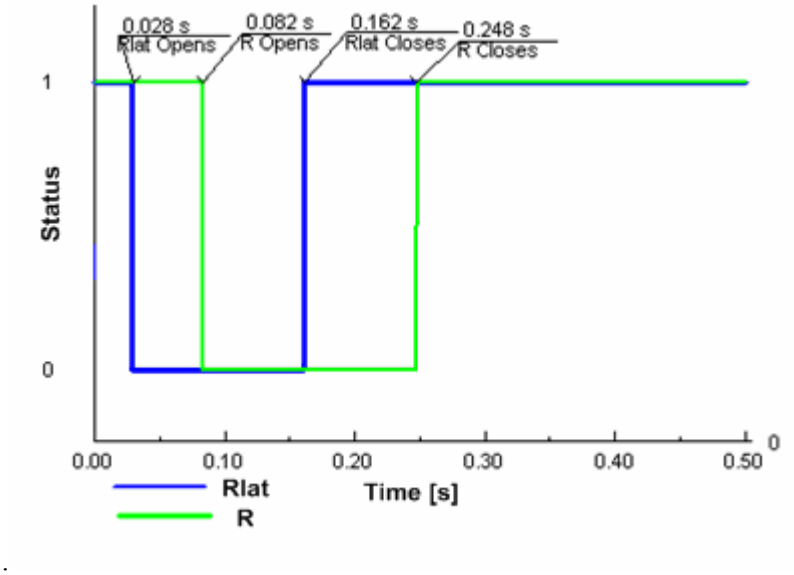

Fig. 23 Case 2: Fuse Misoperation Mitigated after Applying the New Approach

5.2.3. Case 3

This case discussed how the DG impacted the existing OCP scheme when the DG was placed at the remote end of lateral 8. A maximum fault was placed downstream of the lateral

fuses on the IEEE 34 Node Radial Test Feeder with DG at location 3 (node 862) of Fig. 16. Fig. 24 and Fig. 25 give the results before applying the new approach while Fig. 26 and Fig. 27 show the results after the new approach was applied. Fig. 24 illustrates a nuisance fuse blowing issue in which F11 on phase B of the 3-phase lateral blew prior to the recloser operation during the temporary fault. Given the magnitude of the fault current, the fuse underwent fatiguing followed by blowing at 0.060 seconds within the fault duration (0.176seconds). The current through the fuse during the fault is shown in Fig. 25. Again, the current became zero during the 10 cycle fault duration.

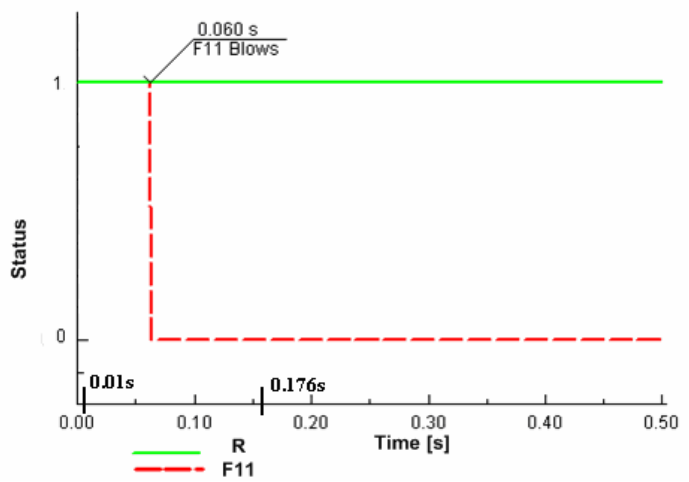

Fig. 24 Case 3: Nuisance Fuse Blowing before Applying the New Approach

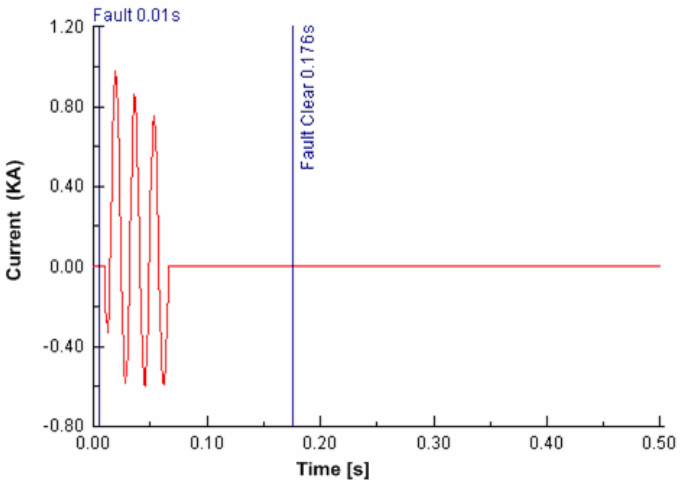

Fig. 25 Case 3: Fault Current through Fuse before Applying the New Approach

Fig. 26 displays the operation of the feeder recloser, lateral recloser, and F11 operation after applying the new approach to mitigate the fuse fatigue and nuisance fuse blowing issues. The duration for the simulation was 0.5s. As the fault is initiated at 0.01seconds, the lateral recloser operated to reduce the infeed current from the DG by opening at 0.030s and closing at 0.163s. R opened at 0.086s and reclosed at 0.252s. F11 did not operate and a permanent outage during the temporary fault was prevented. Therefore the fuse fatigue and nuisance fuse blowing issues were mitigated. Continuity of service was maintained at the lateral protected by the fuse F11.

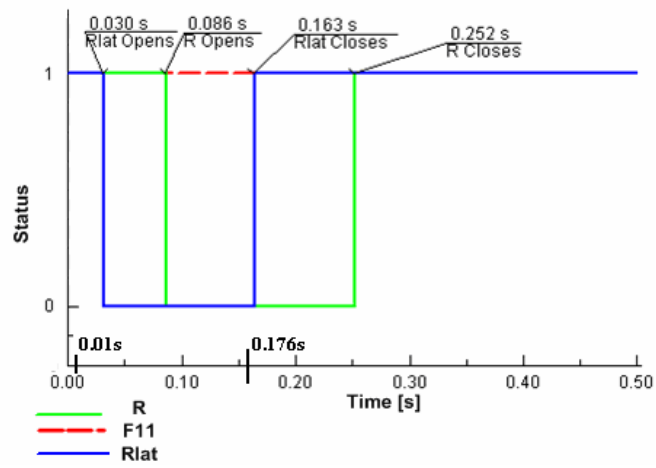

Fig. 26 Case 3: Nuisance Fuse Blowing Mitigated after Applying the New Approach

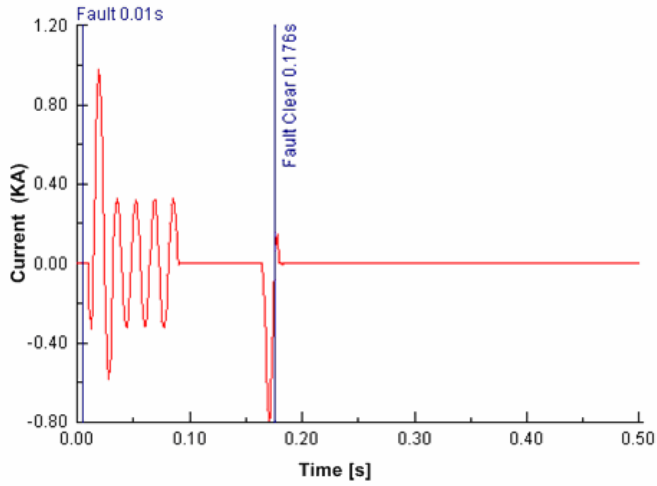

Fig. 27 Case 3: Current through Fuse after Applying the New Approach

The results for the studies performed in this case study are summarized in three tables. Table 12 provides the recloser - fuse coordination results during the staged temporary fault. Again, the results include the worst case scenario where the maximum fault and maximum DG penetration level were applied. The minimum fault was a 1-phase grounded fault with a 20 ohm fault impedance value. When the fault was temporary during the worst case situation, two fuses

F7 and F11 blew and resulted in permanent outages at two locations lateral 7 and 11. The recloser failed to operate during the two nuisance fuse blowing situations. As shown Lateral fuses F1-F4, and F6 did not blow during the temporary fault and were consequently saved. The highlighted sections of the last column of the table correspond to the fastest blowing operation of the three single fuses on a 3-phase lateral which caused the lateral to be unbalanced.

Table 13 provides the reclosers and fuses operation for a temporary fault after implementing the new approach to the existing protection scheme while Table 14 shows the reclosers and fuses operation for a permanent fault after implementing the new approach to the existing protection scheme.

Table 12 Case 3: Temporary Fault Coordination before the New Approach

Fuse #	Fault Type	R Opens (s)	R Closes (s)	Fuse blows (s)
1	1-ph-g	0.037	0.203	-
	1-ph-gZ_f	0.044	0.211	-
2	1-ph-g	0.065	0.232	-
	1-ph-gZ_f	0.354	0.521	-
3	1-ph-g	0.070	0.237	-
	1-ph-gZ_f	0.110	0.277	-
4	1-ph-g	0.141	0.307	-
	1-ph-gZ_f	0.215	0.382	-
6	1-ph-g	0.156	0.323	-
	1-ph-gZ_f	0.252	0.418	-
7	3-ph-g			0.051
	1-ph-gZ_f			0.287
11	3-ph-g			0.060
	1-ph-gZ_f	0.306	0.472	0.422

Table 13 Case 3: Temporary Fault Coordination after the New Approach

Fuse #	Fault Type	R_{lat} opens (s)	R_{lat} Closes (s)	R Opens (s)	R Closes (s)	Fuse blows (s)
1	1-ph-g	0.034	0.167	0.037	0.203	-
	1-ph-gZ_f	0.041	0.175	0.051	0.217	-
2	1-ph-g	0.036	0.170	0.063	0.229	-
	1-ph-gZ_f	0.552	0.686	0.364	0.531	-
3	1-ph-g	0.033	0.167	0.065	0.232	-
	1-ph-gZ_f	0.039	0.172	0.098	0.265	-
4	1-ph-g	0.035	0.168	0.111	0.278	-
	1-ph-gZ_f	0.040	0.174	0.148	0.315	-
6	1-ph-g	0.037	0.170	0.128	0.295	-
	1-ph-gZ_f	0.037	0.170	0.191	0.357	-
7	3-ph-g	0.030	0.164	0.084	0.251	-
	1-ph-gZ_f	0.036	0.169	0.179	0.346	-
11	3-ph-g	0.031	0.164	0.085	0.252	-
	1-ph-gZ_f	0.037	0.170	0.179	0.346	-

Table 14 Case 3: Permanent Fault Coordination before the New Approach

Fuse #	Fault Type	R_{lat} opens (s)	R_{lat} Closes (s)	R Opens (s)	R Closes (s)	Fuse blows (s)
1	1-ph-g	0.034	0.167	0.037	0.203	0.224
	1-ph-gZ_f	0.041	0.175	0.051	0.217	0.289
2	1-ph-g	0.036	0.170	0.063	0.229	0.328
	1-ph-gZ_f	0.552	0.686	0.364	0.531	1.361
3	1-ph-g	0.033	0.167	0.065	0.232	0.292
	1-ph-gZ_f	0.039	0.172	0.098	0.265	0.377
4	1-ph-g	0.035	0.168	0.111	0.278	0.501
	1-ph-gZ_f	0.040	0.174	0.148	0.315	0.752
6	1-ph-g	0.037	0.170	0.128	0.295	0.457
	1-ph-gZ_f	0.037	0.170	0.191	0.357	0.692
7	3-ph-g	0.030	0.164	0.084	0.251	0.218*
	1-ph-gZ_f	0.036	0.169	0.179	0.346	0.771
11	3-ph-g	0.031	0.164	0.085	0.252	0.235*
	1-ph-gZ_f	0.037	0.170	0.179	0.346	0.653

5.2.4. Case 4

This case investigated how the DG impacted the existing OCP scheme when the DG was placed at the remote end of lateral 12. A maximum temporary and permanent fault was placed downstream of each lateral fuse of the IEEE 34 Node Radial Test Feeder with the DG placed at location 4 (node 890) in Fig. 16. No nuisance fuse blowing issues occurred during this case for the temporary fault situation. However, fuse misoperation and fuse fatigue issues occurred during a fault on the feeder and the approach was applied to mitigate the issues.

Table 15 provides the recloser fuse coordination results during the staged temporary fault for the studies performed. The results include the worst case scenario where the maximum fault and maximum DG penetration level were applied. As shown in the table, coordination held between the fuses and the feeder recloser during the fault. Consequently, no nuisance fuse blowing issues occurred. An additional step that was taken was to replace the fuse protecting the step-down transformer with a differential relay. The differential relay operates instantaneously only when the fault is either on the step-down transformer's primary or secondary sides.

Table 16 provides the recloser and fuses operation for a permanent fault before implementing the new approach to the existing protection scheme while Table 17 gives the results after the new approach was implemented. The asterisked sections on the last column of both tables indicate the slowest operating time of the fuse which indicates that the fault would be completely isolated.

Table 15 Case 4: Temporary Fault Coordination before the New Approach

Fuse #	Fault Type	R Opens (s)	R Closes (s)	Fuse Melts (s)
1	1-ph-g	0.037	0.203	0.036
	1-ph-gZ_f	0.124	0.291	-
2	1-ph-g	0.063	0.230	-
	1-ph-gZ_f	0.241	0.408	-
3	1-ph-g	0.065	0.232	-
	1-ph-gZ_f	0.103	0.269	-
4	1-ph-g	0.126	0.293	-
	1-ph-gZ_f	0.180	0.347	-
6	1-ph-g	0.136	0.303	-
	1-ph-gZ_f	0.197	0.364	-
7	3-ph-g	0.084	0.250	-
	1-ph-gZ_f	0.229	0.395	-
8	3-ph-g	0.089	0.255	-
	1-ph-gZ_f	0.261	0.428	-
11	3-ph-g	0.089	0.256	-
	1-ph-gZ_f	0.227	0.394	-

Table 16 Case 4: Permanent Fault Coordination before the New Approach

Fuse #	Fault Type	R Opens (s)	R Closes (s)	Fuse blows (s)
1	1-ph-g	0.037	0.203	0.237
	1-ph-gZ_f	0.124	0.291	0.309
2	1-ph-g	0.063	0.230	0.428
	1-ph-gZ_f	0.241	0.408	1.308
3	1-ph-g	0.065	0.232	0.344
	1-ph-gZ_f	0.103	0.269	0.476
4	1-ph-g	0.126	0.293	0.526
	1-ph-gZ_f	0.180	0.347	0.730
6	1-ph-g	0.136	0.303	0.560
	1-ph-gZ_f	0.197	0.364	0.777
7	3-ph-g	0.084	0.250	0.300
	1-ph-gZ_f	0.229	0.395	0.695
8	3-ph-g	0.089	0.255	0.368*
	1-ph-gZ_f	0.261	0.428	0.792*
11	3-ph-g	0.089	0.256	0.374*
	1-ph-gZ_f	0.227	0.394	0.707*

Table 17 Case 4: Permanent Fault Coordination after the New Approach

Fuse #	Fault Type	R_{lat} opens (s)	R_{lat} opens (s)	R opens (s)	R Closes (s)	Fuse blows (s)
1	1-ph-g	0.042	0.176	0.037	0.203	0.236
	1-ph-gZ_f	0.248	0.370	0.051	0.218	0.237
2	1-ph-g	0.044	0.177	0.063	0.230	0.393
	1-ph-gZ_f	0.344	0.478	0.241	0.408	1.269
3	1-ph-g	0.041	0.174	0.066	0.232	0.323
	1-ph-gZ_f	0.045	0.178	0.094	0.260	0.422
4	1-ph-g	0.045	0.178	0.112	0.279	0.448
	1-ph-gZ_f	0.066	0.199	0.153	0.319	0.593
6	1-ph-g	0.044	0.177	0.122	0.289	0.460
	1-ph-gZ_f	0.046	0.179	0.160	0.327	0.604
7	3-ph-g	0.031	0.165	0.083	0.250	0.391*
	1-ph-gZ_f	0.180	0.346	0.055	0.188	0.614
8	3-ph-g	0.032	0.166	0.087	0.254	0.393*
	1-ph-gZ_f	0.193	0.360	0.050	0.184	0.533
11	3-ph-g	0.032	0.166	0.085	0.252	0.399*
	1-ph-gZ_f	0.177	0.344	0.053	0.186	0.477

5.2.5. Summary of Cases 1 - 4

This summary gives the results from the exhaustive case studies performed on the IEEE 34 node radial test feeder. The studies included the worst case situations and totaled 768. The results are provided in Table 18 where the first column provides the three OCP issues fuse fatigue, nuisance fuse blowing, and fuse misoperation. The second column indicates the DG size on the feeder that caused the OCP issues. The third and fourth columns provide number of the three issues found on the feeder prior to implementing the new approach on the existing OCP scheme of the feeder and after the new approach was implemented. The results indicated that there were a total of 18 nuisance fuse blowing, 46 fuse fatigue issues and 24 fuse misoperation issues prior to implementing the new approach on the existing OCP scheme of the IEEE 34 node radial test feeder. After the new approach was implemented on the OCP scheme of both radial test feeders, there were only 2 fuse fatigue issues (where the fuses began to melt before the recloser's fast operation) and no fuse misoperation or nuisance fuse blowing issues.

Table 18 OCP Issues on the IEEE 34 Node Test Feeder before and after the New Approach

OCP Issues occuring on the Radial Feeder	DG Size (MVA)	Tot. # Before	Tot. # After
Fuse Fatigue	0.406	0	0
	1.075	2	0
	2.5	46	2
Nuisance Fuse Blowing	0.406	0	0
	1.075	0	0
	2.5	18	0
Fuse Misoperation	0.406	0	0
	1.075	12	0
	2.5	12	0

5.3 Simulation Cases on the IEEE 123 Node Radial Test Feeder

5.3.1. Case 5

Similar studies conducted on the IEEE 34 Node were performed on the IEEE 123 Node Radial Test Feeder to investigate how the DG impacted the existing OCP scheme when the DG was placed at the remote end of a 3-phase lateral on location 1 (node 48) of the feeder. A fault was placed downstream of the lateral fuses of the feeder with DG as shown in Fig. 17 .

In one of the studies conducted a temporary L-G fault was placed downstream of a single phase fuse (F10) on a 1-phase lateral (phase A type). The fault was initiated at 0.01 seconds with a 10 cycle duration. During the temporary fault duration, it is expected that the feeder recloser will trip to clear the fault and prevent F10 from melting before the recloser's fast operation began. Fig. 28 provides the operation of F10 and the feeder recloser during the fault period. Here the status of the fuse remained at 1 and changes to 0 when melting began. As shown, after the fault was initiated, R opened at 0.053 seconds and closed at 0.220 seconds. However, F10 became fatigued at 0.053 seconds, around the same time the feeder recloser began its fast operation. Fig. 29 shows the same scenario after implementing the new approach on the

existing OCP scheme in which the fuse did not melt during the 10 cycle fault duration. Therefore, fuse fatigue was mitigated in this situation.

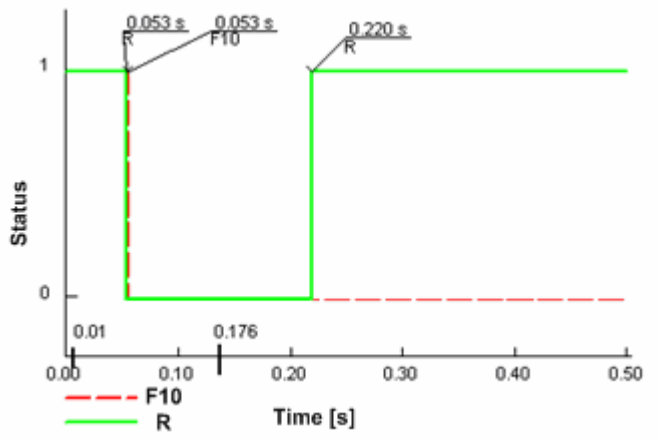

Fig. 28 Case 5: Fuse Fatigue on F10 before Applying the New Approach

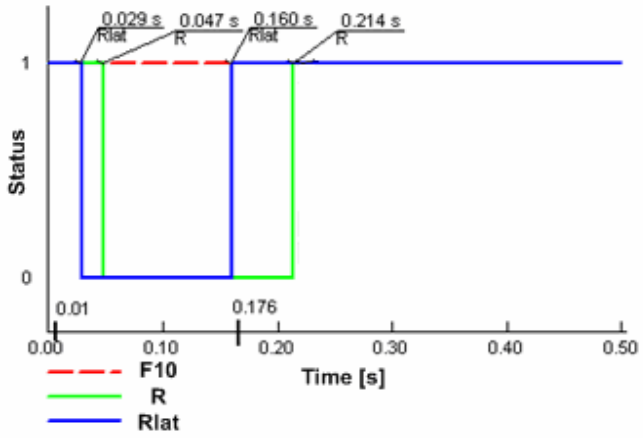

Fig. 29 Case 5: Fuse Fatigue on F10 Mitigated after Applying the New Approach

In another scenario in which nuisance fuse blowing was investigated, a L-G fault downstream of F14 caused the fuse to blow prior to the feeder recloser completing its first operation. This situation occurred when the maximum DG size was placed on the feeder as well.

The illustration in Fig. 30 shows the operation of F14 and the feeder recloser, while Fig. 31 shows the fault current through F14 during the nuisance blowing situation. As the fault is initiated at 0.01seconds, R opened at 0.045seconds and reclosed at 0.211 seconds. However, F14 blew at 0.171 seconds.

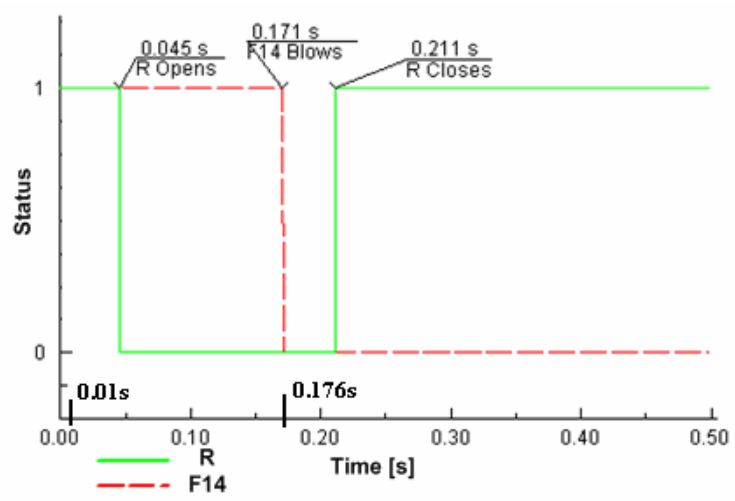

Fig. 30 Case 5: Nuisance Fuse Blowing before Applying the New Approach

The vertical axis in Fig. 31 gives the phase fault current through the fuse, while the horizontal axis corresponds to the fault current duration in seconds. Fig. 32 and Fig. 33 show the same scenario after implementing the new approach on the existing OCP scheme. After implementing the new approach, F14 was saved during the occurrence of the temporary fault. The fuse saving was achieved due to the operation of the lateral recloser with the feeder recloser to allow the temporary fault to clear without blowing the fuse. As shown in Fig. 32, the lateral recloser opened at 0.20s and reclosed at 0.153s while R opened at 0.042s and reclosed at 0.209s. Continuity of service was maintained at the lateral protected by F14 as shown in Fig. 32. For the lateral recloser phase element (51P1), the time dial settings (TDS) was 0.1 and the pickup was

400A. The TDS was 0.1 and the pickup was 3.2A for the ground element (51N1). The TCC type for both elements was 103.

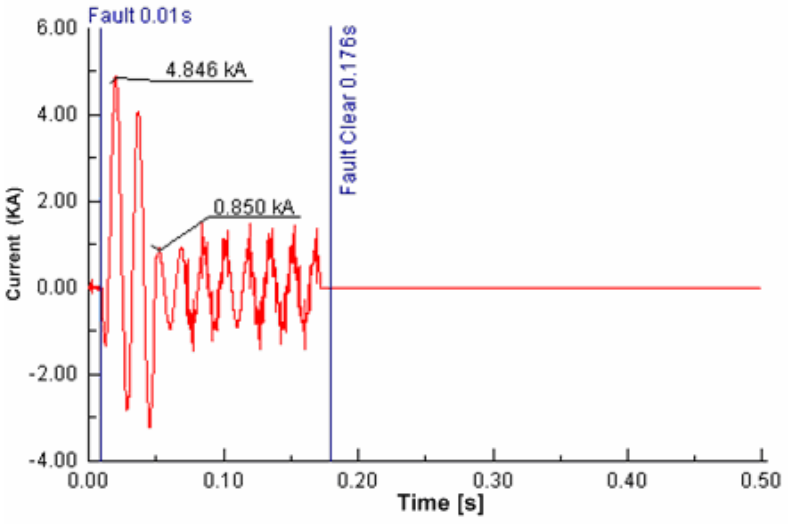

Fig. 31 Case 5: Fault Current through the Fuse before Applying the New Approach

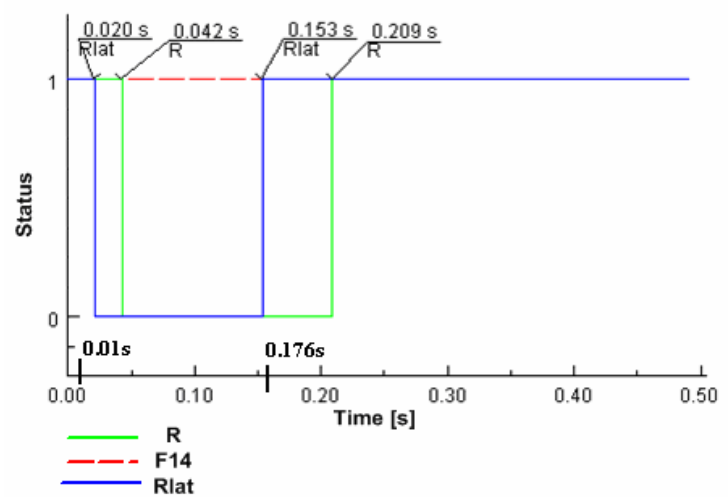

Fig. 32 Case 5: Nuisance Fuse Blowing Mitigated after Applying the New Approach

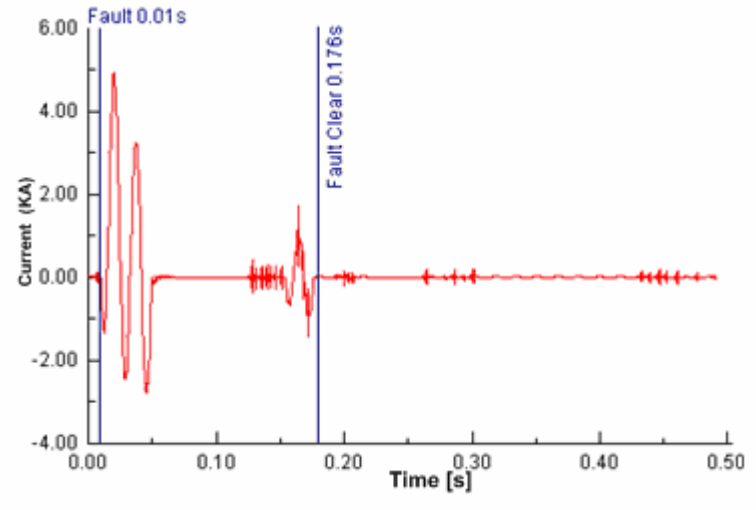

Fig. 33 Case 5: Current through Fuse after Applying the New Approach

Table 19 provides the recloser and fuse coordination results during the staged temporary fault for Case 5. In addition, the results from the worst case scenario where the maximum fault and maximum DG penetration level were applied are included in the table. Table 20 gives the OCPDs' (reclosers and fuses) operation for a temporary fault after implementing the new approach to the existing protection scheme. The highlighted sections on the last column imply that nuisance fuse blowing occurred at the lateral in question. As indicated four fuses underwent fuse blowing when a maximum fault was placed downstream of each fuse. Table 21 provides the OCPDs' operation for a permanent fault after implementing the new approach to the existing protection scheme.

Table 19 Case 5: Temporary Fault Coordination before the New Approach

Fuse #	Fault Type	R Opens (s)	R Closes (s)	Fuse blows (s)
F3	1-ph-g	0.033	0.200	-
F5	1-ph-g	0.030	0.196	-
F6	1-ph-g	0.037	0.203	-
F7	1-ph-g	0.038	0.205	-
F8	1-ph-g	0.041	0.208	-
F9	1-ph-g	0.045	0.212	-
F10	1-ph-g	0.052	0.219	-
F11	1-ph-g	0.033	0.199	-
F12	1-ph-g	0.040		0.171
F13	1-ph-g	0.045	0.211	0.092
F14	1-ph-g	0.045	0.212	0.174
F15	1-ph-g	0.034	0.200	-
F16	1-ph-g	0.045	0.211	-
F17	1-ph-g	0.048	0.214	-
F18	1-ph-g	0.033	0.199	-
F20	1-ph-g	0.067	0.234	-
F21	1-ph-g	0.095	0.261	-
F22	1-ph-g	0.099	0.266	-
F23	1-ph-g	0.092	0.259	-
F24	1-ph-g	0.127	0.294	0.263
F25	3-ph-g	0.033	0.199	-
F26	1-ph-g	0.057	0.224	-
F27	1-ph-g	0.057	0.224	-
F28	1-ph-g	0.062	0.229	-
F29	3-ph-g	0.031	0.197	-

Table 20 Case 5: Temporary Fault Coordination after the New Approach

Fuse #	Fault Type	R_{lat} opens (s)	R_{lat} Closes (s)	R Opens (s)	R Closes (s)	Fuse blows (s)
F3	1-ph-g	0.020	0.154	0.033	0.200	-
F5	1-ph-g	0.016	0.149	0.030	0.196	-
F6	1-ph-g	0.021	0.154	0.036	0.203	-
F7	1-ph-g	0.027	0.160	0.037	0.204	-

Table 20 continued

Fuse #	Fault Type	R_{lat} opens (s)	R_{lat} Closes (s)	R Opens (s)	R Closes (s)	Fuse blows (s)
F8	1-ph-g	0.016	0.150	0.038	0.205	-
F9	1-ph-g	0.017	0.151	0.041	0.207	-
F10	1-ph-g	0.022	0.155	0.046	0.213	-
F11	1-ph-g	0.023	0.080	0.033	0.199	-
F12	1-ph-g	0.016	0.149	0.037	0.204	-
F13	1-ph-g	0.027	0.160	0.042	0.209	-
F14	1-ph-g	0.021	0.154	0.042	0.209	-
F15	1-ph-g	0.027	0.160	0.034	0.200	-
F16	1-ph-g	0.023	0.156	0.042	0.208	-
F17	1-ph-g	0.021	0.154	0.044	0.211	-
F18	1-ph-g	0.015	0.149	0.032	0.199	-
F20	1-ph-g	0.024	0.157	0.057	0.223	-
F21	1-ph-g	0.032	0.166	0.072	0.239	-
F22	1-ph-g	0.024	0.157	0.069	0.236	-
F23	1-ph-g	0.034	0.168	0.090	0.257	-
F24	1-ph-g	0.016	0.149	0.032	0.199	-
F25	3-ph-g	0.015	0.149	0.032	0.199	-
F26	1-ph-g	0.022	0.155	0.049	0.216	-
F27	1-ph-g	0.029	0.162	0.050	0.217	-
F28	1-ph-g	0.024	0.157	0.054	0.221	-

Table 21 Case 5: Permanent Fault Coordination after the New Approach

Fuse #	Fault Type	R_{lat} opens (s)	R_{lat} Closes (s)	R Opens (s)	R Closes (s)	Fuse blows (s)
F3	1-ph-g	0.020	0.154	0.033	0.200	0.320
F5	1-ph-g	0.016	0.149	0.030	0.196	0.306
F6	1-ph-g	0.021	0.154	0.036	0.203	0.289
F7	1-ph-g	0.027	0.160	0.037	0.204	0.334
F8	1-ph-g	0.016	0.150	0.038	0.205	0.346
F9	1-ph-g	0.017	0.151	0.041	0.207	0.363
F10	1-ph-g	0.022	0.155	0.046	0.213	0.297
F11	1-ph-g	0.023	0.080	0.033	0.199	0.350
F12	1-ph-g	0.016	0.149	0.037	0.204	0.246
F13	1-ph-g	0.027	0.160	0.042	0.209	0.215
F14	1-ph-g	0.021	0.154	0.042	0.209	0.260
F15	1-ph-g	0.027	0.160	0.034	0.200	0.249
F16	1-ph-g	0.023	0.156	0.042	0.208	0.361
F17	1-ph-g	0.021	0.154	0.044	0.211	0.373
F18	1-ph-g	0.015	0.149	0.032	0.199	0.308
F20	1-ph-g	0.024	0.157	0.057	0.223	0.336
F21	1-ph-g	0.032	0.166	0.072	0.239	0.318
F22	1-ph-g	0.024	0.157	0.069	0.236	0.341
F23	1-ph-g	0.034	0.168	0.090	0.257	0.334
F24	1-ph-g	0.015	0.149	0.032	0.199	0.309
F25	3-ph-g	0.011	0.145	0.032	0.199	0.280*
F26	1-ph-g	0.022	0.155	0.049	0.216	0.607
F27	1-ph-g	0.029	0.162	0.050	0.217	0.590
F28	1-ph-g	0.024	0.157	0.054	0.221	0.704

5.3.2. Case 6

This case investigated how the DG impacted the existing OCP scheme when the DG was placed at the remote end of a 3-phase lateral (node 450) in Fig. 17. In this case, the DG location was farther away from the substation of the IEEE 123 Node Radial Test Feeder. In the studies, the presence of DG on the feeder lateral caused fuse fatigue, nuisance fuse blowing, and misoperation issues.

In one example which describes the nuisance fuse blowing issue, a maximum fault was placed downstream of lateral fuses of the feeder with the DG (size of 3.85 MVA) at location 2 in

Fig. 17. Fig. 34 shows the operation of the feeder recloser and F21 when a L-G fault in Fig. 35 was initiated at 0.01s and cleared after 10 cycles. The feeder recloser opened at 0.108s and reclosed at 0.273s. During this reclosing interval F21 blew at 0.111s leading to a permanent outage before the fault was cleared. Fig. 36 and Fig. 37 show the operation of the OCPDs after the new approach was applied to mitigate the nuisance fuse blowing issue. When the fault was initiated, R opened at 0.08s and reclosed at 0.247s. The lateral recloser opened at 0.040s and reclosed at 0.202s. Both reclosers' operations provided enough time for the fault to clear and prevented the permanent outage from occurring during the temporary fault.

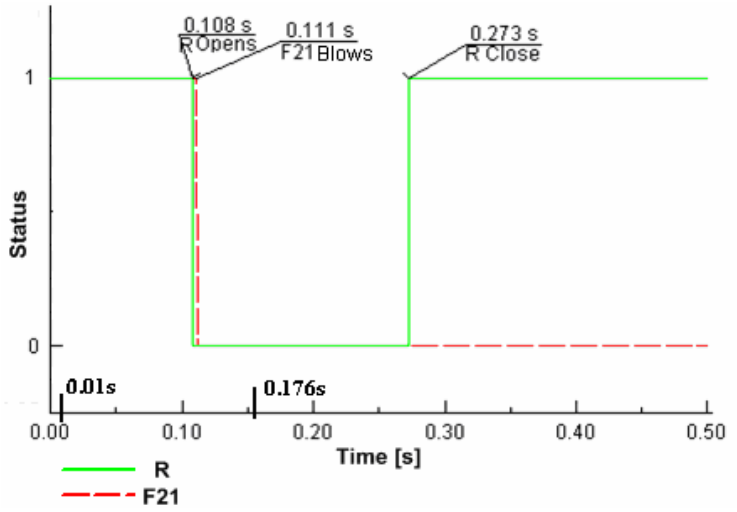

Fig. 34 Case 6: Nuisance Fuse Blowing before Applying the New Approach

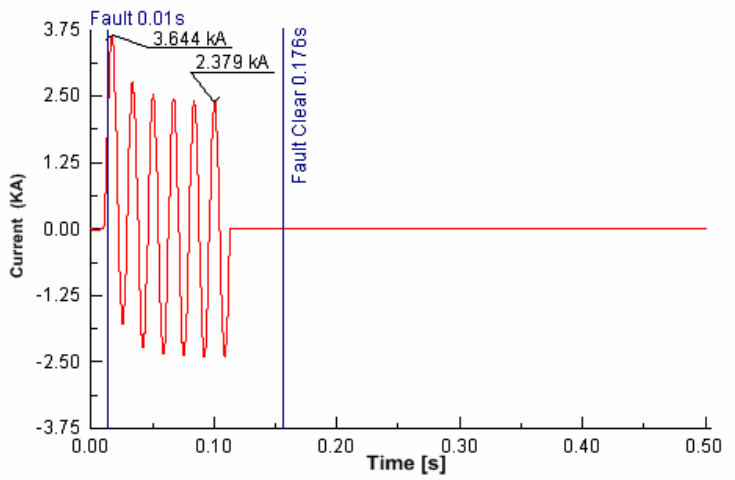

Fig. 35 Case 6: Fault Current through the Fuse before Applying the New Approach

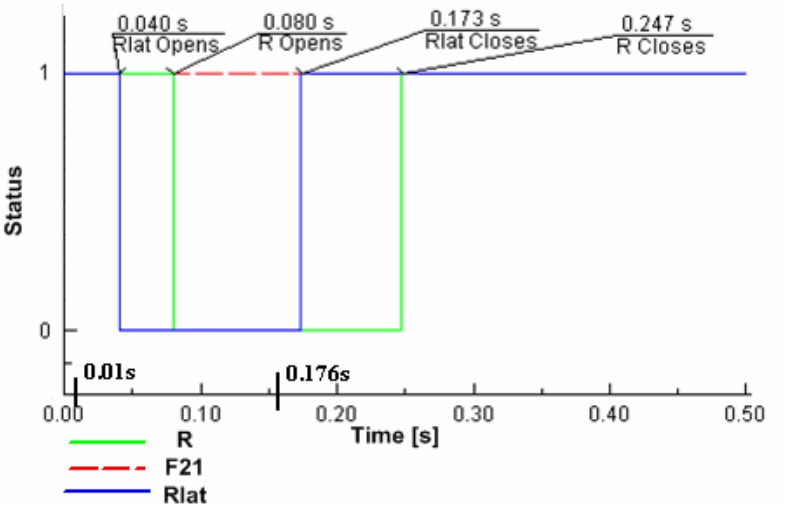

Fig. 36 Case 6: Nuisance Fuse Blowing Mitigated after Applying the New Approach

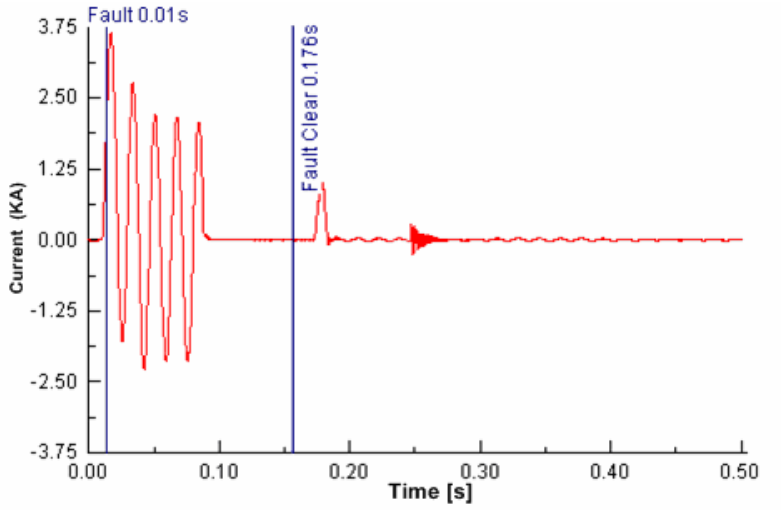

Fig. 37 Case 6: Current through Fuse after Applying the New Approach

Table 22 provides the recloser fuse coordination results during the staged temporary fault for the nuisance fuse blowing issue. In addition, the results are for the worst case scenario in which the OCPDs operation during the maximum fault and the maximum DG penetration level were studied. The nuisance fuse blowing occurred at two locations on the feeder, laterals 21 and 24. Table 23 gives the reclosers and fuses operation for a temporary fault after implementing the new approach to the existing protection scheme while Table 24 shows the devices' operation for a permanent fault after implementing the new approach. The asterisked section of the last column of Table 24 corresponds to the slowest operation of the three single fuses on a 3-phase lateral which caused the entire lateral to be permanently isolated.

Table 22 Case 6: Temporary Fault Coordination before the New Approach

Fuse #	Fault Type	R Opens (s)	R Closes (s)	Fuse blows
F3	1-ph-g	0.033	0.200	-
F4	1-ph-g	0.031	0.197	-
F5	1-ph-g	0.030	0.196	-
F6	1-ph-g	0.037	0.203	-
F7	1-ph-g	0.038	0.205	-
F8	1-ph-g	0.041	0.208	-
F9	1-ph-g	0.044	0.211	-
F10	1-ph-g	0.052	0.218	-
F11	1-ph-g	0.033	0.200	-
F12	1-ph-g	0.039	0.206	-
F13	1-ph-g	0.045	0.211	-
F14	1-ph-g	0.046	0.213	-
F15	1-ph-g	0.034	0.200	-
F16	1-ph-g	0.045	0.212	-
F17	1-ph-g	0.050	0.217	-
F18	1-ph-g	0.032	0.065	-
F20	1-ph-g	0.074	0.241	-
F21	1-ph-g	0.106	0.273	0.108
F22	1-ph-g	0.101	0.268	-
F23	1-ph-g	0.106	0.272	-
F24	1-ph-g	No-op	No-op	0.135
F26	1-ph-g	0.058	0.224	-
F27	1-ph-g	0.061	0.228	-
F28	1-ph-g	0.067	0.233	-
F29	3-ph-g	0.032	0.198	-

Table 23 Case 6: Temporary Fault Coordination after the New Approach

Fuse #	Fault Type	R_{lat} opens (s)	R_{lat} Closes (s)	R Opens (s)	R Closes (s)	Fuse blows (s)
F3	0.031	0.164	0.033	0.200	0.323	-
F5	0.027	0.160	0.030	0.196	0.304	-
F6	0.032	0.165	0.037	0.203	0.274	-

Table 23 continued

Fuse #	Fault Type	R_{lat} opens (s)	R_{lat} Closes (s)	R Opens (s)	R Closes (s)	Fuse blows (s)
F7	0.035	0.169	0.038	0.205	0.333	-
F8	0.044	0.177	0.041	0.208	0.365	-
F9	0.044	0.177	0.045	0.211	0.401	-
F10	0.047	0.181	0.052	0.219	0.279	-
F11	0.029	0.163	0.033	0.200	0.377	-
F12	0.130	0.264	0.129	0.295	0.306	-
F13	0.134	0.267	0.136	0.303	0.325	-
F14	0.042	0.175	0.045	0.212	0.236	-
F15	0.029	0.162	0.034	0.200	0.241	-
F16	0.031	0.165	0.044	0.211	0.368	-
F17	0.027	0.161	0.049	0.215	0.387	-
F18	0.026	0.159	0.032	0.199	0.284	-
F19	0.043	0.176	0.084	0.250	0.363	-
F20	0.036	0.170	0.063	0.230	0.338	-
F21	0.040	0.173	0.080	0.247	0.312	-
F22	0.043	0.176	0.078	0.245	0.355	-
F23	0.043	0.177	0.081	0.247	0.362	-
F24	0.135	0.268	0.192	0.359	0.426	-
F26	0.028	0.161	0.053	0.220	0.554	-
F27	0.029	0.162	0.056	0.222	0.543	-
F28	0.032	0.166	0.060	0.226	0.635	-
F29	0.028	0.161	0.032	0.198	0.244	-

Table 24 Case 6: Permanent Fault Coordination after the New Approach

Fuse #	Fault Type	R_{lat} opens (s)	R_{lat} Closes (s)	R Opens (s)	Fuse blows (s)
F3	1-ph-g	0.031	0.164	0.033	0.200
F5	1-ph-g	0.027	0.160	0.030	0.196
F6	1-ph-g	0.032	0.165	0.037	0.203
F7	1-ph-g	0.035	0.169	0.038	0.205

Table 24 continued

Fuse #	Fault Type	R_{lat} opens (s)	R_{lat} Closes (s)	R Opens (s)	Fuse blows (s)
F8	1-ph-g	0.044	0.177	0.041	0.208
F9	1-ph-g	0.044	0.177	0.045	0.211
F10	1-ph-g	0.047	0.181	0.052	0.219
F11	1-ph-g	0.029	0.163	0.033	0.200
F12	1-ph-g	0.130	0.264	0.129	0.295
F13	1-ph-g	0.134	0.267	0.136	0.303
F14	1-ph-g	0.042	0.175	0.045	0.212
F15	1-ph-g	0.029	0.162	0.034	0.200
F16	1-ph-g	0.031	0.165	0.044	0.211
F17	1-ph-g	0.027	0.161	0.049	0.215
F18	1-ph-g	0.026	0.159	0.032	0.199
F20	1-ph-g	0.036	0.170	0.063	0.230
F21	1-ph-g	0.040	0.173	0.080	0.247
F22	1-ph-g	0.043	0.176	0.078	0.245
F23	1-ph-g	0.043	0.177	0.081	0.247
F24	1-ph-g	0.135	0.268	0.192	0.359
F26	1-ph-g	0.028	0.161	0.053	0.220
F27	1-ph-g	0.029	0.162	0.056	0.222
F28	1-ph-g	0.032	0.166	0.060	0.226
F29	3-ph-g	0.027	0.160	0.032	0.230*

5.3.3. Summary of Cases 5 - 6

Table 25 summarizes results of the case studies conducted during the maximum fault studies on the IEEE 123 Node Radial Test Feeder when the DG is placed at the two locations shown in Fig. 17. The first column of the table provides the three OCP issues, while the second column gives the number of issues found on the feeder prior to implementing the new approach on the existing OCP scheme of the feeder. The number of issues remaining after the new approach was implemented is given in the last column. As observed, all of the nuisance fuse blowing and fuse misoperation issues were completely mitigated after implementing the new approach to the existing OCP scheme. However, the fuse fatigue issues were not fully mitigated for the fuses F13, F21, and F24.

Table 25 OCP Issues on the IEEE 123 Node Test Feeder before and after the Approach

OCP Issues on the Radial Feeder	Tot # Before	Tot # After
Fuse Fatigue	34	3
Nuisance Fuse Blowing	13	0
Fuse Misoperation	6	0

CHAPTER VI

CONCLUSIONS AND FUTURE WORK

6.1. Summary

A new approach to mitigate overcurrent protection issues on radial distribution feeders with DGs was developed in the Power System Automation Lab at Texas A&M University. First, two Radial Test Feeders, the IEEE 34 Node Radial Test Feeder and the IEEE 123 Node Radial Test Feeder, were modeled and provided with conventional protective devices and a fuse-saving overcurrent protection scheme. Load flow and short circuit analysis studies were conducted on these feeders using DIgSILENT Powerfactory software to determine the settings and coordination of the protective devices. Four sizes of the salient pole synchronous generator models were then customized in DIgSILENT and added to the Radial Test Feeders to identify the three OCP issues caused by the DG.

The new approach revises the existing overcurrent protection scheme through protection changes only at the lateral with the DG. The three individual fuses protecting the lateral is replaced with a multi-functional recloser to prevent the infeed current from the DG which causes the OCP issues. The recloser uses phase overcurrent measurements and sequence overcurrent measurements for its settings to provide the required operation with the feeder recloser to mitigate the OCP issues, nuisance fuse blowing, fuse fatigue, and fuse misoperation. In addition, an interconnection protection and DG unit protection were added to prevent long term islanding and backup protection for the DG, respectively. The composite and source-to-load coordination methods were used to provide phase and ground setting coordination between the added OCPDs and the existing feeder recloser.

6.2. Conclusions

This thesis work discussed a new approach to mitigate the impact of DG on the overcurrent protection scheme of radial distribution feeders. Four DG sizes (0.406MVA, 1.075 MVA, 2.50, and 3.85 MVA) individually placed at 3-phase lateral ends of two IEEE Radial Test Feeders proved the validity and generality of the new approach on radial distribution feeders. The OCP issues addressed by the new approach included fuse misoperation, fuse fatigue, and nuisance fuse blowing. The new approach included protection for the feeder and the DG unit, using an off-the-shelf multifunction recloser and a relay to mitigate the three OCP issues found.

The new approach completely mitigated the fuse misoperation and nuisance fuse blowing issues that were present on the radial feeders. However, there were some situations where the fuse fatigue issues were not fully mitigated, meaning a fuse began melting before the feeder recloser and lateral recloser fast operation began. Nevertheless, such issues would not result in unwarranted permanent outages.

6.3. Future Work

The focus of the future work will be to readdress the unmitigated fuse fatigue issues. Furthermore exhaustive studies on the IEEE 123 Node Radial Test Feeder will be performed, considering additional DG location(s) on the feeder. Also, the extension of implementing the new approach to multiple feeders will be investigated.

REFERENCES

[1] T. Gonen, *Electric Power Distribution System Engineering*. New York: McGraw Hill, 1986.

[2] W. H. Kersting, *Distribution System Modeling and Analysis*. New York: CRC Press LLC, 2002.

[3] IEEE Power System Relaying Committee, "Distribution Line Protection Practices Report," 2002.[Online]. Available: http// www.pserc.org/ Apublications.html.

[4] L. A. Kojovic and C. W. Williams, Jr., "Sub-cycle detection of incipient cable splice faults to prevent cable damage," in *Proc. 2000 IEEE Power Engineering Society Summer Meeting*, pp. 1175-1180.

[5] J. D. Glover and M. S. Sarma, *Power Systems Analysis and Design*, 2nd ed. Boston: PWS Publishing Company, 1994.

[6] F. Soudi and K. Tomsovic, "Optimal Trade-Offs in Distribution Protection Design," *IEEE Trans. Power Delivery,* vol. 16, pp. 292–296, Apr. 2001.

[7] P. P. Barker and R. W. d. Mello, "Determining the impact of distributed generation on power systems: Part 1 - Radial Distribution Systems," in *Proc. 2000 IEEE Power Engineering Society Summer Meeting,* pp. 1645–1656.

[8] J. L. Blackburn, *Protective Relaying Principles and Applications*, 2nd ed. New York: Marcel Dekker Inc, 1998.

[9] Cooper Power*, Electrical Distribution-System Protection*. Wisconsin: Cooper Power Systems Inc, 2005.

[10] B. Fardanesh and E. Richards, "Distribution System Protection with Decentralized Generation Introduced into the System," *IEEE Trans. Industry Applications,* vol. IA-20, pp. 122-130, 1984.

[11] *IEEE Guide for Protective Relay Applications to Power Transformers*, IEEE Standard C37.91-2000, Mar.2000.

[12] J. Burke. (2002). Hard to Find Information about Distribution Systems ABB Inc. Consulting Raleigh. [Online].Available:library.abb.com/.../VerityDisplay/4EDF68B14B79751F85256C550053D6B6/$File/Hard-to%20Find%2019c.pdf.

[13] M. Davis, D. Costyk, and A. Narang, Distributed and Electric Power System Aggregation model and Field Configuration Equivalency Validation Testing, 2003. [Online]. Available: http://www.nrel.gov/docs/fy03osti/33909.pdf.

[14] SRP Interconnection Guidelines for Distributed Generation 2000. [Online] Available:www.srpnet.com/electric/pdfx/gen_guidelines.pdf.

[15] W. D. Stevenson, Jr., *Elements of Power System Analysis*, Fourth ed. New York: McGraw-Hill Book Company, 1982.

[16] J. Phillips. (2005).Short Circuit Calculations – Transformer and Source Impedance. [Online].Available:http://www.brainfiller.com/documents/TransformerandSourceImpedance_000.pdf.

[17] SimPower Systems. (2007). MATLAB Manual. [Online].Available:http://www.mathworks.com.

[18] K. Tran and M. Vaziri, "Effects of dispersed generation (DG) on distribution systems," in *Proc. 2005 IEEE Power Engineering Society General Meeting*, pp. 2173 - 2178.

[19] R.C.Dugan and D.T.Rizy, "Electric distribution protection problems associated with the interconnection of small, dispersed generation devices," *IEEE Trans. Power Apparatus and Systems,* vol. PAS103, pp. 1121-1127, 1984.

[20] A. Girgis and S. Brahma, "Effect of distributed generation on protective device coordination in distribution system," in *Proc. Power Engineering Large Engineering Systems* Halifax Canada, 2001, pp. 115-119.

[21] K. L. Butler-Purry and M. Marotti, "Impact of distributed generators on protective devices in radial distribution systems," in *Proc. 2006 IEEE PES Transmission and Distribution Conference and Exhibition*, pp. 87-88.

[22] J. A. Silva, H. B. Funmilayo, and K. L. Butler-Purry, "Impact of distributed generation on the IEEE 34 Node Radial Test Feeder with overcurrent protection," in *Proc. 2007 39th North American Power Symposium*, pp. 49-57.

[23] IEEE Distribution System Analysis Subcommittee. Radial Test Feeders [Online].Available: http://www.ewh.ieee.org/soc/pes/dsacom/testfeeders.html.

[24] C. J. Mozina, "Distributed generator interconnect protection practices," in *Proc. 2005/2006 IEEE PES Transmission and Distribution Conference and Exhibition.*

[25] *IEEE Guide for Electric Power Distribution Reliabilty Indices*, IEEE Std 1366-2003, May 2004.

[26] A. Y. Abdelaziz, H. E. A. Talaat, A. I. Nosseir, and A. A. Hajjar, "An Adaptive Protection Scheme for Optimal Coordination of Overcurrent Relays," [Online]. Available: http://docs.ksu.edu.sa/PDF/Articles13/Article130747.pdf.

[27] S. M. Brahma and A. A. Girgis, "Microprocessor-Based Reclosing to coordinate Fuse and Recloser in a system with High Penetration of Distributed Generation," in *Proc. 2002 IEEE Power Engineering Society Winter Meeting*, pp. 453 - 458.

[28] S. Brahma and A. A. Girgis, "Development of Adaptive Protection Scheme for Distribution Systems With High Penetration of Distribution Generation," *IEEE Trans. Power Delivery,* vol. 19, pp. 56-63, 2004.

[29] J. C. Gomez and M. M. Morcos, "Coordination of Voltage Sag and Overcurrent Protection in DG Systems," *IEEE Trans. Power Delivery,* vol. 20, pp. 214-218, 2005.

[30] H.Y. Li, P.A. Crossley, and N. Jenkins, "Transient directional protection for distribution feeders with embedded generations," in *Proc. 2002 14th PSCC Conf., Sevilla*, pp. 1-5.

[31] *IEEE Standard for Interconnecting Distributed Resources with Electric Power Systems*, IEEE Std 1547-2003, Jun. 2003.

[32] M.T.Brown and R.C.Settembrini, "Dispersed Generation Interconnections via Distribution Class Two-cycle Circuit Breakers," *IEEE Trans. Power Delivery,* vol. 5, pp. 481-485, 1990.

[33] M. Geidl. (2005). Protection of Power Systems with Distributed Generation: State of the Art.[Online].Available:http://www.eeh.ee.ethz.ch/downloads/psl/publications/geidl_protection_dg.pdf.

[34] G. Dalke, A. Baum, B. Bailey, J. M. Daley, B. Duncan, J. Fischer, E. Hesla, R. Hoerauf, B. Hornbarger, W. J. Lee, D. J. Love, D. McCullough, C. Mozina, N. Nichols, L. Padden, S. Patel, A. Pierce, P. Pillai, G. Poletto, R. Rifaat, M. K. Sanders, J. M. Shelton, T. N. Stringer, J. Weber, A. Wu, R. Young, and L. Powell, "Application of islanding protection for industrial & commercial generators a working group report," in *Proc. 2005 IEEE Industrial and Commercial Power Systems Technical Conference*, pp. 38-51.

[35] L. A. Kojovic and J. F. Witte, "Improved protection systems using symmetrical components," in *Proc. 2001 IEEE/PES Transmission and Distribution Conference and Exposition*, pp. 47-52.

[36] B. J. Kirby, J. Dyer, C. Martinez, R. A. Shoureshi, R. Guttromson, and J. Dagle. "Frequency Control Concerns in the North American Electric Power System,"Oak Ridge National Lab., Oak Ridge,TN, ORNL/TM-2003/41, Dec. 2002.

[37] Dromney design. (2007). Synchronous Generation in Distribution Systems. [Online]. Available: www.dromeydesign.com/articles/SynchronousGeneration.pdf.

[38] *IEEE Guide for Automatic Reclosing of Line Circuit Breakers for AC Distribution and Transmisson Lines*, IEEE Standard C7.104, Apr. 2003.

[39] W.-C. Yang and T.-H. Chen, "Analysis of interconnection operation of a radial feeder with a cogeneration plant," in *Proc. 2005 IEEE Power Engineering Society General Meeting*, pp. 2384 - 2389.

[40] A. F. Elneweihi, E. O. Schweitzer, III, and M. W. Feltis, "Negative-sequence Overcurrent Element Application and Coordination in Distribution Protection," *IEEE Trans. Power Delivery* vol. 8, pp. 915-924, 1993.

[41] C. J. Mozina, "A tutorial on the impact of distributed generation (DG) on distribution systems," in *Proc. 2008 61st Annual Conference for Protective Relay Engineers*, pp. 591-609.

[42] G. Chicco, R. Napoli, and F. Spertino, "Performance assessment of the inverter-based grid connection of photovoltaic systems," in *Proc. 2004 ATKAAF Conf.*, pp. 187–197.

[43] P. M. Anderson, *Power System Protection,* New Jersey: IEEE Press Series, 1999.

[44] DIgSILENT (2007). DIgSILENT PowerFactory Manual [Online]. Available: www.digsilent.com.

[45] Windsor Energy Center (2007). System Impact Assessment Report. Ontario. [Online]. Available: http://www.ieso.ca/imoweb/pubs/caa/CAA_SIAReport_2007-281.pdf.

[46] K. Tomsovic and F. Soudi, "Optimized Distribution Protection using Binary Programming," *IEEE Trans. Power Delivery,* vol. 13, pp. 218-222, 1998.

[47] V. K. Sood, *HVDC and FACTS Controllers: Applications of Static Converters in Power Systems*. Boston: Kluwer Power Electronics and Power systems Series, 2004.

APPENDIX A

A. IEEE 34 Node Radial Test Feeder

The IEEE 34 Node test feeder's parameters were downloaded from [23] and include the overhead line configurations along with the impedance and susceptance, line segment data, spot loads, distributed loads, shunt capacitors, transformer data, voltage regulator data and load flow results. The load flow node voltage results and short circuit results were compared to the reference results. The list of existing OCPDs and the settings of the selected OCPDs in the new approach are provided in the tables that follow.

Table 26 Selected OCPDs for the IEEE 34 Node Test Feeder

From Node	To Node	Prot. Device	Nomenclature Type	I_{rated} (A)	Manufacturer
800	802	Recloser	CME-FORM4 (1Fast, 2	100	Cooper/McGraw
808	810	Fuse 1	KEARNEY X4	4	Kearney
816	818	Fuse 2	KEARNEY T15	15	Kearney
824	826	Fuse 3	KEARNEY X4	4	Kearney
854	856	Fuse 4	KEARNEY X4	4	Kearney
832	XFM-1	Fuse 5	COOPER/ NEMA T-TIN10T	10	Cooper/McGraw
858	864	Fuse 6	KEARNEY X4	4	Kearney
834	842	Fuse 7	COOPER/NEMA K-TIN20K	20	Cooper/McGraw
836	862	Fuse 8	KEARNEY X4	4	Kearney
844	Cap-844	Fuse 9	GEEJO-1 (SIZE C)10E	10	General Electric
848	Cap-848	Fuse 10	GEEJO-1 (SIZE D)15E	15	General Electric
836	840	Fuse 11	KEARNEY X4	4	Kearney
888	890	Fuse 12	R200ST – 50E	50E	Westinghouse

Table 27 Base Case: Recloser-Fuse Coordination for the IEEE 34 Node Test Feeder

Fuse #	Fault Type	R Opens (s)	R Closes (s)	Fuse Operates (s)
1	1-ph-gZ_f	0.045	0.212	0.302
	1-ph-g	0.036	0.202	0.234
2	1-ph-gZ_f	0.117	0.284	1.245
	1-ph-g	0.059	0.225	0.500
3	1-ph-gZ_f	0.076	0.243	0.501
	1-ph-g	0.061	0.210	0.385
4	1-ph-gZ_f	0.108	0.275	0.725
	1-ph-g	0.088	0.255	0.558
6	1-ph-gZ_f	0.112	0.279	0.878
	1-ph-g	0.098	0.265	0.702
7	1-ph-gZ_f	0.116	0.282	0.928*
	3-ph-g	0.072	0.238	0.447*
8	1-ph-gZ_f	0.124	0.290	0.881*
	3-ph-g	0.071	0.238	0.498*
11	1-ph-gZ_f	0.117	0.283	0.925*
	3-ph-g	0.072	0.238	0.499*

Table 28 Case 1-4: Interconnect Relay Settings

DG	Phase Settings			Ground Settings		
Location	TDS	Ipickup (A)	TCC	TDS	Ipickup (A)	TCC
840	1	80	101	1	6	101
848	0.55	64	C5	0.9	10	C5
862	0.5	80	101	1.15	8	101
890	0.5	300	101	1	2	101

Table 29 Case 1-4: Lateral Recloser – Instantaneous Curve Settings

DG	Phase Settings			Ground Settings		
Location	TDS	Ipickup (A)	TCC	TDS	Ipickup (A)	TCC
840	0.1	80	102	0.1	3.2	102
848	0.1	61	102	0.1	3	102
862	0.1	80	102	0.1	3.2	102
890	0.1	300	102	0.1	0.1	102

Table 30 Case 1-4: Lateral Recloser - Delayed Curve Settings

DG Location	Phase Settings			Ground Settings		
	TDS	Ipickup (A)	TCC	TDS	Ipickup (A)	TCC
840	2	80	102	2	3.2	120
848	2	70	U3	1.15	3.2	120
862	2	80	102	1.15	3.2	120
890	2	300	102	2	0.1	120

APPENDIX B

B. IEEE 123 Node Radial Test Feeder

The IEEE 123 Node test feeder's parameters were downloaded from [23] and include the overhead line configurations along with the impedance and susceptance, line segment data, spot loads, distributed loads, shunt capacitors, switches, transformer data, voltage regulator data and load flow results. The load flow node votage results and short circuit results were compared to the reference results. There were some variances in the short circuit results owing to the line modifications made. The list of OCPDs and the settings of the selected OCPDs in the new approach are provided below.

Table 31 Selected OCPDs for the IEEE 123 Node Test Feeder

From Node	To Node	Protective Device	Nomenclature Type	Manufacturer's Name	I_{rated} (A)	$I_{asymetric}$ (KA)
1	149	**R main**	SEL351R*	SEL	800	12.00
1	2	**RL1**	SEL351R*	SEL	60	12.00
1	6	**RL2**	SEL351R*	SEL	60	12.00
8	11	**F3**	DOMF3-150	Dominion	150	9.85
8	12	**RL4**	SEL351R*	SEL	60	12.00
13	17	**F5**	R400TL-80E	Westinghouse	80E	9.78
18	20	**F6**	DOMF3-100	Dominion	100	10.00
21	22	**F7**	DOMF3-100	Dominion	100	10.00
23	24	**F8**	DOMF3-100	Dominion	100	10.00
26	32	**F9**	DOMF3-100	Dominion	100	10.00
27	33	**F10**	NEMAT-50T	Cooper	50T	8.17
35	39	**F11**	DOMF3-150	Dominion	150	9.85
40	41	**F12**	NEMAT-50T	Cooper	50T	8.17
42	43	**F13**	NEMAT-50T	Cooper	50T	8.17
44	46	**F14**	NEMAT-50T	Cooper	50T	8.17
57	59	**F15**	DOMF3-100	Dominion	100	10.00
67	71	**F16**	DOMF3-100	Dominion	100	10.00
72	75	**F17**	DOMF3-100	Dominion	100	10.00
76	85	**F18**	DOMF3-100	Dominion	100	10.00
87	88	**F20**	NEMAT-50T	Cooper	50T	8.17
89	90	**F21**	NEMAT-50T	Cooper	50T	8.17
91	92	**F22**	NEMAT-50T	Cooper	50T	8.17
93	94	**F23**	NEMAT-50T	Cooper	50T	8.17
95	96	**F24**	NEMAT-50T	Cooper	50T	8.17
97	450	**F25**	DOMF3-100	Dominion	100	10.00
101	104	**F26**	DOMF3-100	Dominion	100	10.00
105	107	**F27**	DOMF3-100	Dominion	100	10.00
108	114	**F28**	DOMF3-100	Dominion	100	10.00
47	48	**F29**	R400TL-65E	Westinghouse	65E	9.78

Table 32 Total Load Distribution for the Modeled IEEE 123 Node Test Feeder

Node	Load Model	Ph-1 kW	Ph-1 kVAr	Ph-2 kW	Ph-2 kVAr	Ph-3 kW	Ph-3 kVAr
5	Y-I	0	0	0	0	20	10
6	Y-Z	0	0	0	0	40	20
10	Y-I	20	10	0	0	0	0
11	Y-Z	40	20	0	0	0	0
16	Y-PQ	0	0	0	0	40	20
17	Y-PQ	0	0	0	0	20	10
19	Y-PQ	40	20	0	0	0	0
20	Y-I	40	20	0	0	0	0
31	Y-PQ	0	0	0	0	20	10
32	Y-PQ	0	0	0	0	20	10
38	Y-I	0	0	20	10	0	0
39	Y-PQ	0	0	20	10	0	0
45	Y-I	20	10	0	0	0	0
46	Y-PQ	20	10	0	0	0	0
49	Y-PQ	35	25	70	50	35	25
50	Y-PQ	0	0	0	0	40	20
51	Y-PQ	20	10	0	0	0	0
52	Y-PQ	40	20	0	0	0	0
53	Y-PQ	40	20	0	0	0	0
58	Y-I	0	0	20	10	0	0
59	Y-PQ	0	0	20	10	0	0
60	Y-PQ	20	10	0	0	0	0
62	Y-Z	0	0	0	0	40	20
63	Y-PQ	40	20	0	0	0	0
64	Y-I	0	0	75	35	0	0
65	D-Z	35	25	35	25	70	50
66	Y-PQ	0	0	0	0	75	35
68	Y-PQ	20	10	0	0	0	0
69	Y-PQ	40	20	0	0	0	0
70	Y-PQ	20	10	0	0	0	0
73	Y-PQ	0	0	0	0	40	20
74	Y-Z	0	0	0	0	40	20
77	Y-PQ	0	0	40	20	0	0
80	Y-PQ	0	0	40	20	0	0
82	Y-PQ	40	20	0	0	0	0
83	Y-PQ	0	0	0	0	20	10
84	Y-PQ	0	0	0	0	20	10
85	Y-PQ	0	0	0	0	40	20
98	Y-PQ	40	20	0	0	0	0
99	Y-PQ	0	0	40	20	0	0
100	Y-Z	0	0	0	0	40	20
102	Y-PQ	0	0	0	0	20	10
103	Y-PQ	0	0	0	0	40	20
104	Y-PQ	0	0	0	0	40	20
106	Y-PQ	0	0	40	20	0	0
107	Y-PQ	0	0	40	20	0	0
109	Y-PQ	40	20	0	0	0	0
112	Y-I	20	10	0	0	0	0
113	Y-Z	40	20	0	0	0	0
114	Y-PQ	20	10	0	0	0	0
Total		1420	775	915	515	1155	635

The following section of the Appendix provides the reclosers and fuses operation in overcurrent protection scheme for a maximum and minimum permanent fault during the base case condition.

Table 33 Base Case: Recloser - Fuse Coordination for the IEEE 123 Node Test Feeder

Fuse #	Fault Type	R opens (s)	R closes (s)	Fuse Operates (s)
F3	1-ph-g Zf	0.451	0.617	6.483
	1-ph-g	0.032	0.199	0.204
F5	1-ph-g Zf	0.584	0.751	10.898
	1-ph-g	0.029	0.195	0.208
F6	1-ph-g Zf	0.462	0.629	2.834
	1-ph-g	0.035	0.202	0.253
F7	1-ph-g Zf	0.779	0.945	2.861
	1-ph-g	0.034	0.200	0.269
F8	1-ph-g Zf	0.591	0.757	3.082
	1-ph-g	0.035	0.202	0.306
F9	1-ph-g Zf	0.590	0.757	3.082
	1-ph-g	0.037	0.204	0.322
F10	1-ph-g Zf	0.473	0.640	1.532
	1-ph-g	0.043	0.209	0.255
F11	1-ph-g Zf	0.809	0.976	2.648
	2-ph-g	0.032	0.198	0.352*
F12	1-ph-g Zf	0.593	0.760	1.446
	1-ph-g	0.035	0.201	0.229
F13	1-ph-g Zf	0.835	1.001	1.376
	1-ph-g	0.037	0.204	0.228
F14	1-ph-g Zf	0.079	0.245	0.495
	1-ph-g	0.031	0.197	0.228
F15	1-ph-g Zf	0.769	0.935	2.769
	1-ph-g	0.032	0.199	0.234
F16	1-ph-g Zf	0.466	0.633	2.699
	1-ph-g	0.039	0.206	0.322
F17	1-ph-g Zf	0.584	0.751	2.738
	1-ph-g	0.038	0.205	0.333

Table 33 continued

Fuse #	Fault Type	R opens (s)	R closes (s)	Fuse Operates (s)
F18	1-ph-g Zf	0.589	0.756	1.554
	1-ph-g	0.030	0.197	0.236
F20	1-ph-g Zf	0.478	0.644	1.543
	1-ph-g	0.049	0.216	0.303
F21	1-ph-g Zf	1.056	1.223	1.508
	1-ph-g	0.056	0.222	0.292
F22	1-ph-g Zf	0.585	0.752	1.585
	1-ph-g	0.063	0.229	0.320
F23	1-ph-g Zf	0.484	0.651	1.602
	1-ph-g	0.058	0.225	0.330
F24	1-ph-g Zf	1.140	1.306	1.608
	1-ph-g	0.073	0.239	0.324
F25	1-ph-g Zf	0.585	0.751	3.274
	3-ph-g	0.030	0.197	0.239*
F26	1-ph-g Zf	0.585	0.752	2.911
	1-ph-g	0.041	0.208	0.356
F27	1-ph-g Zf	0.955	1.122	2.913
	1-ph-g	0.043	0.210	0.349
F28	1-ph-g Zf	0.482	0.648	2.681
	1-ph-g	0.047	0.213	0.395
F29	1-ph-g Zf	0.476	0.643	7.071
	3-ph-g	0.029	0.196	0.235*

Table 34 Case 5-6: Interconnect Relay Settings

DG	Phase Settings			Ground Settings		
Location	TDS	I_{pickup} (A)	TCC	TDS	I_{pickup} (A)	TCC
48	2	400	101	0.5	30	U1
450	2	500	101	0.5	40	U1

Table 35 Case 5-6: Lateral Recloser - Instantaneous Curve Settings

DG	Phase Settings			Ground Settings		
Location	TDS	Ipickup (A)	TCC	TDS	Ipickup (A)	TCC
48	0.1	400	103	0.05	3.2	103
450	0.1	500	103	0.1	3.2	103

Table 36 Case 5-6: Lateral Recloser - Delayed Curve Settings

DG	Phase Settings			Ground Settings		
Location	TDS	Ipickup (A)	TCC	TDS	Ipickup (A)	TCC
48	1	400	165	0.1	3.2	C1
450	1.15	500	165	0.1	3.2	C1

VITA

Hamed B. Funmilayo received his Bachelor of Science degree in electrical engineering from Kansas State University. He received his Master of Science degree in electrical engineering in December 2008 from Texas A&M University and was a research assistant in the Power System Automation Laboratory at Texas A&M.

He is a student member of IEEE and the honor society of Etta Kappa Nu. He may be reached at Department of Electrical and Computer Engineering, 214 Zachry Engineering Center, Texas A&M, College Station, TX 77843-3128. His email is hfunmilayo@gmail.com.